CELLULAR COMMUNICATION AND MECHANOTRANSDUCTION IN RESPONSE TO FLUID SHEAR STRESS

by

Mia Mia Thi

A dissertation submitted to the Graduate Faculty in Engineering in partial fulfillment of the requirements for the degree of Doctor of Philosophy, The City University of New York.

2004

INFORMATION TO USERS

The quality of this reproduction is dependent upon the quality of the copy submitted. Broken or indistinct print, colored or poor quality illustrations and photographs, print bleed-through, substandard margins, and improper alignment can adversely affect reproduction.

In the unlikely event that the author did not send a complete manuscript and there are missing pages, these will be noted. Also, if unauthorized copyright material had to be removed, a note will indicate the deletion.

ProQuest Information and Learning Company
300 North Zeeb Road
P.O. Box 1346
Ann Arbor, MI 48106-1346

This manuscript has been read and accepted for the Graduate Faculty in Engineering in satisfaction of the dissertation requirement for the degree of Doctor of Philosophy.

9/8/04
Date

Professor Sheldon Weinbaum
Chair of Examining Committee

9/8/04
Date

Professor Mumtaz Kassir
Executive Officer

Professor David C. Spray

Professor Stephen C. Cowin

Professor Susannah P. Fritton

Professor John M. Tarbell

Supervisory Committee

THE CITY UNIVERSITY OF NEW YORK

Abstract

CELLULAR COMMUNICATION AND MECHANOTRANSDUCTION IN RESPONSE TO FLUID SHEAR STRESS

by

Mia Mia Thi

Advisor: Professor Sheldon Weinbaum

Co-Advisors: Professor David C. Spray

Professor Stephen C. Cowin

Cell-cell mechanotransduction which involves sensing mechanical stimuli such as fluid induced shear stress and spreading the signal in the connected network of bone cells or among endothelial cells is still not well understood. Our studies here address several vital links that are overlooked by previous studies. Current knowledge on how these cells behave under fluid shear stress with possible candidates for mechanosensors are discussed in Chapter 1.

In Chapter 2, we first tested the hypothesis that fluid shear stress modifies expression, function and distribution of junctional proteins (Cx43, Cx45, and ZO-1) in cultured bone cells. Cell lines with osteoblastic (MC3T3-E1) and osteocytic (MLO-Y4) phenotypes were exposed to shear stress of 5 or 20 dyn/cm^2 for 1-3 h. Our results indicate that in cultured bone cells fluid shear stress disrupts junctional communication, rearranges junctional proteins and determines *de novo* synthesis of specific connexins to an extent that depends on the magnitude of the shear stress. Such disconnection from the

bone cell network may provide part of the signal whereby the disconnected cells or the remaining network initiate focal bone remodeling.

In Chapter 3, we propose a new conceptual model for the cytoskeletal organization of endothelial cells (ECs) with a major dichotomy in structure and function at its basal and apical aspects. Intracellular distributions of F-actin, vinculin, paxillin, ZO-1 and Cx43 were analyzed following five hours of shear stress. Our results are explained in terms of a 'bumper car' model in which the actin cortical web (ACW) and dense peripheral actin band (DPAB) are only loosely connected to basal attachment sites allowing for two distinct cellular signaling pathways in response to fluid shear stress, one transmitted by glycocalyx core proteins as a torque that acts on the ACW and DPAB and the other emanating from focal adhesions and stress fibers (SFs) at the basal and apical membranes of the cell.

Chapter 4 recapitulates past and present key insights and proposes future directions.

Acknowledgements

I am forever indebted to Professors Sheldon Weinbaum and David C. Spray for their superior mentoring and support and for allowing me to become an independent researcher throughout my graduate studies. Special thanks to Professors Stephen C. Cowin, Susannah P. Fritton and John M. Tarbell for their insightful guidance and advice. I am very honored to be able to explore and expand my knowledge in such a company.

I would also like to thank all the members of Spray Lab at Albert Einstein College of Medicine, especially Drs. Sylvia O. Suadicani, Eliana Scemes, Miduturu Srinivas, Heather Duffy, Andrei and Sanda Iacobas, not yet Drs. Marcia Urban-Maldonado, Fran Andrade, Delia Vieira-Cruz, Michelle Beelitz, Alfredo Fort and Carmen Flores and all the faculty and friends at the CCNY Biomedical Engineering Department, especially Ms. Carol Bamberger and Dr. Laurent Mars for all the collaboration and help that I received during my Ph.D journey.

Last but not the least, my family, for their unrelenting support, understanding and believing in me. My parents, U Saw Win and Daw Khin Win Myint, for all the sacrifices they made for my education. My uncle Dr. Ronald Findlay, aunts Mrs. Tin Tin Aye Findlay, Ms. C.K. Khoo and Daw Hnin Hline for giving me a new life to my education. My husband, Myo Min Latt, and daughter, Megan Zune Latt, who have made my world special, for standing by me and encouraging me through thick and thin. In memory of my late father, I dedicate this dissertation to my family and friends.

Table of Contents

List of Figures

MC3T3-E1 and MLO-Y4 cells. Cells were subjected to low shear stress (5 dyn/cm^2) and high shear stress (20 dyn/cm^2) for 1 or 3 h; control cells were maintained for the same periods of time under no flow conditions. The effect of fluid shear stress on the distribution and arrangement of Cx43, Cx45 and ZO-1 in MC3T3-E1 and MLO-Y4 were analyzed using immunofluorescence microscopy. Formaldehyde fixed, triton X-100 permeabilized samples of control (A, D), $\tau = 5$ dyn/cm^2 exposure for 3 h (B, E), or $\tau = 20$ dyn/cm^2 exposure for 3 h (C, F) cells were stained with primary polyclonal or monoclonal antibodies against Cx43, ZO-1 and Cx45 followed by fluorescein-conjugated goat anti-rabbit IgG or goat anti-mouse IgG. A. Control MC3T3-E1 cells possessed abundant punctate and linear appositional staining of Cx43 and ZO-1 at cell borders as well as Cx43 immunoreactivity in perinuclear regions. Cx45 was present at appositional regions but was mainly concentrated at perinuclear regions of the cells. (B) Exposure to low shear stress of 5 dyn/cm^2 caused cells to become elongated and moderately decreased Cx43 and ZO-1 at the appositional membranes while perinuclear distribution of Cx43 notably increased. (C) Low shear stress led to reduced appositional and increased cytoplasmic staining of Cx45; at shear stress of 20 dyn/cm^2 significant disruptions of both Cx43 and ZO-1 at the opposing cell membranes were observed as exposure time increased from 1 to 3h. Cx45 distribution in perinuclear regions was more prominent at 20 dyn/cm^2. (D) In control MLO-Y4 cells, Cx43 and ZO-1 were concentrated at the tips of the cell processes at regions of contact with neighboring cells, with perinuclear distribution of Cx43. There was very faint staining for Cx45 at the tips of opposing cell processes of the control cells. Dramatic morphological changes were observed at both low and high levels of shear stress. (E) When cells were exposed to low shear stress of 5

Chapter 1

Introduction

Fluid induced shear stress has become well established as an important biophysical signal in cell-cell mechanotransduction (Weinbaum et al., 1994; Duncan and Turner, 1995; Davies, 1995; Turner and Pavalko, 1998; Burger and Klein-Nulend, 1999; Weinbaum et al., 2003). However, the cellular mechanisms that are involved in sensing mechanical stimuli and spreading the signal in the connected network of bone cells or among vessel wall endothelial cells (ECs) are still not well understood. The goal of the studies in this dissertation is to elucidate the cellular mechanisms of how cells can work in synchrony and propagate locally generated signals throughout the skeletal tissue or the endothelium by means of junctional, cytoskeletal and focal adhesion proteins.

In this Chapter, we present an overview of the structures and functions of cell junctions, actin cytoskeleton and focal adhesions in terms of scaffolding organization and stabilization (Fig. 1.1). Next, we discuss the unique aspects and multi-faceted roles of the cell surface glycocalyx. Finally, we focus our attention on the current knowledge of bone and endothelial cell mechanotransduction and critical aspects of mechanosensory function that have been overlooked in previous studies. We proposed a novel 'bumper car' model to explain how endothelial cells sense fluid shear. This has led to a new view of complex signaling cascades involved in cell-cell mechanotransduction in terms of their cytoskeletal activation.

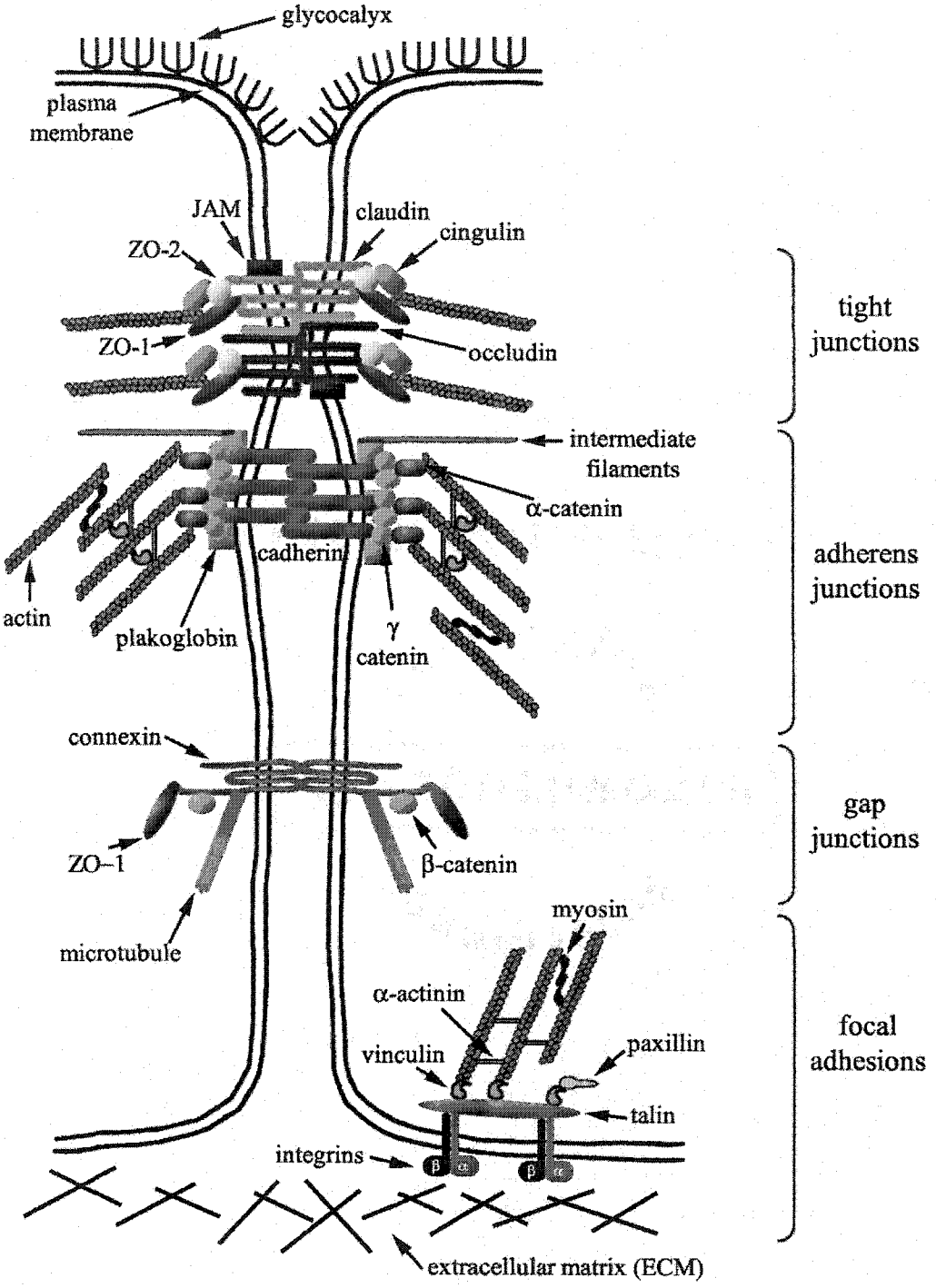

Figure 1.1. An overview of the organization of cell junctions (tight junctions, adherens junctions, and gap junctions) and focal adhesions showing their linkage with the actin cytoskeleton (adapted slightly from Ogunrinade et al., 2002).

Cell junctional complexes

Most cells are linked to one another at specialized cell-cell and cell-matrix contact sites termed cell junctions. These junctions are characterized as tight junctions, adherens junctions and gap junctions. An overview of these junctions in a bone cell network and in a confluent endothelial layer is discussed below.

Tight or occluding junctions are the most apical intercellular junctions in a variety of cells, including epithelial and endothelial cells. They serve as selective permeability barriers to regulate diffusion of nutrients and small molecules between individual cells as well as act as a fence within the membrane bilayer to control the migration of distinct carrier proteins from apical to basolateral side (Adamson and Michel, 1993; Mitic and Anderson, 1998; Ogunrinade et al., 2002). Tight junctions in osteoblasts are thought to be involved in compartmentalization of the early matrix and final polarization (Arana-Chavez et al., 1995). Tight junctions in endothelial cells form discontinuous junctional strands (~ 300 nm long) with 15-20 nm wide clefts (Adamson and Michel, 1993). Occludin, claudins (a family of 24 members) (Tsukita and Furuse, 2002) and the junctional adhesion molecule (JAM) are transmembrane proteins associated with tight junctions. Their extracellular loops weave together appositional membranes of the neighboring cells and form a tight junction with a pore size on the order of 8-20 Å as shown in Fig. 1.2 (Mitic and Anderson, 1998). Peripheral proteins such as ZO-1, 2 and cingulin are known to be involved in the tight junction scaffold of many cell types including epithelial cells, cardiac myocytes, astrocytes, bone and endothelial cells (Howarth et al., 1992; Furuse et al., 1994; Toyofuku et al., 1998; Laing et al., 2001; Thi

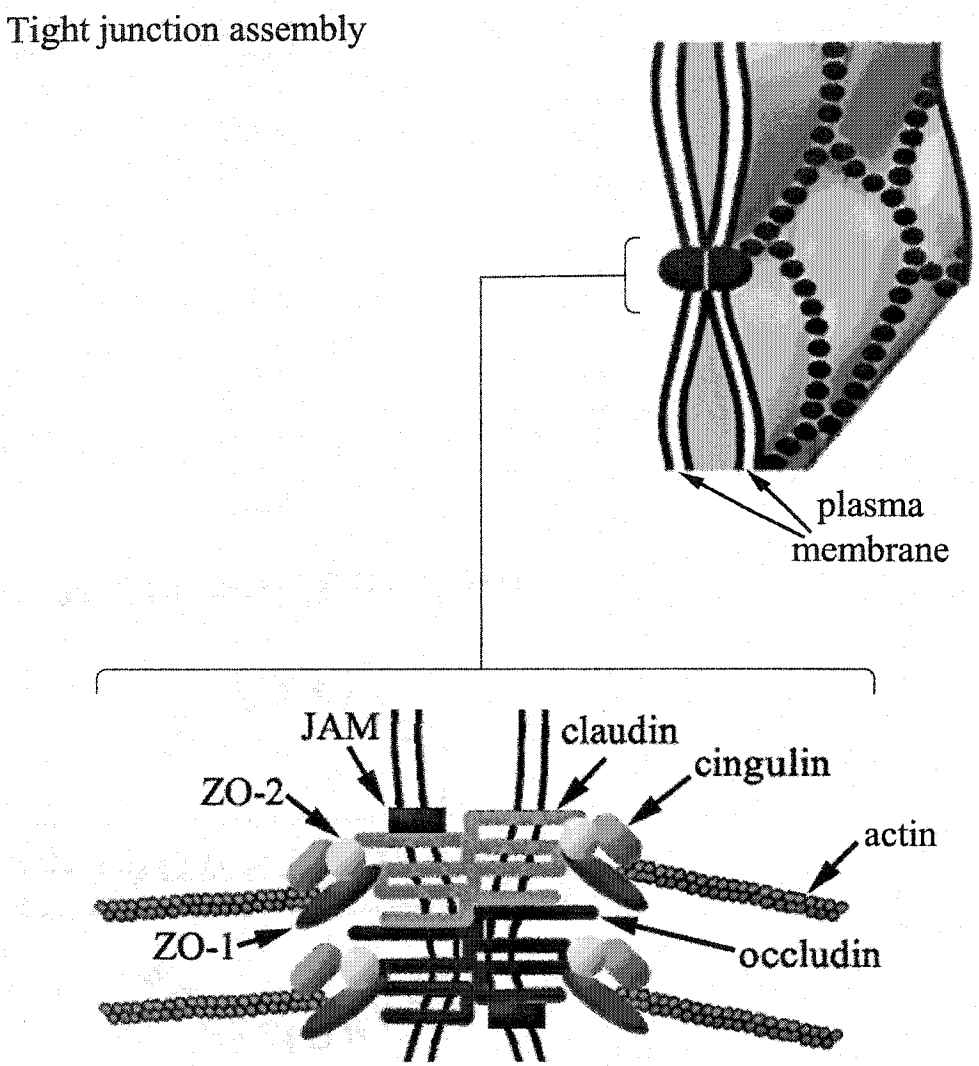

Figure 1.2. Sketches of a tight junction and its potential binding proteins. The extracellular loops of occludin and claudin from opposing cells knit together to form a tight junction. These integral tight junction proteins have four transmembrane domains with both amino and carboxyl termini in the cytoplasm. Peripheral proteins ZO-1, 2 and cingulin are associated with the tight junction scaffold. The connection between the tight junction scaffold and the cytoskeleton is achieved through either cingulin or ZO-1 (adapted slightly from Ogunrinade et al., 2002).

et al., 2003). Among these, ZO-1, a relatively large protein about 220kD in size, has been suggested to interact not only with other tight and gap junction proteins but also with the cell cytoskeleton; it is thus believed to play a role in stabilization of both tight and gap junction proteins (Itoh et al., 1997; Giepmans and Moolenaar, 1998; Fanning et al., 1998; Laing et al., 2001). In this dissertation, the adaptation of this scaffolding protein complex in response to fluid shear stress will be discussed in more detail in Chapters 2 and 3.

Cell-cell adherens junctions are large multiprotein complexes that are made up of cadherins, α-, β-, and γ-catenin, and plakoglobin. Cadherins, single pass transmembrane glycoproteins, of adjacent cells interact and hold the appositional cells together in a calcium-dependent manner, thereby forming an adhesion belt (Angst et al., 2001). As shown in Fig. 1.3 external cadherin domains act as a zipper between the two neighboring cells and their internal domains via attachment proteins that link the actin filament system of one cell with its neighboring cell (Tepass, 2002). Major cadherins found in the adherens junction of osteoblasts are cadherin-11 and N-cadherin and in endothelial cells, VE-cadherin (Schnittler, 1998; Luegmayr et al., 2000; Ogunrinade et al., 2002). Studies of interactions between the external domain of VE-cadherins in endothelial cells (Baumgartner et al., 2000) using single molecule atomic microscopy suggest that the binding is regulated by low-affinity Ca^{++} binding sites (K_D ~ 1.15 mM) with a comparatively low unbinding forces in the vicinity of 35-120 pN. The linkage between actin, myosin, and the α-actinin rich dense peripheral band and this complex of multiproteins is achieved through α-catenin. In Chapter 3, we investigated the role of the adherens junctions from a cytoskeletal point of view.

Adherens junction assembly

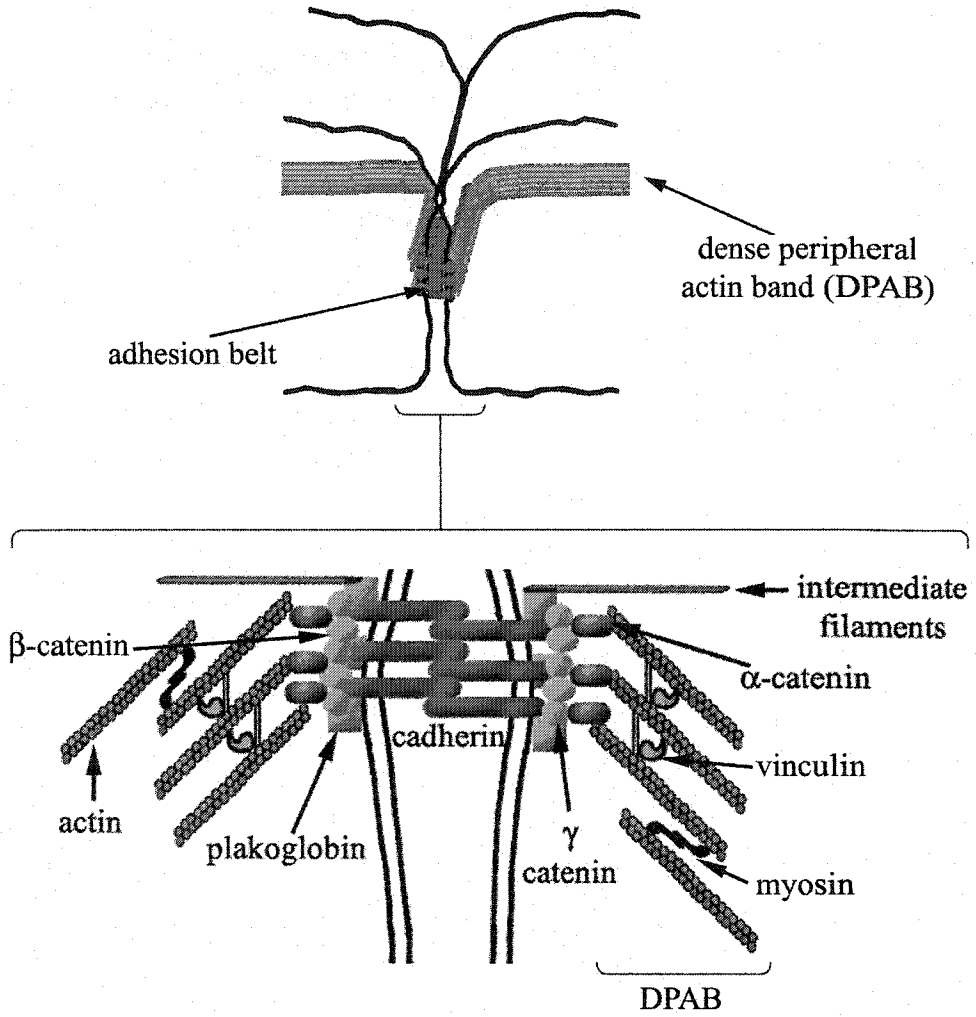

Figure 1.3. Diagrams of multiprotein adherens junction complexes and the dense peripheral actin band. External domains of single pass transmembrane cadherins from neighboring cells interact and form an adhesion belt. The internal domains connect the dense peripheral actin band (DPAB) from one cell to that of the adjacent cell by means of α-, β-, and γ-catenin. The DPAB consists of contractile bundles of actin and myosin-II filaments. (Adapted slightly from Ogunrinade et al., 2002).

Gap or communicating junctions are intercellular channels across the extracellular space formed by the connection of two hemichannels or connexons. Each connexon is made up of six protein subunits, called connexins (Cx) (Willecke et al., 2002). Each connexin has both intracellular amino and carboxyl termini and spans the membrane four times. The extracellular loops of the connexons from two adjacent cells interact and form a pore that joins the cytoplasms of the cells. Gap junction channels are permeable to small ions and molecules, including second messenger molecules with molecular weights up to approximately 1kD (kilodalton) and are impermeable to proteins, cellular organelles, DNA and RNA (Spray, 1996; Spray, 1998) (Fig. 1.4). Different types of connexins are named for their approximate molecular weight in kDa (Beyer, 1990). The connexin proteins that form gap junctions are encoded by a gene family with as many as 21 members in mammals (Willecke et al., 2002). The bone cell network, which consists of osteoblasts, bone lining cells along the surface, and osteocytes within the bone matrix, and vessel wall lining endothelial cells are functionally connected by means of gap junction channels (Shaklai et al., 1978; Jeansonne et al., 1979; Doty, 1981). Gap junction plaques are generally quite large, consisting of hundreds or thousands of connexons. The gap junction proteins Cx43 and Cx45 are expressed by bone cells (Civitelli et al., 1993; Minkoff et al., 1994; Steinberg et al., 1994; Yamaguchi et al., 1994; Lecanda et al., 1998; Minkoff et al., 1999) and Cx37, Cx40, and Cx43 are expressed in the vascular wall endothelium (Polacek et al., 1993; Bruzzone et al., 1993; Reed et al., 1993). Gap junctional communication is believed to play an important role during embryogenesis, osteogenesis, bone remodeling, bone mineralization, propagation of intercellular signals, vessel wall homeostasis and atherogenesis (Warner, 1992; Minkoff et al., 1994; Polacek

Gap junction assembly

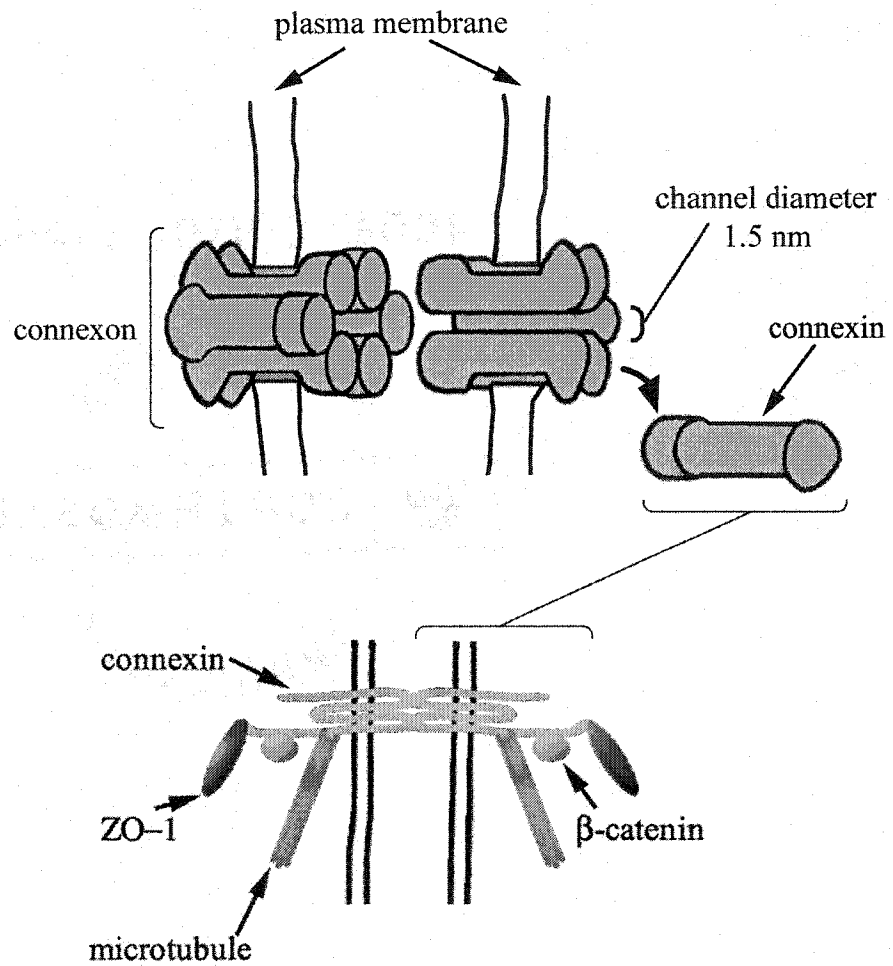

Figure 1.4. Schematic of gap junction channel and a few of its prospective binding partners. Gap junction channels are formed by bridging two connexons across oppositional membranes of two cells (approximately 1.5 nm in diameter); each connexon is formed of six connexin molecules. Connexin topology includes both intracellular amino and carboxyl termini and spans the membrane four times. There are as many as 21 encoded connexins in the mouse and human genome. Various connexins bind to many proteins such as ZO-1, occludin, claudin, and β-catenin and thus form a scaffolding complex termed the 'Nexus' (Spray et al., 1999).

et al., 1997; Lecanda et al., 1998; Depaola et al., 1999; Donahue, 2000; Kwak et al., 2002). The role of gap junction communication in bone cell mechanotransduction is briefly discussed later in this Chapter and is more thoroughly explored in Chapter 2. Gap junctional communication in endothelial cell mechanotransduction is analyzed from the viewpoint of adaptation to shear stress in Chapter 3. Recent findings of connexin interactions with other proteins, such as ZO-1, occludin, claudin, β-catenin, microtubule and caveolin-1 forming a 'Nexus' suggest that in addition to forming communicating junctions, connexins may also play other roles in signaling, trafficking, scaffolding, and organization (Toyofuku et al., 1998; Kojima et al., 1999; Ai et al., 2000; Nusrat et al., 2000; Schubert et al., 2002; Duffy et al., 2002; Giepmans, 2004).

This dissertation attempts to elucidate the process of cell-cell communication and adaptation in response to mechanical stimuli from the environment. The regulation of tight and gap junctional protein complexes by fluid shear stress is further discussed in both Chapters 2 and 3. Although junctional changes in response to mechanical stimuli have been the subject of a number of previous studies, this dissertation has examined these changes in the context of changes in the cell's actin cytoskeleton and its focal adhesions, and more importantly the involvement of the cell glycocalyx. Through consideration of the broader context of cytoskeletal linkage of junctional proteins, we believe that we have contributed to further understanding of the cellular mechanisms of mechanotransduction in response to shear stress.

Focal adhesions

The basal surfaces of most cells adhere to the underlying substratum at specific regions of their plasma membrane called focal adhesions or focal contacts. These focal contacts are sites of anchorage for intracellular actin filaments and stress fibers to extracellular matrix (ECM) molecules. Besides their role as cell anchors, the interactions at these sites are important for cell morphology, motility, proliferation, migration, and signaling for a variety of cells including the bone cell network and endothelial cells (Burridge et al., 1988; Burridge et al., 1992; Pavalko and Otey, 1994; Duncan and Turner, 1995; Davies, 1995; Pavalko et al., 1998). The assembly of the entire focal adhesion plaque involves transmembrane integrin receptors linking ECM proteins such as fibronectin, collagens, and vitronectin, to actin filaments and stress fibers through an array of cytoskeletal proteins such as talin, vinculin, paxillin, and filamin as shown in Fig. 1.5 (Burridge et al., 1988; Burridge et al., 1992; Critchley, 2000; Turner, 2000). Moreover, the construction of focal adhesive contacts is regulated by activation of numerous kinases including p125 focal-adhesion kinase, focal adhesion kinase (FAK), protein kinase C, and Src family tyrosine kinases (Burridge et al., 1992; Critchley, 2000). Recent findings indicate that the minimal applied force on the apical surface of endothelial cells required to initiate the signal transduction and translocation at the focal adhesion sites lies in the range 0.9 - 1.45 nN (Mack et al., 2004). Moreover, analysis of individual focal adhesions using 130 pN magnetic force application to integrin receptors via ligand coated magnetic microbeads suggests that those beads that formed focal adhesion assembly (either via vinculin, paxillin or actin) were stiffer and thus more

Focal adhesions

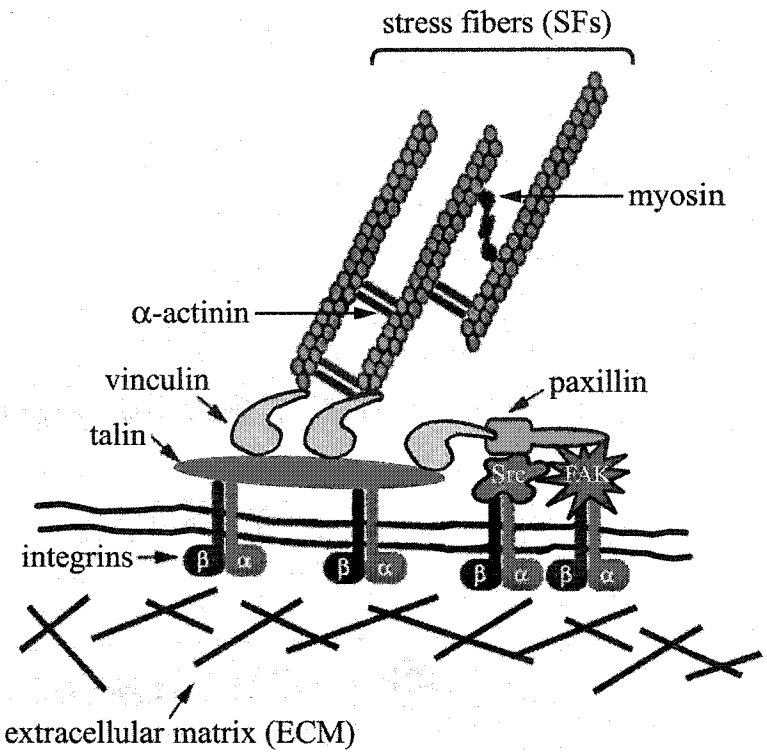

Figure 1.5. Assembly of a focal adhesion plaque. A sketch of interactions among ECM proteins, integrins, cytoskeletal and adaptor proteins: vinculin, talin, paxillin, numerous activated kinases: FAK, Src, and stress fibers. Modified from (Turner, 2000).

effectively retarded maximal displacement compared to integrins that were not attached to the adhesion proteins (Matthews et al., 2004).

In the past, focal adhesions comprised of the α, β family of integrins have been extensively studied in both the bone cell network and endothelial cells (Duncan and Turner, 1995; Davies, 1995). In Chapter 3, we have reevaluated two of the cytoskeletal proteins, vinculin and paxillin, which have been shown to play critical roles in actin polymerization, contact assembly and stabilization (Critchley, 2000; Bailly, 2003). We observed strikingly different distributions of vinculin in response to fluid shear depending on whether the glycocalyx was present or not in contrast to paxillin whose distribution was insensitive to the structural intactness of this layer.

Cell actin cytoskeleton

The cytoskeleton of eukaryotic cells is a network of spatially organized actin filaments, microtubules, and intermediate filaments. Among the three types of filaments, actin filaments form he substratum of the plasma membrane of the cells. Studies have shown that actin filaments (5-8 nm in diameter) and a variety of other actin binding proteins form a layer termed the actin cortical web (ACW), a cortex or fence-like elastic structure just beneath the plasmalemma in various cell types including fibroblasts, erythrocytes, osteoblasts, osteocytes, epithelial, and endothelial cells as shown in Fig. 1.6 (King and Holtrop, 1975; Hirokawa and Heuser, 1981; Sako and Kusumi, 1995; Kusumi and Sako, 1996; Drenckhahn and Ness, 1997; Tanaka-Kamioka et al., 1998; You et al., 2004). This layer is only visible in ultrastructural quick-freeze, deep-etch studies (Drenckhahn and Ness, 1997). More recent freeze fracture EMs close to the plasma membrane of

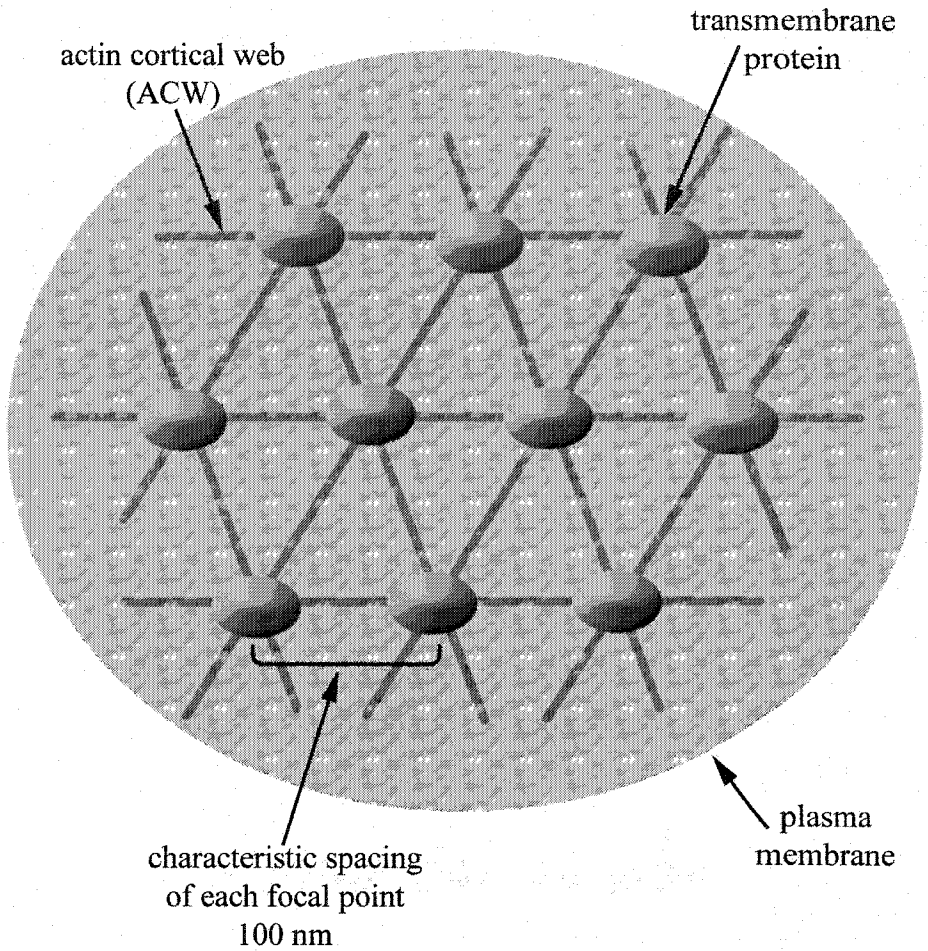

Figure 1.6. A model for the actin cortical web (ACW). This ACW possesses an ordered hexagonal meshwork. This geodesic canopy is located just beneath the palsmalemma.

endothelial cells have revealed an ordered hexagonal meshwork with a characteristic spacing of 100 nm between each focal point (Squire et al., 2001). The properties of this actin rich layer are as follows: (1) it regulates the shape and movement or scaffolding and remodeling of the plasma membrane, and (2) it serves as anchoring site for

transmembrane proteins. Studies have shown that the ACW most likely accounts for the viscoelastic nature of the membrane with the approximate viscoelastic constant of 700-900 dyn/cm^2; the fence-like elastic elements in the ACW can withstand forces in the vicinity of 0.1 pN (Sato et al., 1990; Sako and Kusumi, 1995). In addition, depolymerization of actin filaments by cytochalasin B decreases the viscoelasticity of membranes and increases the endocytotic activity in ECs (Liu et al., 1993; Drenckhahn and Ness, 1997). Various studies have indicated that the ACW acts as an attachment site for transmembrane proteins such as glycoprotein CD44, protein 4.1 and transmembrane proteoglycans in a variety of cells (Saunders et al., 1989; Tsukita et al., 1994; Drenckhahn and Ness, 1997). These transmembrane proteins enable the connection between cell surface glycocalyx and the ACW, which we discuss later in this Chapter.

A second type of actin filament structure emerges at cell-cell junctions of endothelial, epithelial and osteoblast cells (Nusrat et al., 1995; Pavalko et al., 1998; Galbraith et al., 1998; Kano et al., 2000; Thi et al., 2003) and around the cell body of the osteocytes (Tanaka-Kamioka et al., 1998; Thi et al., 2003). This structure takes the form of a contractile ring or dense peripheral actin band (DPAB). It is made up of contractile bundles of actin and myosin-II filaments. The DPAB lies adjacent to the adhesion belt, which serves as a linkage to Ca^{++} dependent cell-cell adhesion proteins called cadherins, at the appositional membrane and runs parallel to the plasma membrane as shown in Fig. 1.3. This peripheral band is situated in proximity to tight junction and has been proposed to be involved in the regulation of the permeability of the tight junctions (Nusrat et al., 1995; Drenckhahn and Ness, 1997). The essential role of this band is to stabilize the weak anchoring of intercellular adherens junction by means of α-, β-, and γ-catenin, and

plakoglobin and provide lateral alignment shown in Fig. 1.3 (Drenckhahn and Ness, 1997; Schnittler, 1998; Baumgartner et al., 2000; Ogunrinade et al., 2002). Due to the DPAB's contractile nature, several investigator have suggested that, in addition to cell-cell adhesion, the DPAB also regulates retraction and intercellular spacing of cells in response to various inflammatory stimuli and to fluid shear stress in both osteoblastic and endothelial cell layers (Schnittler et al., 1997; Pavalko et al., 1998; Galbraith et al., 1998; Schnittler, 1998; Noria et al., 1999; Seebach et al., 2000).

A third type of actin filament structure, which is readily seen in immunofluorescence studies are stress fibers (SFs), which form myofibril-like contractile bundles of dozens if not hundreds of actin filaments. These bundles are typically 0.7 μm thick and 25 μm long (Drenckhahn and Ness, 1997). SFs are known to form in response to tension generated across the cell. Numerous *in vitro* studies have shown the formation of SFs in response to fluid shear stress in both bone and endothelial cells (Pavalko et al., 1998; Galbraith et al., 1998; Schnittler et al., 2001). One end of these stress fibers in the cell body is often associated with focal contacts or focal adhesion plaques and the other end either is attached to another focal plaque or to a network of intermediate filaments. Stress fibers in osteocyte processes are bundled primarily with fimbrin are parallel whereas those in the cell body are bundled with only α-actinin and are anti-parallel (King and Holtrop, 1975; Tanaka-Kamioka et al., 1998; You et al., 2004). In endothelial cells, previous studies have shown the presence of thick SFs in basal regions and thin SFs in apical regions (Satcher et al., 1997; Schnittler, 1998; Kano et al., 2000). In addition SFs from apical plaques seem to link either to the basal plaque or DPAB at the lateral region.

Moreover, SFs endings in endothelial cells at focal adhesion sites are associated with α-actinin and vinculin (Drenckhahn and Wagner, 1986; Drenckhahn and Ness, 1997).

In general, the existence of the geodesic-like ACW canopy usually is undetectable in most *in vitro* immunofluorescence studies and thus the significant role of this structure in cell-cell mechanotransduction is often ignored. Moreover, direct evidence of changes in adherens junction and stress fiber formation is routinely observed in confluent cell monolayers exposed to fluid shear stress but the association was previously with the surface glycocalyx. In Chapter 3 we will address the unique functions of the ACW, the DPAB and the SFs in relation to the glycocalyx.

Cell surface layer glycocalyx

The surface of all eukaryotic cells is decorated with carbohydrate rich layer which is often termed cell coat or pericellular matrix or glycocalyx. It is composed mainly of glycoproteins and proteoglycans. The existence of a glycocalyx was first proposed by Luft (1966) almost four decades ago and has been studied extensively in endothelial cells (Adamson, 1990; Vink and Duling, 1996; Squire et al., 2001). Depending on the species, this layer is between 100 to 500 nm thick. Although the pericellular matrix that fills the fluid annulus surrounding the osteocyte processes in canaliculi and cell body in lacunae was identified 40 years ago (Wassermann and Yaeger, 1965), studies regarding its detailed structure and composition have been somewhat hampered by the difficulty in assessing living cells in mineralized tissue. Recent data by You et al. (2004)

quantitatively identified the presence of transverse elements in the pericellular matrix (~ 100 nm) that bridge between the mineralized bone matrix and the osteocyte cell processes using special staining techniques. Additional findings by the same group suggest that these transverse elements are regularly spaced between 38 to 41 nm apart both longitudinal and transverse sections as shown in Fig. 1.7. Sauren et al. (1992) showed that chondroitin sulfate proteoglycans play a role in the pericellular matrix assembly of rat and human bone. In the past 10 years, a number of theoretical models have suggested the possible role of fluid flow through the pericellular matrix as the activation in bone cell signalling (Zeng et al., 1994; Cowin et al., 1995; Cowin and Weinbaum, 1998; Weinbaum et al., 2001; You et al., 2001). This role has yet to be verified experimentally in bone cells *in vivo*. Our study on bone cells presented in Chapter 2 of this dissertation focuses on other aspects of cell-cell mechanotransduction but does not address the role of the pericellular matrix. At the time of our study, due to the lack of knowledge on the structure of the pericellular matrix, many *in vitro* studies including ours were not aware of the presence of this surface layer on cultured bone cells. So far only one *in vitro* study has shown the presence of a hyaluronic acid rich layer with undetectable sulfated proteoglycans on osteoblastic and osteocytic cells and it role as mechanotransducer has yet to be clearly defined (Reilly et al., 2003).

Similarly, the presence of surface layer glycocalyx in endothelial cells was first identified in the mid 60s (Luft, 1966). Since then, the endothelial glycocalyx (EG) has been more thoroughly studied than bone pericellular matrix. Numerous researchers have studied its possible roles as a molecular sieve in determining oncotic pressures (Michel, 1997; Weinbaum, 1998), as a barrier and modulator of interactions between blood cells

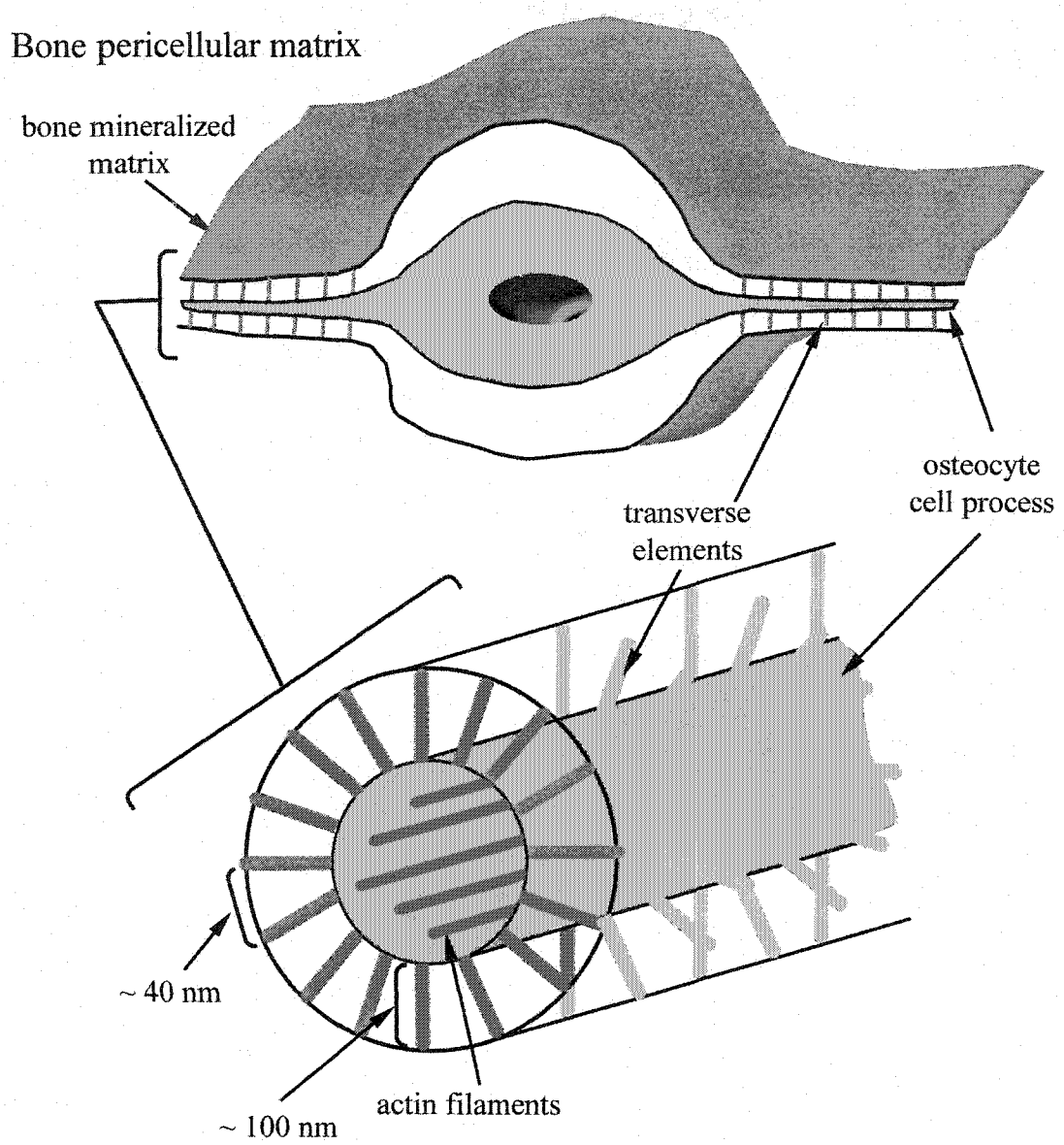

Figure 1.7. The glycocalyx in bone pericellular matrix. It consists of regularly spaced transverse and longitudinal proteoglycans spanning from the cell process of osteocyte to mineralized bone matrix. The dimension of lacunae and canaliculi are not drawn to scale.

and ECs (Adamson, 1990; Desjardins and Duling, 1990; Huxley and Williams, 2000; Mulivor and Lipowsky, 2002), and whereas its role as a mechanotransducer of fluid shear stress has only been studied more recently (Secomb et al., 2001; Damiano and Stace, 2002; Weinbaum et al., 2003). Findings by Adamson and Clough, (1992) suggested that the integrity of this layer depends on the presence of plasma proteins. This layer serves as an exclusion zone for molecules with radii greater than 5.7 nm and hinders the transport of molecules with radii between 0.5 to 4.7 nm (Vink and Duling, 2000). The ultrastructural organization of the EG was largely a mystery until the recent study by Squire et al. (2001) showed that the EG was a quasi-periodic bush-like structure that was anchored to an actin cortical web just beneath the plamalemma as shown in Fig 1.8. Relatively little is known about the specific proteins in the EG. Henry and Duling (1999) showed that hyaluronan and chondroitin sulfate play a significant role in its assembly and that the heparin sulfate family of proteoglycans, specifically the syndecans, participate in signal transduction (Ihrcke et al., 1993; Bass and Humphries, 2002). Heparan sulfate is the most abundant glycosaminoglycan on the endothelial glycocalyx (~ 50-90%) and generally co-exists with chondroitin sulfate in a ratio of 4:1 (Mulivor and Lipowsky, 2004). The recent theoretical model by Weinbaum et al. (2001) predicted that these proteoglycan core proteins serve as stiff bristles with flexural rigidity, EI, on the order of 700 $pN \cdot nm^2$ and thus, they are capable of transmitting fluid drag on their tips as a bending moment that acts on the ACW. Syndecan I is the most abundant EC surface proteoglycan (Mulivor and Lipowsky, 2004) and syndecan IV is involved in mechanotransduction at focal adhesion sites (Bass and Humphries, 2002). Florian et al. (2003) recently verified the presence of heparin sulfate in the glycocalyx of cultured

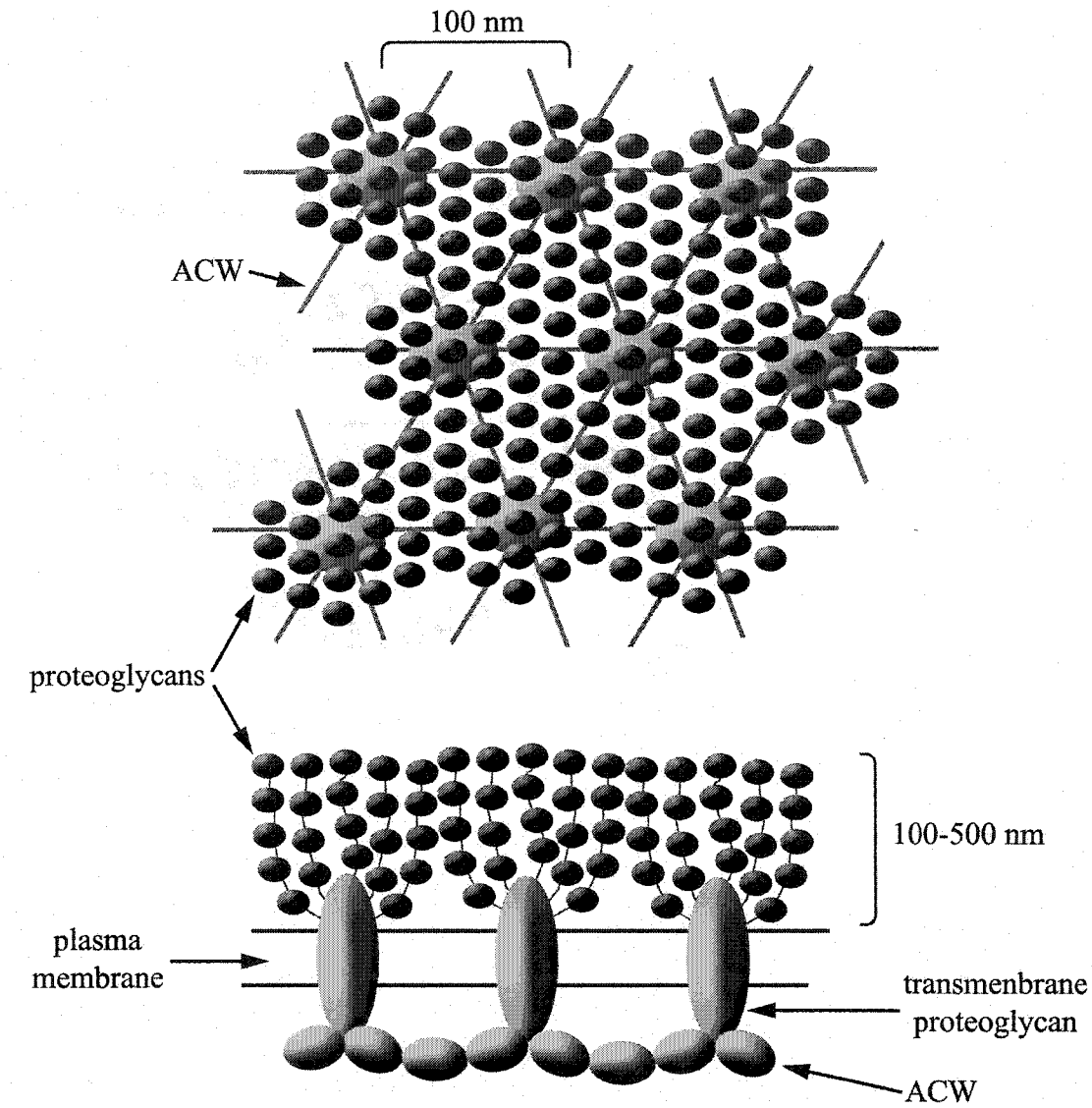

Figure 1.8. Surface layer glycocalyx. The glycocalyx is composed of proteoglycans and is present on the cell surface as a quasi-periodic bush-like structure. The core proteins from the proteoglycan are assumed to link to the ACW beneath the apical surface of the cell (adapted from Squire et al. (2001) model).

monolayers of bovine aortic endothelial cells (BAECs) and demonstrated that its presence was necessary for the release of NO in response to fluid shear. We analyze another important aspects of the EG, its function as a mechanosensor of fluid shear and its transmission to the ACW, in Chapter 3 of this dissertation.

Bone cell mechanotransduction

Attempts to unravel the mystery surrounding bone mechanotransduction have become a major area of research for more than a decade. Depending on the mechanical environment, bone structure and mass can change dramatically. Many bones are exposed to repetitive loads every day. In response to these mechanical loads, the skeleton optimizes its architecture by subtle adaptation. For example, dynamic loading causes new bone formation whereas removal of load bearing or reduced loading causes bone loss (Rubin and Lanyon, 1984; Rubin and Lanyon, 1985; Duncan and Turner, 1995; Fritton et al., 2000). Bone remodeling is a life-long process, which includes replacing aging tissue and repairing injuries. In the 1980's Lanyon hypothesized that under mechanical load bone formation is primarily induced by mechanical stimuli while resorption is mostly controlled by hormonal, biochemical, and genetic factors (Lanyon, 1984). Although it is well established that load-induced mechanical signals play a critical role in maintaining bone mass and structure, the cellular mechanisms by which bone remodels or resorbs its tissue are poorly understood. Among the many proposed mechanical signals, such as deformation (mechanical strain) (Burr et al., 1996; Cowin and Weinbaum, 1998; Fritton

et al., 2000) and microcracks or microdamage (Carter and Hayes, 1977; Burr and Martin, 1993), the one that has received the most attention is that load-induced interstitial fluid shear stress in the lacunar-canalicular porosity resulting from small deformations in the bone matrix (Hillsley and Frangos, 1994; Turner et al., 1994; Weinbaum et al., 1994; Cowin et al., 1995; Duncan and Turner, 1995; Burger and Klein-Nulend, 1999; Burr et al., 2002). In addition, these studies strongly suggest that in the bone cell network, osteocytes act as sensors of the mechanical environment and relay the signals via gap junctions to osteoblasts or bone lining cells to regulate bone homeostasis.

Over the last decade the adaptation responses of the bone cell network in response to fluid shear stress have been studied extensively. In order to better understand the cellular mechanisms of this network, Weinbaum et al. (1994) first proposed a model predicting the magnitude of fluid shear stress, that excites osteocytes, resulting from a physiological loading to be on the order of 8-30 dyn/cm^2. Subsequent models, based on the different aspects of the first model, attempted to determine the anatomical site of strain generated potentials (SGPs), the electrical signal propagation in the bone cell network, and the fluid movement resulting from cyclic loading (Harrigan and Hamilton, 1993; Zeng et al., 1994; Cowin et al., 1995; Zhang et al., 1997; Zhang et al., 1998; Wang et al., 2000). Experimental evidence has also indicated that fluid flow is a more potent stimulator of bone cells, especially osteocytes, than hydrostatic compression and substrate deformation at physiological strain levels (Burger et al., 1995; Klein-Nulend et al., 1995a; Owan et al., 1997; You et al., 2000). Many investigators have performed *in vitro* fluid shear stress studies on osteoblastic and osteocytic cell lines in the range of 5 to 60 dyne/cm^2 in flow chambers. These investigators showed that, similar to endothelial

cells, both steady and pulsatile fluid flow cause rapid and continuous release of NO, prostaglandins (PGI_2 and PGE_2), early response gene expression (c-fos), second messenger production, cytoskeletal adaptation, and Ca^{++} responses in bone cells (Reich et al., 1990; Reich and Frangos, 1991; Hung et al., 1995; Klein-Nulend et al., 1995b; Hung et al., 1996; Johnson et al., 1996; Klein-Nulend et al., 1996; Hillsley and Frangos, 1997; Klein-Nulend et al., 1998; Pavalko et al., 1998; Chen et al., 2000; Cheng et al., 2001a; Donahue et al., 2003; Norvell et al., 2004; Ponik and Pavalko, 2004). Recently, several investigators have experimentally explored the fluid shear stress regulation of gap junctional communication in bone cells. While others focused their attentions mainly on the gap junctional communication and its regulation on PGE_2 and Ca^{++} release (Saunders et al., 2001; Cheng et al., 2001b; Alford et al., 2003; Saunders et al., 2003), we are the first to explore the effects of fluid shear stress on junctional complexes (Cx43 and ZO-1) as shown in Chapter 2 of this dissertation (Thi et al., 2003).

Although countless attempts were made to resolve the mystery behind bone cell mechanotransduction, no one was able to clarify the fundamental question of how cells are sensing the signals from the mechanical environment. Recent theoretical models and morphological data compellingly suggest that tissue level strains (~ 0.2%) resulting from mechanical loading can be amplified 20- to 100-fold at the cellular level by the fluid flow-induced drag forces on the transverse elements of the pericellular matrix (Weinbaum et al., 2001; You et al., 2001; You et al., 2004). All of the *in vitro* flow studies in bone neglect the existence of the pericellular matrix that surrounds the bone cells *in vivo*. As a result, the importance of this layer is routinely ignored. The role of this pericellular layer will be further discussed in Chapter 4.

Endothelial cell mechanotransduction

Mechanotransduction due to fluid shear on endothelial cells has been extensively studied for almost 30 years in contrast to the bone cell network. It is well accepted that hemodynamic shearing forces acting on the endothelium play a central role in the regulation of vessel wall remodeling, transient and sustained cellular signaling, frequent restructuring, mass transport and atherogenesis (Davies, 1995; Davies et al., 1997; Takahashi et al., 1997; Ogunrinade et al., 2002; Tarbell, 2003). The endothelium is strategically located between the vessel wall and various patterns of flowing blood (pulsatile, laminar, turbulent flows) regulate homeostasis of the vessel wall. However, the mechanism as to how ECs sense and communicate the changes in hemodynamic forces to neighboring cells and underlying smooth muscle cells is still not well understood. Numerous candidates, such as cell surface plasma membrane proteins, mechanosensitive ion channels, stress-activated channels, integrins, and focal adhesions have been proposed as mechanosensors of the fluid shearing forces to the actin cortical cytoskeleton (see Davies (1995)).

While many investigators have attempted to elucidate endothelial mechanotransduction the actual mechanics of the process is not know. Evidence accumulated over the past several decades suggests that fluid shear stress regulates EC functions. Similar to bone cells, past *in situ* and *in vitro* flow studies routinely observed morphological changes, adaptation of the cytoskeleton, focal adhesions and junctional proteins, release of prostaglandins (PGE_2), acute and sustained released of NO, changes in gene expression such as c-fos, COX2, protein kinase C, focal adhesion kinase (FAK)

and formation of caveolae (Dewey, Jr. et al., 1981; Pohl et al., 1991; Burridge et al., 1992; Ookawa et al., 1993; Kuchan and Frangos, 1994; Berk et al., 1995; Girard and Nerem, 1995; Frangos et al., 1996; Davies, 1997; Hu and Chien, 1997; Cowan et al., 1998; Barakat and Davies, 1998; Fleming et al., 1998; Galbraith et al., 1998; Depaola et al., 1999; Noria et al., 1999; Bao et al., 2000; Helmke et al., 2000; Park et al., 2000; Seebach et al., 2000; DeMaio et al., 2001; Sawyer et al., 2001; Schnittler et al., 2001; Sun et al., 2003; Boo and Jo, 2003). Although several investigators have proposed that endothelial glycocalyx (EG) plays a possible role as mechanosensor, this role has not quite proven due in part to the lack of knowledge on its structure and composition.

Based on recent proposed structural model (Squire et al., 2001), a new theoretical model has predicted a primary mechanotransduction pathway through the EG to underlying actin cytoskeleton (Weinbaum et al., 2003). In addition, Florian et al. (2003) ultimately verified the existence of EG as well as its role as a mechanotransducer in an in vitro flow study. Thus, we further explored this significant role of the EG in response to fluid shear stress with regard to cell cytoskeleton, junctional complexes, and focal adhesion in Chapter 3 of this dissertation. Consequently, we propose a new conceptual model for the cytoskeletal organization of ECs with a major dichotomy in structure and function at its basal and apical aspects.

Organization of the dissertation

This dissertation is organized into four chapters. The present chapter provides a

background and introduction to the entire dissertation. The last chapter summarizes the important contributions of the dissertation with the new insights and proposes future research directions. The other two chapters deal with the search for possible candidates for the mechanosensor, and address several vital links hat have been overlooked by previous cell-cell mechanotransduction studies and propose and verify the role of a key mechanosensor.

Chapter 2, entitled "Flow-induced Fluid Shear Stress Remodels Expression and Function of Junctional Proteins in Cultured Bone Cells" was published in the *American Journal of Physiology Cell Physiology* 284(2003):C389-C403. We proposed and tested the hypothesis that fluid shear stress modifies the expression, function and distribution of junctional proteins in two types of cultured bone cells. Our findings of impaired cell-cell communication as well as rearranged and newly synthesized junctional proteins suggest that such disconnection from the bone cell network due to the fluid shear stress may provide part of the signal whereby the disconnected cells or the remaining network initiate focal bone remodeling.

Chapter 3, entitled "The Role of the Glycocalyx in the Reorganization of the Actin Cytoskeleton under Fluid Shear Stress: A 'Bumper Car' Model" will be submitted to the *Proceedings of the National Academy of Science.* We present results from experiments that compared for the first time the role of fluid shear stress on the structural organization of the endothelial cytoskeleton in the presence or absence of an EG. We propose a new conceptual model for the cytoskeletal organization of endothelial cells with a major dichotomy in structure and function at its basal and apical aspects. Intracellular distributions of F-actin, vinculin, paxillin, ZO-1 and Cx43 were analyzed in

the presence and absence of endothelial glycocalyx. Our results are explained in terms of a 'bumper car' model in which the actin cortical web and dense peripheral actin band are only loosely connected to basal attachment sites allowing for two distinct cellular signaling pathways in response to fluid shear stress, one transmitted by glycocalyx core proteins involving the release of NO by caveolae, and the other emanating from focal adhesions and stress fibers at the basal and apical membranes of the cell involving the release of PGI_2.

Chapter 2

Flow-induced fluid shear stress remodels expression and function of junctional proteins in cultured bone cells *

* Reprinted from *American Journal of Physiology Cell Physiology,* Vol 184, Thi et al., pp. C389-C403, Copyright (2003), with permission from the American Physiological Society.

Abstract

We have tested the hypothesis that fluid shear stress modifies expression, function and distribution of junctional proteins (Cx43, Cx45, and ZO-1) in cultured bone cells. Cell lines with osteoblastic (MC3T3-E1) and osteocytic (MLO-Y4) phenotypes were exposed to shear stress of 5 or 20 dyn/cm^2 for 1-3 h. Immunostaining indicated that at 5 dyn/cm^2 distribution of Cx43, Cx45 and ZO-1 were moderately disrupted at cell membranes; at 20 dyn/cm^2, disruption was more severe. Intercellular coupling was significantly decreased at both shear stress levels. Western blots showed the down-regulation of membrane bound Cx43 and ZO-1 and up-regulation of cytosolic Cx43 and Cx45 at different levels of shear stress. Similarly, northern blots revealed that expressions of Cx43, Cx45, and ZO-1 were selectively up- and down-regulated in response to different shear stress levels. These results indicate that in cultured bone cells fluid shear stress disrupts junctional communication, rearranges junctional proteins and determines *de novo* synthesis of specific connexins to an extent that depends on the magnitude of the shear stress. Such disconnection from the bone cell network may provide part of the signal whereby the disconnected cells or the remaining network initiate focal bone remodeling.

Abbreviations

Cx43, connexin43; Cx45, connexin45; dyn/cm^2, unit of shear stress; τ, shear stress, ZO-1, zonula occludens-1.

Introduction

Bone dramatically changes its structure and mass in response to static and dynamic loads. It has been well established that bending loads in bone cause small deformations in the bone matrix, which in turn generate fluid pressure differences that lead to fluid flow from the compression to the tension side. The resulting fluid shear stress (τ) is proposed to be one of the factors transducing mechanical loading to the bone cell network senses mechanical loading (Turner et al., 1994; Weinbaum et al., 1994; Zeng et al., 1994; Cowin et al., 1995). At physiological whole tissue strain levels (<0.2%), culture studies have demonstrated that fluid flow is a more potent stimulator of bone cells than is substrate deformation itself (Owan et al., 1997; You et al., 2000). Previous experimental studies have been shown that bone cells release signaling molecules such as prostaglandins, nitric oxide (NO), Ca^{++}, and other second messengers in response to the fluid shear stress (Reich et al., 1990; Hillsley and Frangos, 1994; Klein-Nulend et al., 1995b; Hung et al., 1996; Cheng et al., 2001a).

One mechanism of bone remodeling by which second messenger signals spread throughout the bone cell network involves gap junction channels that connect osteoblasts and bone-lining cells along the surface of Haversian and Volkmann canals and osteocytes that are embedded within the bone matrix (Jeansonne et al., 1979; Doty, 1981; Zhang et al., 1997). The connexin proteins that form gap junctions are encoded by a gene family with as many as 21 members in mammals (Willecke et al., 2002). Connexins are expressed with an overlapping pattern of tissue specificity; Cx43 and Cx45 are the gap junction proteins that have been associated with bone cells (Civitelli et al., 1993; Minkoff

et al., 1994; Steinberg et al., 1994; Yamaguchi et al., 1994; Minkoff et al., 1999).

Gap junction channels, including those formed by Cx43 and Cx45, are permeable to ions and molecules with M_r lower than approximately 1kD (kilodalton), including second messenger molecules (Spray, 1996). Gap junctional communication of such signals between bone cells gives rise to modulation of hormonal responses in the osteoblastic network (Vander Molen et al., 1996), regulation of gene expression (Lecanda et al., 1998) and propagation of intracellular signals (Donahue, 2000). Moreover, connexin expression and function are essential for normal osteogenesis and bone mineralization (Minkoff et al., 1994; Li et al., 1999; Lecanda et al., 2000).

Connexins may also play roles in addition to the formation of pathways for intercellular communication. Recent studies have shown that connexins directly interact with both adherens and tight junction associated proteins, including zona occludens-1 (ZO-1), claudins, and β-catenin (Giepmans and Moolenaar, 1998; Toyofuku et al., 1998; Kojima et al., 1999; Ai et al., 2000; Nusrat et al., 2000). Accordingly it has been proposed that connexins are part of a multi-molecular signaling complex, the "Nexus" (Spray et al., 1999). From the standpoint of the studies described here, ZO-1 has been shown to interact with gap junction proteins Cx43 and Cx45 in osteoblastic cells (Laing et al., 2001), where ZO-1 binding to connexins may play a role in the organization, trafficking and/or stabilization of gap junction proteins (Laing et al., 2001; Toyofuku et al., 2001).

Regulation of gap junctional communication in response to load-induced biophysical signals has been examined in both vascular endothelial cells (Cowan et al., 1998; Depaola et al., 1999) and in bone cells (Zhang et al., 1997; Ziambaras et al., 1998;

Donahue et al., 2000; Cheng et al., 2001b). Although such studies have generally reported an increase in Cx43 expression, changes in functional coupling in the bone cell network have not been so consistently demonstrated.

In this study, we have tested the hypothesis that fluid shear stress of the magnitude expected to occur in bone tissue modifies expression, distribution, and function of connexins (Cx43 and Cx45) and an associated protein (ZO-1). Well-characterized cell lines, MC3T3-E1 osteoblastic cells and MLO-Y4 osteocytic cells, were used in our experiments. Our results demonstrate that in both osteoblastic and osteocytic cell lines fluid shear stress disrupts cell-cell junctional communication, rearranges gap junction proteins and determines *de novo* synthesis of specific connexins to an extent that depends on the magnitude of shear stress. Such disconnection from the bone cell network due to the fluid shear stress may provide part of the signal whereby the disconnected cells or the remaining network initiate focal bone remodeling.

Materials and Methods

Cell Culture

Osteoblast-like MC3T3-E1 cells (obtained from Dr. Kenneth J. McLeod, SUNY, Stony Brook) were cultured in Eagles's minimal essential medium (α-MEM, Gibco BRL, Grand Island, NY) containing 1% penicillin-streptomycin (Gibco BRL) and 5% fetal bovine serum (FBS) (Gemini Bio-Product, Woodland, CA) and osteocyte-like MLO-Y4 cells (obtained from Dr. Lynda F. Bonewald, University of Texas Health Science Center)

were cultured in α-MEM containing 1% penicillin-streptomycin, 10% FBS and 2.5% calf serum (Gibco BRL) at 37°C with 95% O_2/ 5% CO_2. For each cell type, confluent monolayers of cells were grown on glass slides in static condition and transferred to the flow apparatus to expose the monolayers to a fluid shear stress of 5 or 20 dyn/cm^2 for 1, 2, or 3 h. These durations were chosen based on the turnover rate of Cx43 and Cx45, which exhibit half-lives of 1.5 and 3 h, respectively (Darrow et al., 1995).

Flow Chamber and Experiment

The fluid flow setup consisted of a parallel plate flow chamber (Cytodyne, La Jolla, CA) and a re-circulating flow circuit. This circuit included a variable speed peristaltic pump (Taitec, Japan), pulse dampener (Cole-Palmer Instrument Company, Vernon Hills, IL) and a reservoir with culture medium (α-MEM with 1% FBS) maintained at 37°C with 95% O_2/ 5% CO_2. This system produces laminar flow over a cell monolayer. A flow rate was chosen to yield a shear stress (τ) of 5 dyn/cm^2 or 20 dyn/cm^2 using the equation $\tau = 6Q\mu/bh^2$, where Q is the flow rate, μ is medium viscosity, b is channel width, and h is channel height. Control cells were kept under static conditions with the same culture medium at 37°C.

Alkaline Phosphatase Staining

To determine whether cells retained their differentiated phenotypes, both cell lines were routinely checked for alkaline phosphatase activity. Cells were fixed with 4% formaldehyde and permeabilized with 70% ethyl alcohol (ETOH). Cells were then rinsed with 0.2M Tris[hydroxymethyl]-aminomethane (Sigma, St. Louis, MO) and incubated in

naphthol AS-BI phosphate (Sigma) + fast red violet LB salt (Sigma) + Tris-HCl for 30 min (Burstone, 1961). After several washes with distilled water, cells were counterstained with Mayer's hematoxylin (Sigma) for 2 min. The cells were then washed with distilled water and mounted for analysis.

Cells Viability Studies

Cells from both control and shear stress exposed samples were analyzed for their health and viability using the LIVE/DEAD Viability/Cytotoxity Kit (Molecular Probes, Eugene, OR). Cells were rinsed a few times with 1X PBS and incubated with 4μM of Eithidium homodimer-1 (EthD-1) and 2μM of Calcein AM in 1XPBS for 30 min as recommended by the manufacturer. Live cells, which retained the polyanionic dye calcein, gave rise to green fluorescence and dead cells, which took up EthD-1 through membrane damage, produced red fluorescence. Live and dead cells were counted from 10 cell fields for all the samples, and percentages of live and dead cells were calculated.

Immunofluorescence Studies

Both control and shear stress exposed cells were fixed with 2% formaldehyde, permeabilized with 0.4% Triton-X100 (Sigma) and blocked with 10% goat serum (GibcoBRL) in 1X PBS. The cells were then incubated with primary polyclonal antibodies against Cx43, Cx45 (courtesy of Dr. E. Hertzberg, AECOM, and Dr. T. Steinberg, Washington University School of Medicine), ZO-1 (Zymed, South San Francisco, CA) and secondary antibody conjugated to Alexa 488 (Molecular Probes). For F-actin staining, cells were incubated with rhodamine-labeled phalloidin (Sigma)

immediately after fixation. The coverslips were mounted on slides, examined on a Nikon Eclipse TE300 microscope and photographed using a SPOT-RT digital camera (Diagnostic Instruments, Inc., Sterling Heights, MI).

Western Blot Analysis

Controls and shear stress exposed (1 and 3 h) samples were lysed in 80μl of lysis buffer (10mM Tris-HCl pH 7.5, and 2mM PMSF), sonicated, and centrifuged (14,000 rpm, 30min) as described in Guan et al., (Guan et al., 1996). Pellets and supernatants from the samples were collected for crude membrane and cytosolic protein analyses. Samples were loaded onto 10% SDS-PAGE gels (BIO-RAD Laboratories, Hercules, CA) for separation and electrophoretically transferred to nitrocellulose membranes (Schleicher & Schuell Inc., Keene, NH). The membranes were probed with primary polyclonal and monoclonal antibodies to Cx43, Cx45 and ZO-1 (described above), polyclonal β-actin (Sigma) and monoclonal GAPDH (Research Diagnostics Inc., Flanders, NJ), followed by secondary antibodies incubation with horseradish peroxidase (HP)-conjugated anti-rabbit IgG and anti-mouse IgG (Santa Cruz Biotechnology, Santa Cruz, CA). The protein bands were detected using the Amersham ECL detection kit (Amersham Biosciences, Piscataway, NJ) and exposed on Fuji X-ray film. The intensity of the bands was analyzed using Scion NIH Image software (Scion Corporation, Frederick, MD). Measured intensities for all experiments were first normalized with respect to their internal controls, GAPDH for cytosolic proteins and β-actin for membrane bound proteins, and then with respect to controls.

Northern Blot Analysis

Total RNA from the samples was extracted using TRIzol reagent (Gibco BRL) and quantified as previously described (Urban et al., 1999). 10 μg of total RNA from the samples were separated on 1.2% formaldehyde-agarose gel and transferred onto the Gene Screen hybridization transfer membrane (NEN Life Science Products, Inc., Boston, MA). Membranes were hybridized with appropriate denatured random-primed probes. The rat cDNA probes used were full length Cx43 and Cx45 (obtained from Dr. Eric Beyer, University of Chicago Medical School) and 18S labeled with [^{32}P]dCTP using the Megaprime labeling system (Amersham Biosciences). The membranes were then exposed to phosphor screen overnight, scanned on a Storm PhosphorImager system and quantified using ImageQuaNT (Molecular Dynamics, Sunnyvale, CA). All acquired data were first normalized with respect to 18S RNA band intensity and then all experimental data were normalized with respect to control data.

Reverse Transcription Polymerase Chain Reaction (RT-PCR) and semi-quantitative RT-PCR Analysis

RT-PCR was performed as previously described (Urban et al., 1999). For semi-quantitative PCR, a 9:1 ratio of competimers / 18S primers (Ambion, Austin, TX) was added to the PCR mixture. Conditions applied for PCR using a PTC-100 Programmable Thermal Controller (M.J. Research, Inc., Watertown, MA) were: 94°C for 30 s, 55°C for 30 s, 72°C for 30 s for 30 cycles and 72°C for 8 min. Reaction products were analyzed by electrophoresis on 2% agarose gels and quantified using Kodak 1D Scientific Imaging Systems. The following primers were used for each cDNA amplification: mCx43: sense

TACCACGCCACCACTGGC, antisense AATCTCCAGGTCATCAGG; mCx45: sense AAAGAGGAGAGCCAACCAAA, antisense GTCCCAAACCCTAAGTGAAGC (Dermietzel et al., 2000); mZO-1: sense CATAGAATAGACTCCCCTGG, antisense GC TTGAGACCTCATACCTGT (Itoh et al., 1993), mOsteocalcin: sense GACAAAGCCTT CATGTCCAAGC, antisense TTTGAG ACCGTCGAGCCGAAA (Kato et al., 1997).

Scrape loading

Quantitative scrape loading as described in De Pina-Benabou et al., (Pina-Benabou et al., 2001) was used to analyze the gap junctional communication after cells were exposed to shear stress. Incisions on the cell monolayers of control and shear stress exposed samples were made with a fine razor blade in two or three different regions on the slides. The slides were incubated with 0.5% Lucifer Yellow (Sigma) at 37°C, rinsed with 1× PBS, and fixed with 2% formaldehyde. The intensity of the dye spread from the damaged cells to their neighboring cells was observed using a Nikon Eclipse TE300 microscope and photographed with a SPOT-RT digital camera (Diagnostic Instruments, Inc., Sterling Heights, MI). Extent of dye spread was quantified as linear distance perpendicular to the scrape using Scion NIH Image software.

Statistical Analysis

Data were analyzed using one-way ANOVA (SigmaStat, Chicago, IL). Northern blot analyses are presented as the mean ± SEM of 6 experiments. Western blot, quantitative RT-PCR, and scrape loading analyses are presented as the mean ± SEM of 3 experiments. Asterisks indicate a significant difference compared to controls ($*p < 0.05$).

Results

Osteoblast and osteocyte cell lines express gap junction proteins associated with osteogenesis and the tight junction associated protein ZO-1.

We have used the osteoblastic cell line MC3T3-E1 (Yamaguchi et al., 1994) and the osteocytic cell line MLO-Y4 (Kato et al., 1997) in order to compare expression, distribution and function of gap junctions associated with osteogenesis (Minkoff et al., 1994). As shown in Fig. 2.1A in which cell cytoskeleton was stained with phalloidin, these cell lines show quite different morphologies. Whereas the osteoblast cells exhibit flattened, epitheliod shapes and a close packing arrangement, the osteocyte cells exhibit a more stellate shape, with rounded somata and multiple processes extending for variable distance to neighboring cells. Because phenotypic expression of differentiated cell markers may vary in cell lines maintained under different conditions and after prolonged passage, we determined expression levels of alkaline phosphatase and osteocalcin in the MC3T3-E1 and MLO-Y4 cell lines under conditions used in our studies. Alkaline phosphatase activity was higher in the osteoblasts than in the osteocytes (Fig. 2.1B), whereas the osteocytic cell line, but not the osteoblastic cell line, expressed measurable osteocalcin mRNA (Fig. 2.1C). RT-PCR results showed that under normal conditions both types of immortalized cell lines expressed mRNAs encoding Cx43, Cx45 and ZO-1 (Fig. 2.1C). These data indicate that mRNAs corresponding to the osteogenic gap junction proteins and to the tight junction protein ZO-1 are expressed in both cell lines. Additional methods presented below were used to determine changes in abundance and distribution of these junctional proteins and their mRNAs.

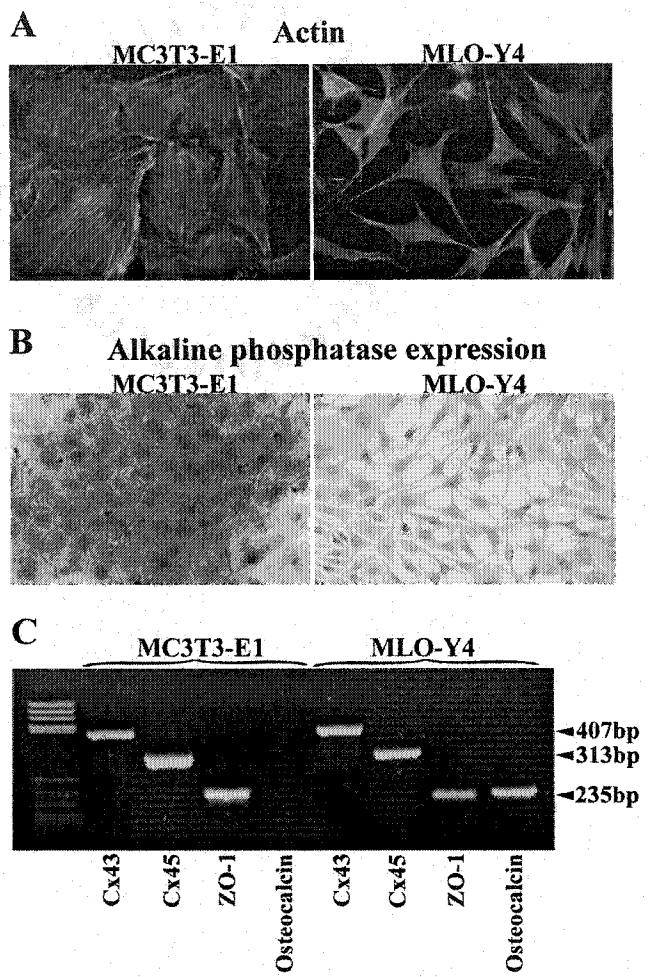

Figure 2.1. **Morphologies, osteoblastic and osteocytic phenotypes, and expression of junctional mRNAs in MC3T3-E1 and MLO-Y4 cell lines.** Phalloidin staining for F-actin (A) indicated that the cell types possessed quite different morphologies. The osteoblastic cell line (MC3T3-E1) expressed more alkaline phosphatase (B), whereas the osteocytic cell line (MLO-Y4) expressed more osteocalcin (C), as described previously (Kato et al., 1997). (C) RT-PCR results showed that under normal conditions both of these cell lines expressed mRNAs corresponding to osteogenic gap junction proteins Cx43 and Cx45 and the tight junction associated protein, ZO-1.

Fluid shear stress does not affect cell viability but disrupts cell-cell communication and rearranges gap junction proteins Cx43 and Cx45 and the associated ZO-1 protein in cultured bone cells

The overall experimental design critically depends on maintenance of cell viability during the periods of shear stress exposure. In order to determine the extent to which cells were injured by the procedure, we performed the LIVE/DEAD assay on both cell types with no shear stress and with 5 and 20 dyn/cm^2 for 3 h. Both MC3T3-E1 and MLO-Y4 cells were viable after 3 h exposure to fluid shear stress. As shown, applying this assay to osteoblastic (Fig. 2.2A) and osteocytic (Fig. 2.2B) cells revealed that the percentage of live cells in normal and shear stress exposed cells were all above 80%. ANOVA analysis revealed that the percentage of dead cells was lower than of live cells for controls and each treatment, but percentage of dead cells did not significantly differ among the groups.

Immunofluorescence microscopy was used to analyze the effect of fluid shear stress on the distribution and arrangement of Cx43, Cx45 and ZO-1 at cell borders as well as in perinuclear areas in cultured osteoblast and osteocyte cell lines. Under control (no flow) conditions, MC3T3-E1 cells possessed extensive contact with neighboring cells. Immunostaining of control MC3T3-E1 cells revealed abundant punctate and linear appositional staining of Cx43 and ZO-1 at cell borders as well as Cx43 immunoreactivity in perinuclear regions; both Cx43 and ZO-1 also showed diffuse cytoplasmic staining throughout the osteoblastic cells (Fig. 2.3A). Overlays of images acquired from cells double labeled for Cx43 and ZO-1 (Fig. 2.4A) indicated that overlap was virtually complete at membrane appositions, although more Cx43 was detected intracellularly.

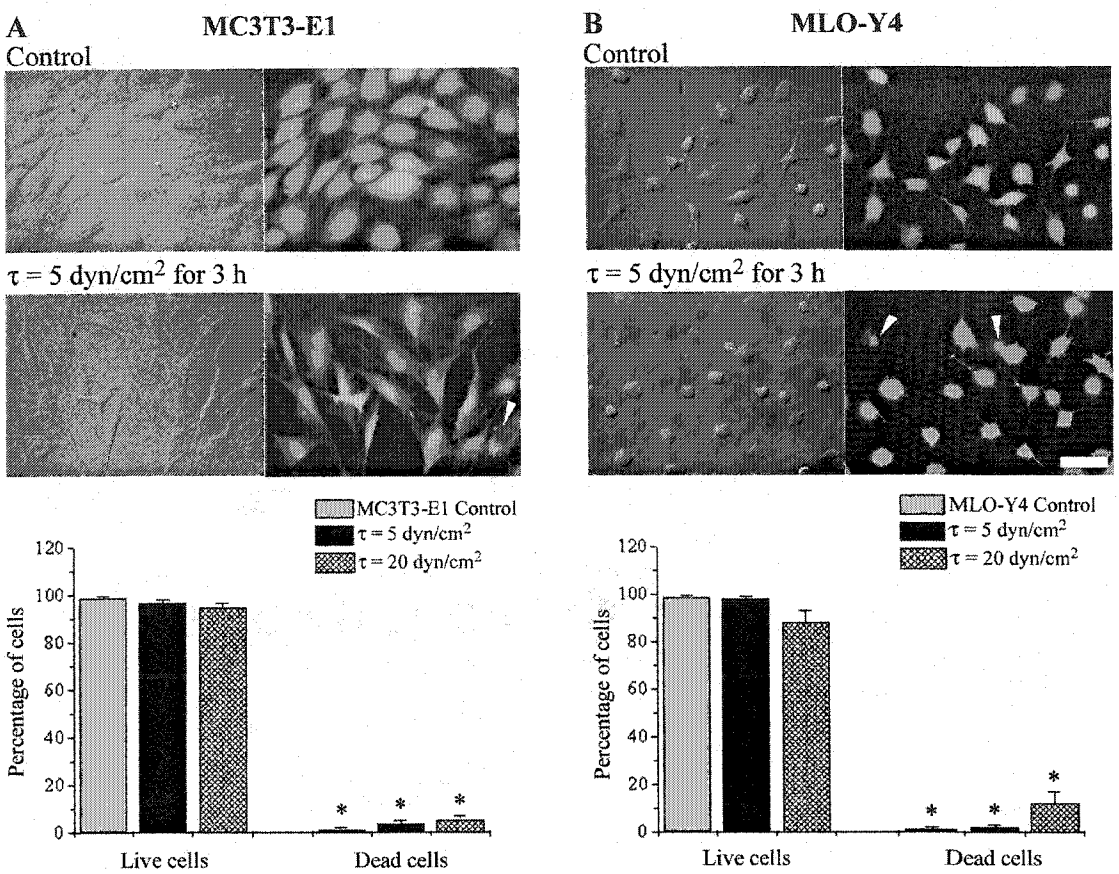

Figure 2.2. **Assessment of MC3T3-E1 and MLO-Y4 cells health and viability.** Cells were subjected to low and high shear stresses (5 dyn/cm^2 and 20 dyn/cm^2) for 3 h; control cells were maintained for the same periods of time under no flow conditions. In order to assess cell health and viability, cells were incubated with 4μM of Eithidium homodimer-1 (EthD-1) and 2μM of Calcein AM. Live cells, which retain calcein, gave rise to green fluorescence and dead cells, which retain EthD-1 through damaged membranes, produced red fluorescence (arrowheads). MC3T3-E1 (A) and MLO-Y4 (B) cell viability as well as morphological changes were observed after exposure to fluid shear stress. Live and dead cells were counted from 10 cell fields for all the samples and percentages of live and dead cells were calculated. All data are presented as mean ± SEM, n = 10 (*, $p < 0.05$).

Wispy Cx45 immunostaining was also present at appositional regions, although it was mainly concentrated at perinuclear regions within the cells (Fig. 2.3A).

Exposure of MC3T3-E1 osteoblast cells to both levels of shear stress resulted in changes in cell morphology (Fig 2.3B, C) and in re-distribution of connexins and ZO-1 within the cells. Even as early as 1 h after exposure to 5 dyn/cm^2, cells began to elongate with respect to flow direction and lost the majority of direct cell body contact with neighboring cells; such anisotropy was even more apparent after longer duration exposure to higher shear stress. Shear stress (τ) rapidly affected Cx43 distribution in osteoblastic cells when MC3T3-E1 cells were exposed to τ = 5 dyn/cm^2. The distribution of Cx43 was moderately disrupted at cell membranes with increased perinuclear and cytoplasmic staining being detectable as early as 1 h of exposure time (data not shown). Increased perinuclear and cytoplasmic staining for Cx43, with concomitant further reduction in appositional staining, was even more apparent at 3 h of 5 dyn/cm^2 (Fig. 2.3B). Although ZO-1 distribution was also altered by flow, it was altered differently from Cx43. At 1 h of low shear stress ZO-1 distribution was largely appositional (data not shown), similar to the controls, whereas disruption was observed only at 3 h (Fig. 2.3B). In contrast to Cx43, diffuse cytoplasmic ZO-1 staining was only occasionally detectable. Exposure to τ = 20 dyn/cm^2 for both 1 and 3 h produced more pronounced disruption of both Cx43 and ZO-1 at the cell membrane and moderate increase of Cx43 perinuclear and cytoplasmic staining (Fig. 2.3C). Overlay images of Cx43 and ZO-1 from shear stress exposed samples clearly showed a dramatic reduction in overlap of these proteins at the contact cell borders (Fig 2.4A). With regard to Cx45, low shear stress (especially at 3 h) led to reduced appositional and increased cytoplasmic staining; this

change in Cx45 distribution was more prominent at 20 dyn/cm^2 (Fig. 2.3C).

Control MLO-Y4 osteocyte cells possessed rounded cell bodies with numerous cell processes and were connected to neighboring cells via these processes. Immunostaining of these control cells revealed that Cx43 and ZO-1 were concentrated at the tips of the cell processes at regions of contact with neighboring cells, with Cx43 also showing perinuclear distribution (Fig. 2.3D). Similar to MC3T3-E1 cells, colocalization of Cx43 and ZO-1 in control MLO-Y4 cells indicated that overlap was found at the tips of opposing cell processes (Fig. 2.4B). For Cx45, there was very faint staining at the tips of some opposing processes of the control cells (Fig. 2.3D). Dramatic morphological changes were observed at both low and high levels of shear stresses. The cell processes became smaller in diameter and somewhat more numerous while the cell bodies became smaller and more rounded. When MLO-Y4 cells were subjected to $\tau = 5$ dyn/cm^2 for 1 or 3 h, Cx43 and ZO-1 at the tips of opposing cell processes were moderately decreased while perinuclear distribution of Cx43 notably increased (Fig. 2.3E). At $\tau = 20$ dyn/cm^2 significant disruption of both Cx43 and ZO-1 at the opposing membrane tips was observed for both exposure durations (Fig. 2.3F, illustrating results for 3 h) with a slight increase in cytoplasmic and perinuclear staining of Cx43. Colocalization of Cx43 and ZO-1 was also reduced at the opposing tips of the cell processes after exposing to both fluid shear stress levels of 5 and 20 dyn/cm^2 (Fig 2.4B). Immunofluorescence for Cx45 indicated that perinuclear distribution became more prominent as shear stress increased (Fig. 2.3E, F). These results suggest that both levels of fluid shear stress reorganize the distribution of junctional proteins as early as 1 h of exposure time, which would be expected to produce an effect on junctional communication.

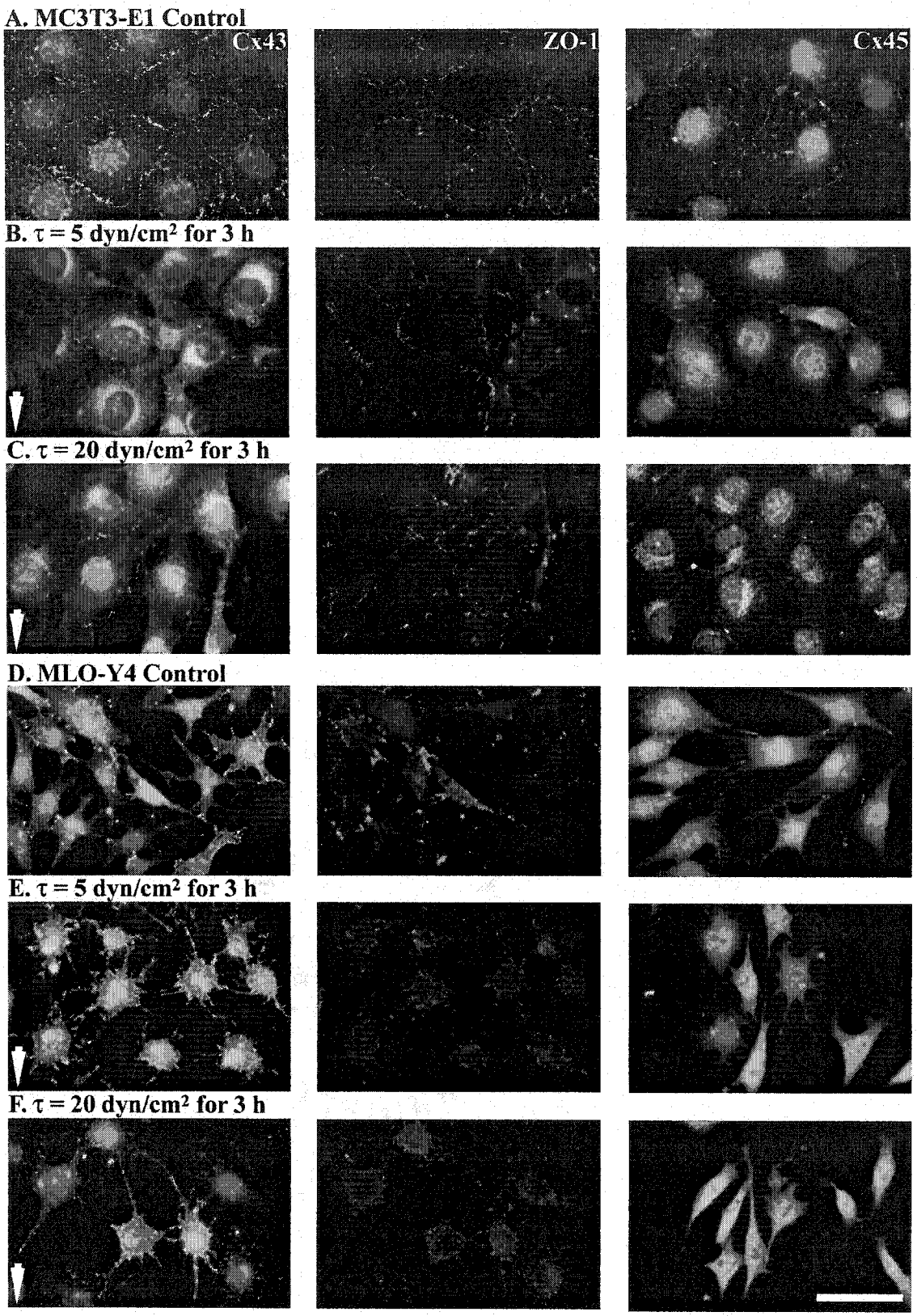

Figure 2.3. **Fluid shear stress disrupts cell-cell communication and rearranges gap**

junction proteins Cx43 and Cx45 and the tight junction associated protein ZO-1 in MC3T3-E1 and MLO-Y4 cells. Cells were subjected to low shear stress (5 dyn/cm^2) and high shear stress (20 dyn/cm^2) for 1 or 3 h; control cells were maintained for the same periods of time under no flow conditions. The effect of fluid shear stress on the distribution and arrangement of Cx43, Cx45 and ZO-1 in MC3T3-E1 and MLO-Y4 were analyzed using immunofluorescence microscopy. Formaldehyde fixed, triton X-100 permeabilized samples of control (A, D), τ = 5 dyn/cm^2 exposure for 3 h (B, E), or τ = 20 dyn/cm^2 exposure for 3 h (C, F) cells were stained with primary polyclonal or monoclonal antibodies against Cx43, ZO-1 and Cx45 followed by fluorescein-conjugated goat anti-rabbit IgG or goat anti-mouse IgG. A. Control MC3T3-E1 cells possessed abundant punctate and linear appositional staining of Cx43 and ZO-1 at cell borders as well as Cx43 immunoreactivity in perinuclear regions. Cx45 was present at appositional regions but was mainly concentrated at perinuclear regions of the cells. (B) Exposure to low shear stress of 5 dyn/cm^2 caused cells to become elongated and moderately decreased Cx43 and ZO-1 at the appositional membranes while perinuclear distribution of Cx43 notably increased. (C) Low shear stress led to reduced appositional and increased cytoplasmic staining of Cx45; at shear stress of 20 dyn/cm^2 significant disruptions of both Cx43 and ZO-1 at the opposing cell membranes were observed as exposure time increased from 1 to 3h. Cx45 distribution in perinuclear regions was more prominent at 20 dyn/cm^2. (D) In control MLO-Y4 cells, Cx43 and ZO-1 were concentrated at the tips of the cell processes at regions of contact with neighboring cells, with perinuclear distribution of Cx43. There was very faint staining for Cx45 at the tips of opposing cell processes of the control cells. Dramatic morphological changes were observed at both

low and high levels of shear stress. (E) When cells were exposed to low shear stress of 5 dyn/cm^2, Cx43 and ZO-1 at the tips of the opposing cell processes were moderately decreased while perinuclear distribution of Cx43 increased; perinuclear distribution of Cx45 moderately increased when exposed to low shear stress of 5 dyn/cm^2. (F) At shear stress of 20 dyn/cm^2 significant disruption of both Cx43 and ZO-1 at the opposing cell membranes was observed for all exposure durations, with the slight increase in cytoplasmic and perinuclear staining of Cx43; high shear stress significantly increased perinuclear distribution of Cx45 as exposure time increased from 1 to 3 h. Arrows indicate flow direction; Bar, 50μm.

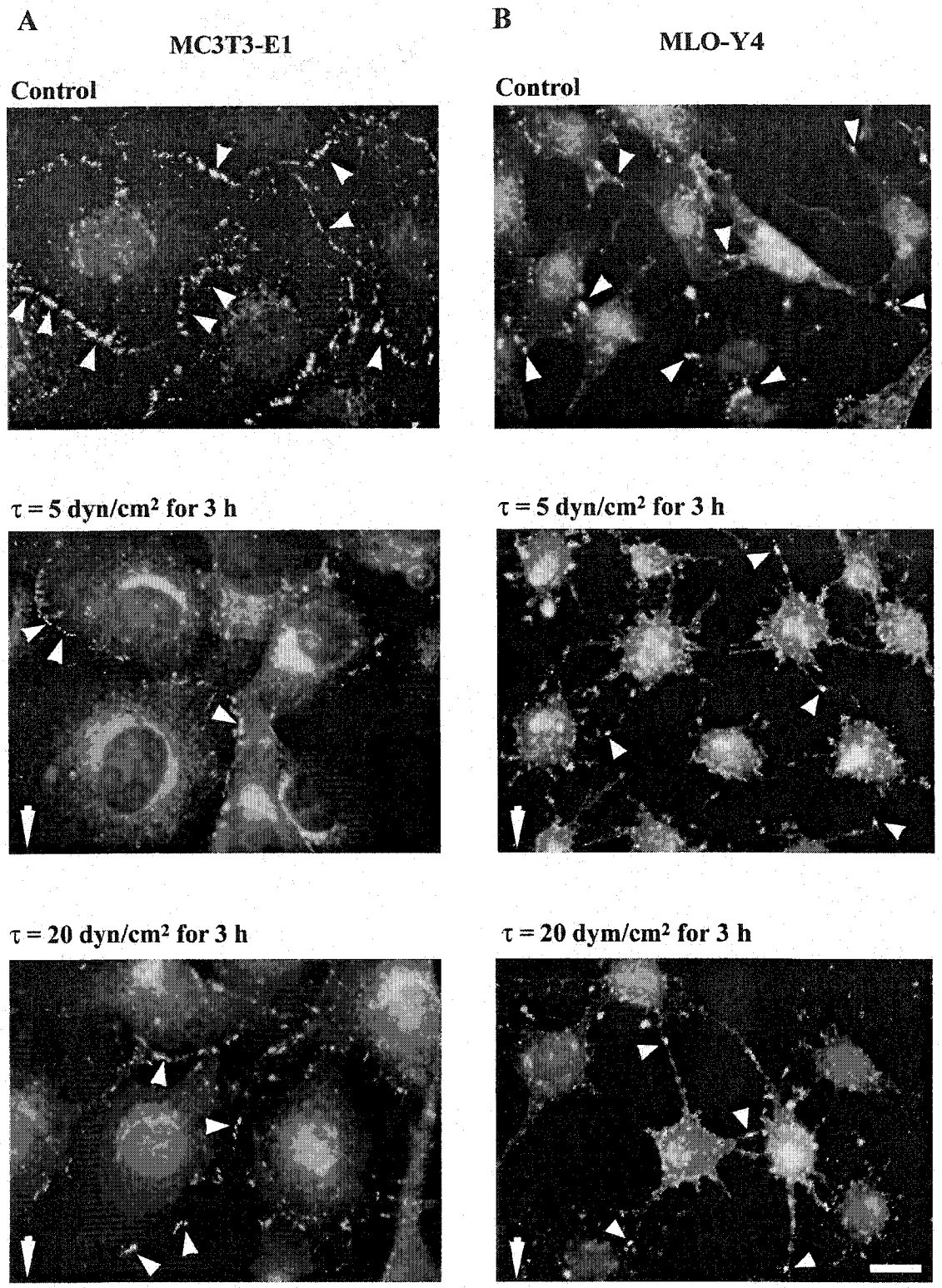

Figure 2.4. **Fluid shear stress dramatically reduced the colocalization of Cx43 and ZO-1 is both MC3T3-E1 and MLO-Y4 cells.** Cells were subjected to low shear stress

level of 5 dyn/cm^2 and high shear stress level of 20 dyn/cm^2 for 1 or 3 h and control cells were kept in static condition. The effect of fluid shear stress on the colocalization of Cx43 and ZO-1 in MC3T3-E1 (A) and MLO-Y4 (B) were analyzed using immunofluorescence microscopy. Formaldehyde fixed, triton X-100 permeabilized samples were double labeled with primary polyclonal and monoclonal antibodies against Cx43 and ZO-1 followed by fluorescein-conjugate goat anti-rabbit IgG and goat anti-mouse IgG. Arrow, flow direction; arrowhead, colocalization of Cx43 and ZO-1; Bar, 20μm.

Intercellular coupling in cultured bone cells is significantly decreased by fluid shear stress

Previous studies (Yamaguchi et al., 1994; Cheng et al., 2001b) have shown that both MC3T3-E1 and MLO-Y4 cells are coupled by functional gap junction channels. In this study, we used the scrape loading technique to quantitatively examine the effects of fluid shear stress on cell-cell coupling. Our scrape loading data indicated that intercellular coupling significantly decreased in MC3T3-E1 cells; this change was more pronounced at the higher shear stress and the longer duration. As shown in Fig. 2.5A, the extent of dye spread in control MC3T3-E1 cells was 270.4 ± 10.7 μm. This dye transfer distance was reduced to 237.4 ± 4.7 or 120.8 ± 5.0 μm when cells were exposed to the lower shear stress of 5 dyn/cm^2 for 1 or 3 h, respectively. At the high shear stress level of 20 dyn/cm^2 the degree of dye transfer was dramatically reduced to 168.4 ± 4.7 μm for the shorter duration and to 106 ± 6.3 μm for the longer duration (results shown in bar graph).

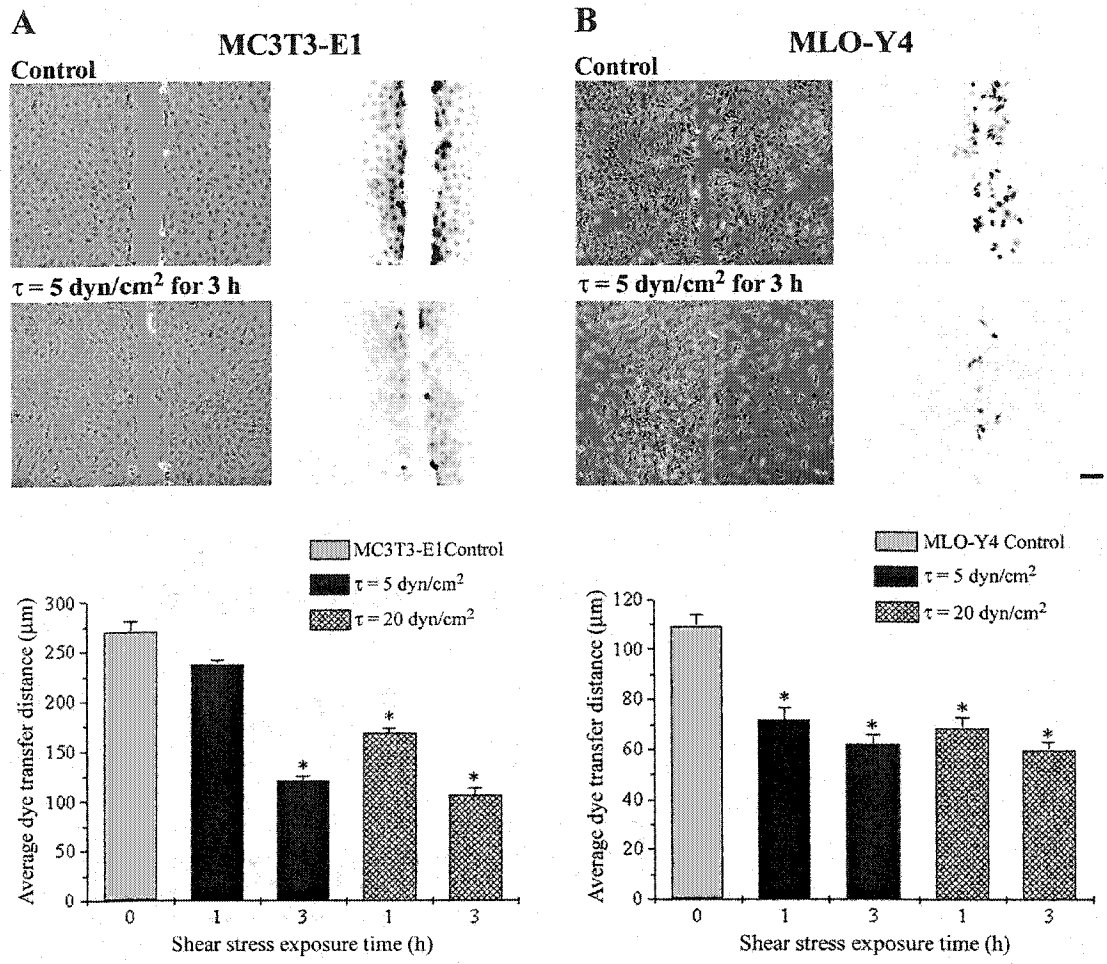

Figure 2.5. **Intercellular coupling in MC3T3-E1 and MLO-Y4 cells is significantly decreased by fluid shear stress.** Cell-cell coupling in MC3T3-E1 (A) and MLO-Y4 (B) cells after the exposure of fluid shear stress was quantitatively examined using the scrape loading technique. Incisions on the cell monolayers of control and shear exposed samples incubated with 0.5% Lucifer Yellow were made with a razor blade. Dye spread distance from the damaged cells to their neighboring cells was quantified using Scion NIH Image software. Data are presented as mean ± SEM, and n = 4 (*, $p < 0.05$). Bar, 100μm.

MLO-Y4 cells showed more uniform changes in dye coupling when exposed to shear stress. As shown in Fig. 2.5B the average dye transfer distance for control MLO-Y4 cells was 109.5 ± 4.3 μm. When cells were exposed to 5 dyn/cm^2 for 1 or 3 h this dye transfer distance was significantly decreased to 72 ± 4.9 or 62.1 ± 3.7 μm (see bar graph). Similar decreases were observed with the samples that were exposed to high shear stress of 20 dyn/cm^2 for 1 or 3 h. These data imply that both levels of fluid shear stress inhibited intercellular coupling which in turn supports the conclusion that they also disrupt cell-cell junctional communication and redistribute the junctional proteins depending on the duration and the level of shear stress.

Fluid shear stress downregulates ZO-1 and phosphorylated Cx43 in cultured bone cells

We have performed Western blot analyses for crude membrane and cytosolic proteins to determine the extent to which fluid shear stress regulates levels of Cx43, Cx45 and ZO-1 within each cell type. For Cx43, multiple bands were detected in Western blots corresponding to different extent and/or type of phosphorylation (Musil et al., 1990; Musil and Goodenough, 1991), where NP is the dephosphorylated form and P1 and P2 designate phosphorylated Cx43 species. For both cell lines at all shear stress levels, there was a similar pattern, in which the P2 form of Cx43 from the membrane was significantly decreased in the membrane fraction, whereas all three forms of Cx43 were dramatically increased in the cytosolic fraction. For osteoblastic MC3T3-E1 cells, densitometric analysis of membrane bound Cx43 bands showed significant downregulation of the P2 form of Cx43 at 3 h for both 5 and 20 dyn/cm^2. By contrast, NP, P1 and P2 forms of cytosolic Cx43 increased after exposure to both levels of shear stress (Fig. 2.6A).

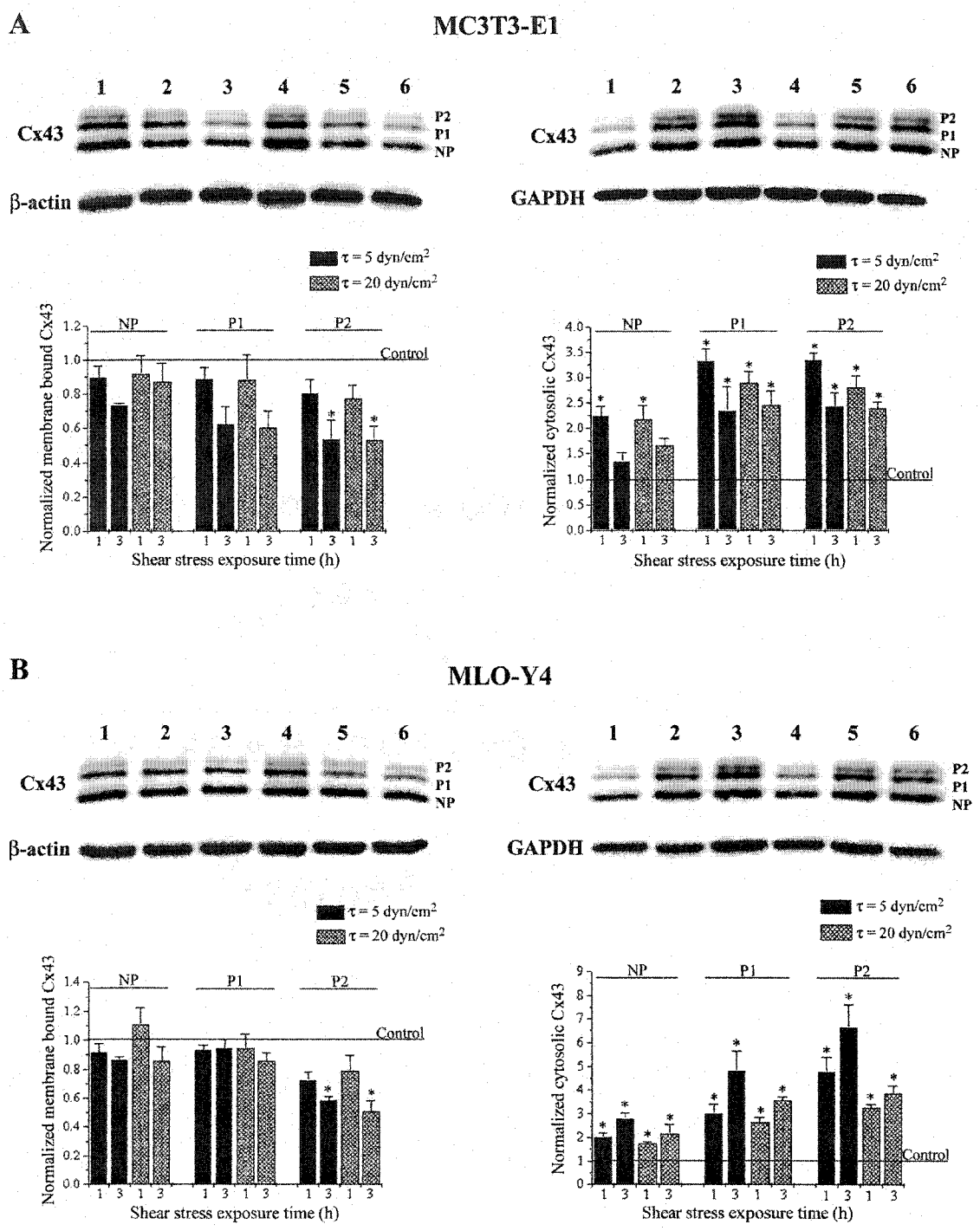

Figure 2.6. **Fluid shear stress downregulates phosphorylation of membrane bound Cx43 and upregulates all three forms of cytosolic Cx43 in both MC3T3-E1 and**

MLO-Y4 cells. Western blot analysis for both membrane bound and cytosolic proteins was performed to determine the extent to which fluid shear stress regulates levels of Cx43 and Cx45. Cells were lysed and membrane bound and cytosolic proteins were prepared from controls (lanes 1 and 4), 1 h exposure of $\tau = 5$ dyn/cm^2 (lane 2), 3 h exposure of $\tau = 5$ dyn/cm^2 (lane 3), 1 h exposure of $\tau = 20$ dyn/cm^2 (lane 5), or 3 h exposure of $\tau = 20$ dyn/cm^2 (lane 6) cells. Western blot analysis was performed using antibodies against Cx43, β-actin and GAPDH for membrane and cytosolic portions of MC3T3-E1 (A) and MLO-Y4 cells (B). Densitometric analysis of Cx43 bands (NP, non-phosphorylated band; P1, phosphorylated band 1; and P2, phosphorylated band 2) from three independent experiments were performed using Scion NIH Image software. All acquired data were first normalized with respect to their internal controls, β-actin for membrane bound proteins and GAPDH for cytosolic proteins, and then normalized with respect to control data. All data are presented as mean ± SEM, n = 3 (*, $p < 0.05$).

Similarly, densitometric analysis of membrane-bound Cx43 for MLO-Y4 revealed downregulation of the P2 form at both 5 and 20 dyn/cm^2, whereas cytosolic Cx43 noticeably increased in response to both levels of shear stress, especially to 5 dyn/cm^2 (Fig. 2.6B). In both MC3T3-E1 and MLO-Y4 cells Cx45 was detectable only in the cytosolic fraction and low levels of shear stress seemed to down-regulate Cx45, whereas high level of shear stress appeared to up-regulate Cx45 at both exposure times (Fig. 2.7A). Western blots using ZO-1 specific antibodies revealed that for both shear stress levels this membrane bound protein was downregulated at longer exposure time in

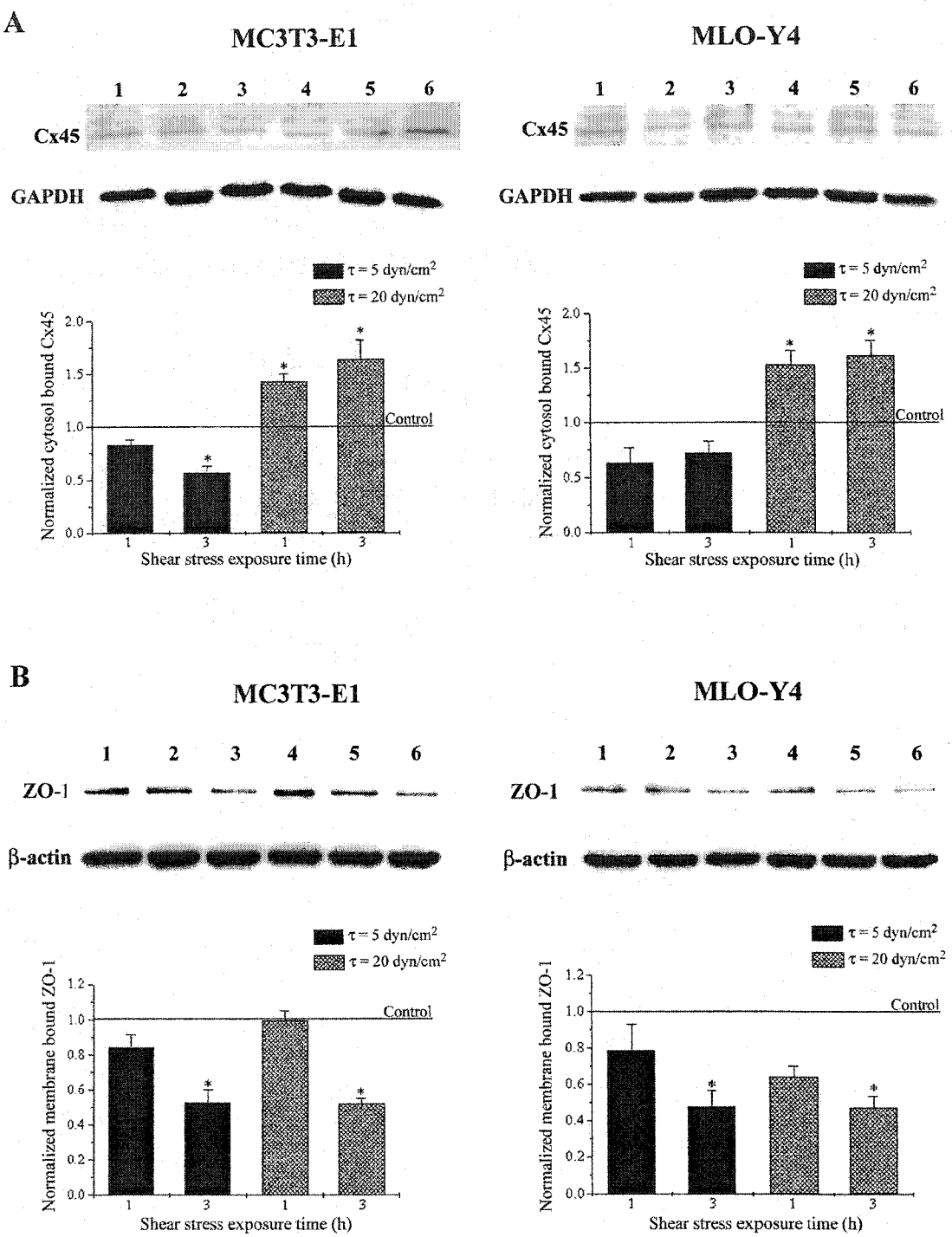

Figure 2.7. **High magnitude shear stress upregulates cytosolic Cx45 whereas both levels of shear stress downregulate membrane ZO-1 in cultured bone cells.** The effect of fluid shear stress on the protein levels of Cx45 and ZO-1 were determined using

Western blot analysis. Cells were lysed and membrane bound and cytosolic proteins were prepared from controls (lanes 1 and 4), 1 h exposure of $\tau = 5$ dyn/cm^2 (lane 2), 3 h exposure of $\tau = 5$ dyn/cm^2 (lane 3), 1 h exposure of $\tau = 20$ dyn/cm^2 (lane 5), or 3 h exposure of $\tau = 20$ dyn/cm^2 (lane 6) cells. Western blot analysis was performed using antibodies against Cx45, GAPDH (A), ZO-1 and β-actin (B) for MC3T3-E1 and MLO-Y4 cells. Densitometric analysis of cytosolic Cx45 and membrane bound ZO-1 proteins from three independent experiments were performed using Scion NIH Image software. All acquired data were first normalized with respect to their internal controls, β-actin for membrane bound proteins and GAPDH for cytosolic proteins, and then normalized with respect to control data. All data are presented as mean ± SEM, n = 3 (*, $p < 0.05$).

both MC3T3-E1 and MLO-Y4 cells (Fig. 2.7B). These data indicate that fluid shear stress regulates the level of Cx45 and ZO-1 expression and abundance of all three forms of Cx43. Notably the P2 form of the membrane bound Cx43 decreased as duration of the shear stress increased. Such correlation of decrease in P2 with decreased dye coupling is consistent with previous reports on other cell types (see Discussion).

Expression of Cx43, Cx45, and ZO-1 were selectively regulated in response to different shear stress levels

Previous studies on endothelial cells have shown that fluid flow and mechanical stretch alter the expression of Cx43 (Cowan et al., 1998; Depaola et al., 1999). Therefore in this study we analyzed the consequence of fluid shear stress on the expression of Cx43,

Cx45, and ZO-1 mRNAs in osteoblastic and osteocytic cell lines using northern blot analysis and semi-quantitative RT-PCR. In both cell lines different levels of shear stress seemed to regulate expression of Cx43 and Cx45 in a reciprocal or compensatory manner. As shown in Fig. 2.8A, Cx43 mRNA levels increased 1.5 - 2 fold for MC3T3-E1 cells and 1.25 – 1.5 fold for MLO-Y4 cells at 5 dyn/cm^2 for 1, 2, or 3 h, yet no apparent changes were found from the controls at 20 dyn/cm^2 for any of the durations for either cell types. By contrast, Cx45 mRNA remained the same as the controls at the lower shear stress level for all durations and increased to 1.25 – 1.75 fold at 20 dyn/cm^2 for 1, 2, or 3 h (Fig. 2.8B). With regard to ZO-1 mRNA there were no detectable changes with respect to control in MC3T3-E1 cells at the lower shear stress level, whereas the mRNA level was decreased to half that of controls at the higher shear stress level (Fig. 2.9A). However, more dramatic effects on ZO-1 expression were seen in MLO-Y4 cells, where ZO-1 mRNA was profoundly decreased at both 5 and 20 dyn/cm^2 for 1, 2, or 3 h of exposure times (Fig. 2.9B). These data suggest that for both cell lines, lower shear stress (5 dyn/cm^2) upregulates the expression of Cx43, whereas the higher shear stress (20 dyn/cm^2) upregulates the expression of Cx45. By contrast, ZO-1 is downregulated at high shear stress levels in the osteoblastic cell line and, even more strikingly, at both shear stresses in the osteocytic cell line.

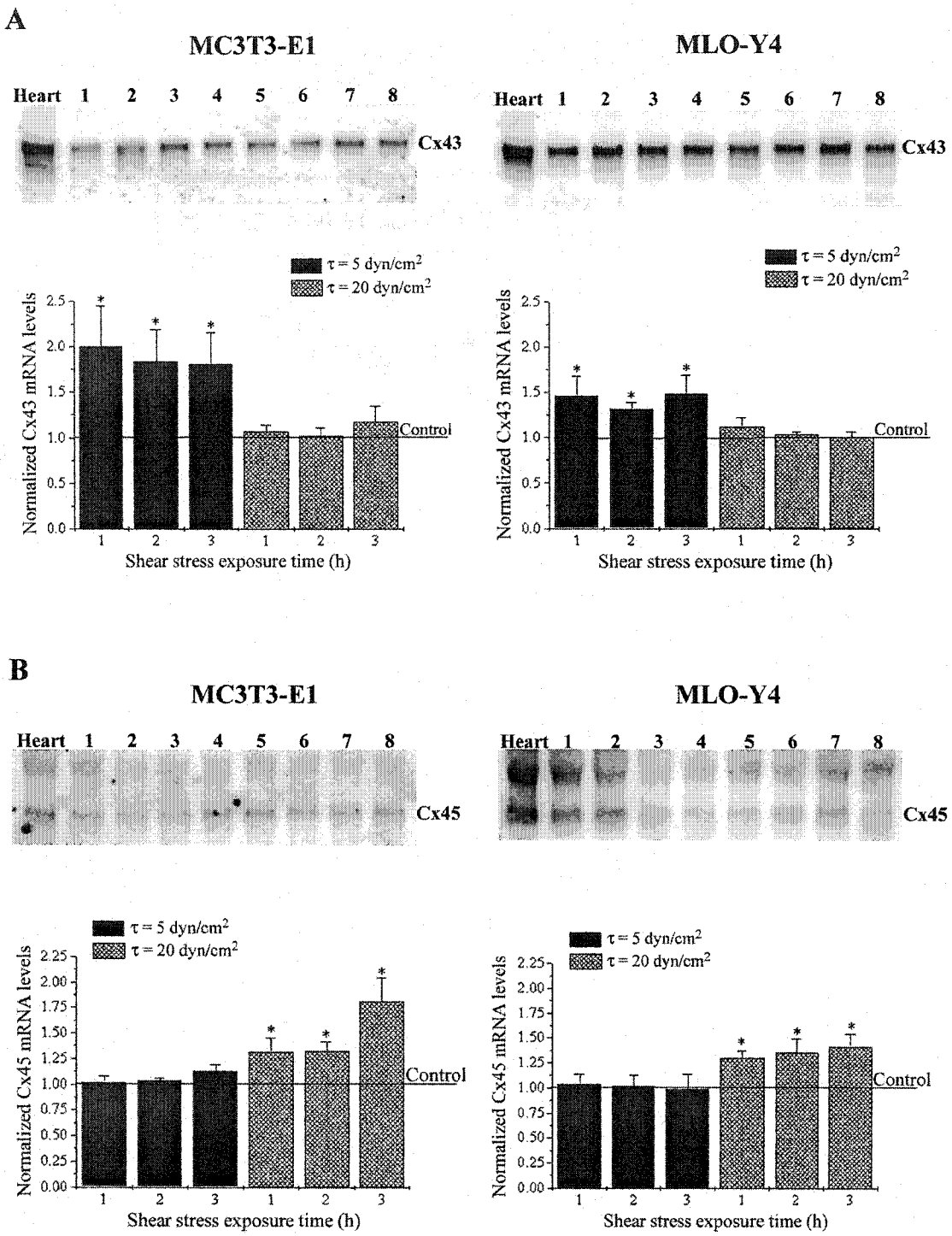

Figure 2.8. **Low magnitude shear stress upregulates Cx43 whereas high magnitude shear stress upregulates Cx45 in both MC3T3-E1 and MLO-Y4 cells.** Northern blot analysis of Cx43 (A) and Cx45 (B) expression in MC3T3-E1 and MLO-Y4 cells. Total

RNA was prepared from controls (lanes 1 and 5), 1 h exposure of $\tau = 5$ dyn/cm^2 (lane 2), 2 h exposure of $\tau = 5$ dyn/cm^2 (lane 3), 3 h exposure of $\tau = 5$ dyn/cm^2 (lane 4), 1 h exposure of $\tau = 20$ dyn/cm^2 (lane 6), 2 h exposure of $\tau = 20$ dyn/cm^2 (lane 7), or 3 h exposure of $\tau = 20$ dyn/cm^2 (lane 8) cells. 10 μg of RNA were loaded in each lane and probed by hybridization at high stringency with [^{32}P]-labeled rat Cx43 cDNA as described in Materials and Methods. Densitometric analysis of Cx43 mRNA bands from six independent experiments was performed using Scion NIH Image software. All acquired data were first normalized with respect to corresponding 18S intensity and then all experiments data were normalized with respect to control data. All data are presented as mean ± SEM, n = 6 (*, $p < 0.05$).

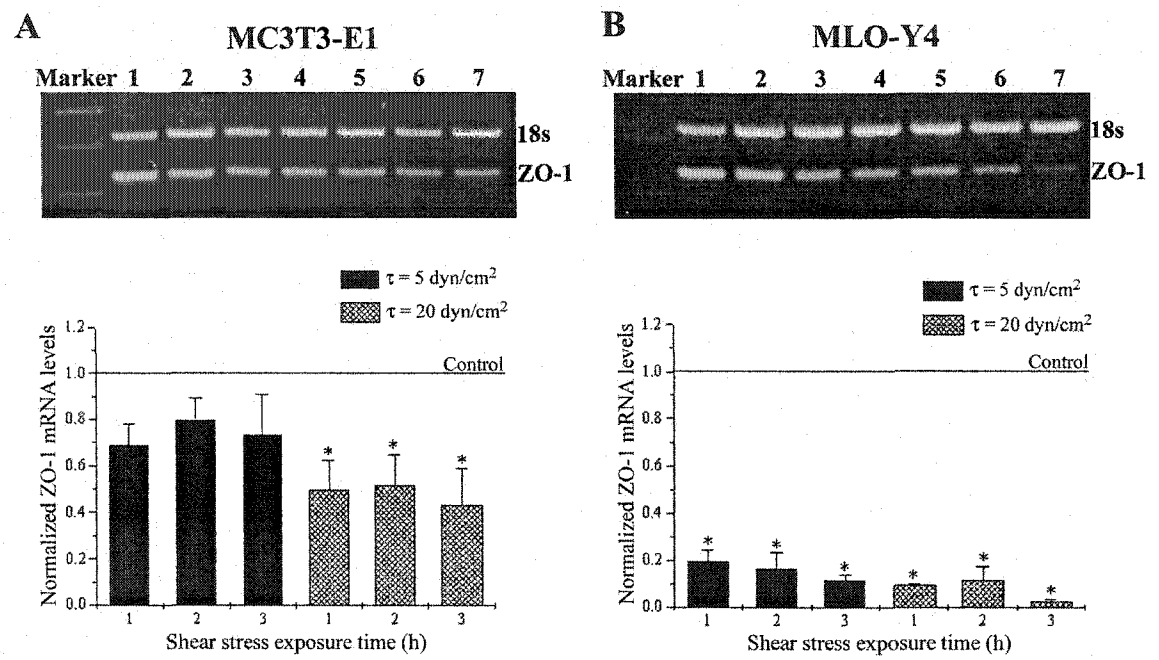

Figure 2.9. **Fluid shear stress downregulates ZO-1 mRNA in both MC3T3-E1 and MLO-Y4 cells.** Semi-quantitative RT-PCR analysis of ZO-1 in MC3T3-E1 (A) and MLO-Y4 cells (B). Total RNA was prepared from controls (lanes 1), 1 h exposure of τ = 5 dyn/cm^2 (lane 2), 2 h exposure of τ = 5 dyn/cm^2 (lane 3), 3 h exposure of τ = 5 dyn/cm^2 (lane 4), 1 h exposure of τ = 20 dyn/cm^2 (lane 5), 2 h exposure of τ = 20 dyn/cm^2 (lane 6), or 3 h exposure of τ = 20 dyn/cm^2 (lane 7) cells. RT-PCR was performed using the Thermoscript RT-PCR System. Densitometric analysis of ZO-1 mRNA bands from three independent experiments were performed using 1D Kodak Scientific Imaging Systems. All acquired data were first normalized with corresponding 18S and then all experimental data were normalized with respect to control data. All data are presented as mean ± SEM, n = 3 (*, $p < 0.05$).

Discussion

In this study, we have found that steady fluid shear stress modifies expression, function and distribution of connexins (Cx43 and Cx45) and an associated tight junction protein (ZO-1) in cultured bone cells. Our results strongly suggest that fluid shear stress disrupts cell-cell communication and rearranges the gap junction proteins Cx43, and Cx45 and an associated protein ZO-1 in both MC3T3-E1 and MLO-Y4 cells. This disrupted gap junctional communication and rearrangement of Cx43, Cx45 and ZO-1 depended on the magnitude of shear stress as well as exposure duration. Our results as well as others; (Donahue et al., 1995; Yamaguchi et al., 1994; Kato et al., 1997; Yellowley et al., 2000)indicate that the major gap junction protein mediating cell-cell communication in both cell types is Cx43. Our finding that the selective reduction in the P2 form of membrane bound Cx43 correlates with the loss of dye coupling is consistent with previous reports indicating that Cx43 phosphorylation is important for its function (Musil et al., 1990; Musil and Goodenough, 1991). Elevated levels of all three forms (NP, P1 and P2) of cytosolic Cx43 after exposure to fluid shear stress suggests that newly synthesized as well as internalized Cx43 contributed to the increase in cytosolic Cx43 level. We believe that this significant increase in cytosolic Cx43 level was mainly due to the internalization of membrane bound Cx43 because newly synthesized Cx43 should mostly be in NP form. Furthermore, based on the cytosolic Cx43 analysis, low shear stress seemed to be regulating Cx43 in both cell types, whereas high shear stress appeared to be upregulating cytosolic Cx45. At the level of mRNA, Cx43, Cx45 and ZO-1 all showed interesting changes with fluid-induced shear stress. Expression of Cx43 and

Cx45 mRNA were selectively upregulated in response to different shear stress levels, whereas both magnitudes of shear stress inhibited ZO-1 expression. Together, these results show for the first time that in cultured bone cells, fluid shear stress disrupts cell-cell junctional communication, rearranges junctional proteins and determines *de novo* synthesis of specific connexins in a manner that depends on the magnitude of shear stress.

There is increasing evidence that fluid shear stress regulates Cx43 in vascular smooth muscle cells (Cowan et al., 1998), vascular endothelial cells (Depaola et al., 1999), and cultured bone cells (Cheng et al., 2001b). Our observation on the disruption and translocation or internalization of Cx43 from the membrane after exposure to laminar flow in both MC3T3-E1 and MLO-Y4 cells agree with the findings of DePaola and coworkers (Depaola et al., 1999) for endothelial cells in the laminar flow region at 5 h of exposure time. We speculate that fluid shear stress of short duration (t = 1 or 3 h) reduces intercellular communication as a consequence of morphological changes (Pavalko et al., 1998; Cheng et al., 2001b), loss and/or internalization of membrane bound Cx43 (Musil et al., 1990; Musil and Goodenough, 1991; Krutovskikh et al., 1995; Depaola et al., 1999), and possibly also through the inhibited trafficking of newly synthesized Cx43 to the membrane. Our finding that plasmalemmal ZO-1 immunostaining decreased in a somewhat similar manner to Cx43 indicates that ZO-1 and Cx43 might interact in MC3T3-E1 and MLO-Y4 cells as has been reported for other cell types (Howarth et al., 1992; Giepmans and Moolenaar, 1998; Toyofuku et al., 1998; Laing et al., 2001). Because interaction with ZO-1 has been suggested to stabilize Cx43 at the cell surface (Toyofuku et al., 2001), the downregulation of ZO-1 by shear stress might lead to

redistribution of Cx43 to intracellular compartments.

Functional studies on junctional communication indicated that during shear stress exposure, dye coupling was reduced as gap junction protein expression decreased on the appositional membranes. Our observation of impaired dye coupling during the early period of laminar shear stress in cultured bone cells is similar to that reported in endothelial cells (Depaola et al., 1999). Hence, these results verify our conclusion that fluid shear stress disrupts cell-cell communication. Biochemical evidence for redistribution of Cx43 due to fluid shear stress is provided by the observed decrease in Cx43 P2 from the membrane, which is believed to be the predominant form of this gap junction protein forming functional gap junction channels (Musil et al., 1990; Musil and Goodenough, 1991), and increase in all three forms of Cx43 in the cytosol.

Our findings on the distribution of Cx43, intercellular coupling and the phosphorylation level of Cx43 after the steady shear stress exposure in MLO-Y4 cells differ from a recent report that migration of Cx43 from perinuclear region towards the dendritic processes and intercellular coupling increased after MLO-Y4 cells were subjected to fluid flow (Cheng et al., 2001b). Although differences might have arisen from usage of different antibodies, the analytical methods applied, or the composition of culture media, the previous study noted a lack of correlation between Cx43 distribution and the enhanced intercellular coupling, suggesting that another connexin might upregulate cell-cell communication after shear stress exposure. We analyzed both Cx43 and Cx45 in our experiments, and our data suggest that although Cx43 is the major gap junction protein regulating junctional communication in MC3T3-E1 and MLO-Y4 cells, Cx45 can be upregulated under high shear stress conditions. The previous study also

analyzed various osteoblastic cells (2T3, ROS17/2.8, MC3T3-E1) reporting no effect of fluid flow on cell-cell communication, and concluded that osteoblasts are less responsive than osteocytes to such stimuli (see also Klein-Nulend et al. (1995a)). However, numerous previous studies on osteoblastic cells have clearly demonstrated that stress enhances production of second messengers such as cAMP, NO, Ca^{++}, prostaglandin (Reich et al., 1990; Hillsley and Frangos, 1994; Klein-Nulend et al., 1995b; Hung et al., 1996; Smalt et al., 1997), and alters cell morphology, including reorganization of the actin cytoskeleton (Pavalko et al., 1998). Our data indicate that osteoblastic MC3T3-E1 cells do respond to fluid shear stress.

We have observed differential mRNA expression of Cx43, Cx45, and ZO-1 in response to different shear stress levels. Low shear stress upregulated Cx43 expression in both cell types, whereas high shear stress upregulated Cx45 expression in both cell types. Previous studies have shown that when Cx43 function is inhibited in avian osteogenic tissue, Cx45 is upregulated to fulfill at least some aspect of the missing functions (Minkoff et al., 1999). Such selective upregulation of Cx43 and Cx45 by different levels of shear stress provides evidence that patterns of gene expression are transduced by the mechanical stimulus that would be expected to qualitatively alter the junctional phenotype and may correspond to either differentiation or dedifferentiation of bone cells (Minkoff et al., 1994; Schiller et al., 1997; Li et al., 1999; Minkoff et al., 1999; Donahue et al., 2000; Romanello et al., 2001).

Although the mechanochemical transduction cascade leading from shear stress to altered gene expression patterns remains to be fully elucidated, fluid shear stress has been shown to enhance second messenger production in cultured bone cells. In bone cells,

cAMP is regulated by prostaglandin, and both are increased under fluid flow conditions (Reich et al., 1990); cAMP has been shown to upregulate both mRNA and protein of both Cx43 and Cx45 in cultured cardiac myocytes (Darrow et al., 1996). Therefore a possible mechanism by which cultured bone cells might respond to fluid flow would involve disruption of cell-cell communication and enhanced production of prostaglandins. This would elevate cAMP, which in turn would upregulate expression and phosphorylation of either Cx43 or Cx45 depending on the magnitude of shear stress and duration of exposure period. Subsequently, cellular differentiation would be initiated and disconnected cells or the remaining network would begin focal bone remodeling.

The decrease in ZO-1 mRNA and protein expression with increased level of shear stress we have observed may also play an important role in bone remodeling. Truncation mutants of the tight junction protein ZO-1 have been shown to disrupt epithelial cell morphology suggesting that ZO-1 may be involved in regulation of cellular differentiation (Ryeom et al., 2000). Moreover, downregulation of ZO-1 and occludin appear to be related to phenotypic changes associated with epithelial cell transformation (Marzioni et al., 2001). Therefore, it seems likely that ZO-1 may also be involved in mediating cell differentiation in cultured bone cells.

The results described in this manuscript were obtained under *in vitro* conditions in tissue culture. *In vivo*, there is increasing evidence that osteocyte cell processes are surrounded by the pericellular matrix with transverse tethering filaments (Weinbaum et al., 2001) whereas in culture there is no encircling support structure. In addition, the recent theoretical model by You et al. (2001) brings to our attention that *in vivo*, the fluid shear stresses on the cell body are much smaller than those on the membrane in cell

processes so that the fluid drag force on the transverse filaments in the pericellular matrix is much greater than the fluid shear force on the cell process membrane. Therefore, it is possible that under *in vitro* conditions the actin cytoskeleton in the cell body responds to the fluid shear stress rather than the more rigid actin bundle in the cell process. However, You et al. (2001) predicted that the fluid drag on the tethering filaments can produce a 20-100-fold amplification in the strain on the actin filament bundle in the cell process. This amplification is sufficient to elicit intracellular signaling responses in all cell cultures with deformed substrates.

In summary, we have shown that fluid-induced shear stress is an important biophysical signal in bone mechanotransduction. Our observations suggest that in both osteoblastic and osteocytic cell lines fluid shear stress of the magnitude expected to occur in bone tissue disrupts junctional communication, rearranges junctional proteins, and determines *de novo* synthesis of specific connexins to an extent that depends on the magnitude of the shear stress. Such disconnection from the bone cell network due to the fluid shear stress may provide part of the signal whereby the disconnected cells or the remaining network initiate focal bone remodeling.

Acknowledgements

We thank Ms. Marcia Urban for her technical assistance, Dr. Wei Li for advice on separating membrane and cytosolic Cx43, Dr. Karen Cusato for advice on use of the LIVE/DEAD cell assay, Dr. Elliot L. Hertzberg (Albert Einstein College of Medicine) and Dr. Thomas H. Steinberg (Washington University School of Medicine) for their generous supply of Cx43 and Cx45 antibodies and Dr. Kenneth J. McLeod (SUNY, Stony Brook) and Dr. Lynda F. Bonewald (University of Texas Health Science Center) for graciously providing us with MC3T3-E1 and MLO-Y4 cell lines.

This work was supported primarily by NIH HL19454 (PI: Sheldon Weinbaum) and a Gillecce Fellowship (CUNY Graduate School), with additional support provided by NIH DK41918 and NIH NS34931 (PI: David C. Spray).

Chapter 3

The Role of the Glycocalyx in Reorganization of the Actin Cytoskeleton under Fluid Shear Stress: A 'Bumper Car' Model*

* Will be submitted to the *Proceedings of the National Academy of Science.*

Abstract

We propose a new conceptual model for the cytoskeletal organization of endothelial cells (ECs) based on a major dichotomy in structure and function at basal and apical aspects of the cells. Intracellular distributions of F-actin, vinculin, paxillin, ZO-1 and Cx43 were analyzed from confocal micrographs of rat fat pad ECs following 5 h shear stress. With intact glycocalyx there was severe disruption of the dense peripheral actin bands (DPABs) and migration of vinculin to cell borders under a uniform shear stress (10.5 dyn/cm^2). This behavior was augmented in corner flow regions of the flow chamber where high shear stress gradients were present. In striking contrast, no such reorganization was observed if the glycocalyx was compromised. These results are explained in terms of a 'bumper car' model in which the actin cortical web and DPAB are only loosely connected to basal attachment sites allowing for two distinct cellular signaling pathways in response to fluid shear stress, one transmitted by glycocalyx core proteins as a torque that acts on the ACW and DPAB and the other emanating from focal adhesions and stress fibers at the basal and apical membranes of the cell.

Abbreviations

EC, endothelial cell; EG, endothelial glycocalyx; HSPG, heparan sulfate proteoglycan; ACW, actin cortical web; DPAB dense peripheral actin band; SFs, stress fibers; TJ, tight junction; USS, uniform shear stress; HSSG, high shear stress gradient.

Introduction

Hemodynamic shearing stresses on endothelial cells (EC) are widely recognized to play a vital role in regulation of vessel wall remodeling, cellular signaling, mass transport, red and white cell interaction and atherogenesis (Davies, 1995; Ogunrinade et al., 2002; Tarbell, 2003). The possible roles of the endothelial glycocalyx (EG) in this regulation as a molecular sieve, as a barrier and modulator of interactions between blood cells and ECs, and as a mechanotransducer of fluid shear stress have only been studied more recently (Vink and Duling, 1996; Hu and Weinbaum, 1999; Mulivor and Lipowsky, 2002; Weinbaum et al., 2003). Relatively little is known about the specific proteins in the EG, although hyaluronan, chondroitin and heparan sulfate play a significant role in its assembly(Ihrcke et al., 1993; Henry and Duling, 1999). In the early 1990's investigators first observed that the shear induced dilation of small arteries was abolished when sialic acids were removed from the EG by neuraminidase (Pohl et al., 1991). Florian et al. (Florian et al., 2003) recently verified the presence of heparan sulfate proteoglycan (HSPG) in the glycocalyx of cultured bovine aortic endothelial cells (BAECs) and demonstrated that partial removal of HSPG with heparinase completely blocked shear-induced NO release. A puzzling and still not understood consequence of EG degradation was the observation that shear-induced NO production was greatly inhibited without apparent effect on shear-dependent vasodilation due to PGI_2 release (Hecker et al., 1993).

Squire et al. (Squire et al., 2001) showed that the ultrastructural organization of EG was quasi-periodic, anchored to a geodesic-like scaffold of hexagonally arranged F-actin filaments forming an actin cortical web (ACW) (Drenckhahn and Ness, 1997) just

beneath the plasmalemma. A fundamental question addressed in (Weinbaum et al., 2003) is how fluid shear stresses acting at the surface of the EG are transmitted to this ACW if there is essentially no flow in the EG and hence nearly zero fluid shear stress acting at the level of the cell membrane. This model predicted that the core proteins in the EG serve as stiff bristles (flexural rigidity EI, 700 $pN \cdot nm^2$) that transmit the fluid drag on their tips as a bending moment that acts on the ACW.

While numerous studies have been performed on the intracellular rearrangement of cytoskeletal structural components (microfilaments, intermediate filaments and microtubules) in EC cultures subject to fluid shear (Galbraith et al., 1998; Helmke et al., 2000), none have compared cytoskeletal reorganization in the absence or presence of the EG. Moreover, all previous parallel plate flow chamber studies have been conducted in the uniform shear stress (USS) region in the central portion of the chamber and have assiduously avoided the disturbed corner flow region associated with high shear stress gradients (HSSGs) because of its complexity. The HSSGs examined in this study vary from 0 to $\approx$ 2500 $dyn/cm^2/cm$ and are more than one order of magnitude greater than other flow chamber designs (Depaola et al., 1999) and closer to those observed near arterial bifurcations and branch sites (Ku et al., 1985; Davies, 1995). These high shear gradients are of special interest in atherogenesis since it has been proposed that these regions are prone to lesion development (Davies et al., 1986; White et al., 2001; Tarbell, 2003). The present study attempts to explain these various observations within the context of a new mechanical model for the actin cytoskeleton.

Materials and Methods

Flow Chamber Design and Flow Characteristics

We have modified the gasket of the conventional parallel plate flow chamber (Cytodyne) to obtain a very narrow flow space (4 × 60 mm × 220 μm gap height) which has enabled us to analyze the effects of USS as well as spatial HSSGs in the corner flow region. The flow loop consisted of a parallel plate flow chamber and a re-circulating flow circuit as previously described (Thi et al., 2003). Spatial variations of shear stress gradients in the entire chamber cross section were calculated using an infinite series solution of the two-dimensional steady Navier-Stokes equation. (see *Appendix A*)

Cell Culture and Flow Experiments

Rat fat pad ECs (RFPEC, passage 14-20, obtained from Dr. Anthony Ashton, AECOM, Bronx) were cultured in DMEM containing 1% penicillin-streptomycin and 10% fetal bovine serum (FBS). Cells were grown on glass slides until confluency and transferred to the flow chamber for experiments. Cells were exposed to USS of 10.5 dyne/cm^2 for 5 h with different perfusion media (DMEM, DMEM+10%FBS, DMEM+1% bovine serum albumin (BSA)). Sham controls were the no flow condition for each perfusion medium. Each set of experiments was repeated four times.

Immunofluorescence and Confocal Microscopy

To detect the changes in stress fibers (SFs) and DPAB (F-actin, rhodamine-labeled phalloidin (Sigma)), focal adhesions (Vinculin and Paxillin, (Chemicon)), and

tight junction (TJ; ZO-1 (Zymed)) and gap junction complexes (Cx43, courtesy of Dr. E. Hertzberg, AECOM)), immunofluorescence analyses were performed on both controls and shear stress exposed cells (Thi et al., 2003). 15mU/ml of heparinase III (Sigma) was used to digest the glycocalyx (Florian et al., 2003) and HSPG antibody (US Biological) and CellTracker Orange (Molecular Probes) were used to assess heparan sulfate removal. Image stacks were collected using an Olympus FluoView FV500 Laser Scanning Confocal Microscope (Olympus). Four images from each flow treatment and eight images from HSPG control treatments were taken for each set of experiments. For detailed methods see *Appendix B*.

Protein Distribution and Statistical Analysis

Overall average density profiles of 10 cell pairs from each stacked image were plotted using Scion Image (NIH) and changes in protein distribution were detected using kurtosis analysis. HSPG reduction was measured and analyzed using Scion Image and Imaris (Bitplane AG). For detailed analysis, see *Appendix B*. Statistical comparisons were performed using one-way ANOVA (SigmaStat). Asterisks in figures indicate significant difference compared with controls (* $p < 0.05$).

Results

Presence and Absence of Glycocalyx. Previous studies have suggested the existence of a structured EG in the presence of BSA or plasma in the lumen and its absence or

collapse in simple Ringer solution (Adamson and Clough, 1992; Florian et al., 2003). Thus, our *in vitro* flow experiments compared different perfusion media: DMEM, DMEM + 10% FBS, and DMEM + 1% BSA. Fig. 3.1 shows the expression of HSPG under various control conditions. The surface of ECs in the presence of FBS was abundantly decorated with HSPG (Fig. 3.1A, XZ view). When serum proteins were removed, 27.4 ± 1.1% reduction of cell surface heparan sulfate was observed (Fig. 3.1B, XZ view and graph). This finding together with previous observations of EG closely adherent to EC in protein-free Ringer solution (Adamson and Clough, 1992) suggested that the EG collapsed and the core proteins of HSPGs clumped in the absence of serum proteins. In addition, enzymatic removal of HSPG by 2 h heparinase III (Hep III) showed 53.2 ± 2.4% reduction, and this removal was not greatly changed during 5 h post incubation with 1% BSA+DMEM (Fig. 3.1C, XZ view and graph).

Cytoskeleton Organization. To study the participation of EG in the process of transmitting fluid shear stress to the ACW, distribution of F-actin fibers was analyzed among samples that were exposed to various perfusion media and no flow controls. In controls, F-actin fibers were distributed mostly at the peripheral cell borders as a DPAB, with some randomly distributed SFs linking basal and apical adhesion plaques (thin arrows, Fig. 3.2). Exposure of ECs to both USS and HSSG with DMEM alone caused no noticeable changes in F-actin organization compared to control (Fig. 3.2, graph). Similarly, for cells with digested glycocalyx (Hep III), there was insignificant F-actin redistribution in both USS and HSSG regions compared to controls. Exposure of the cells to USS with 1% BSA or 10% FBS perfusion media resulted in dramatic redistribution of

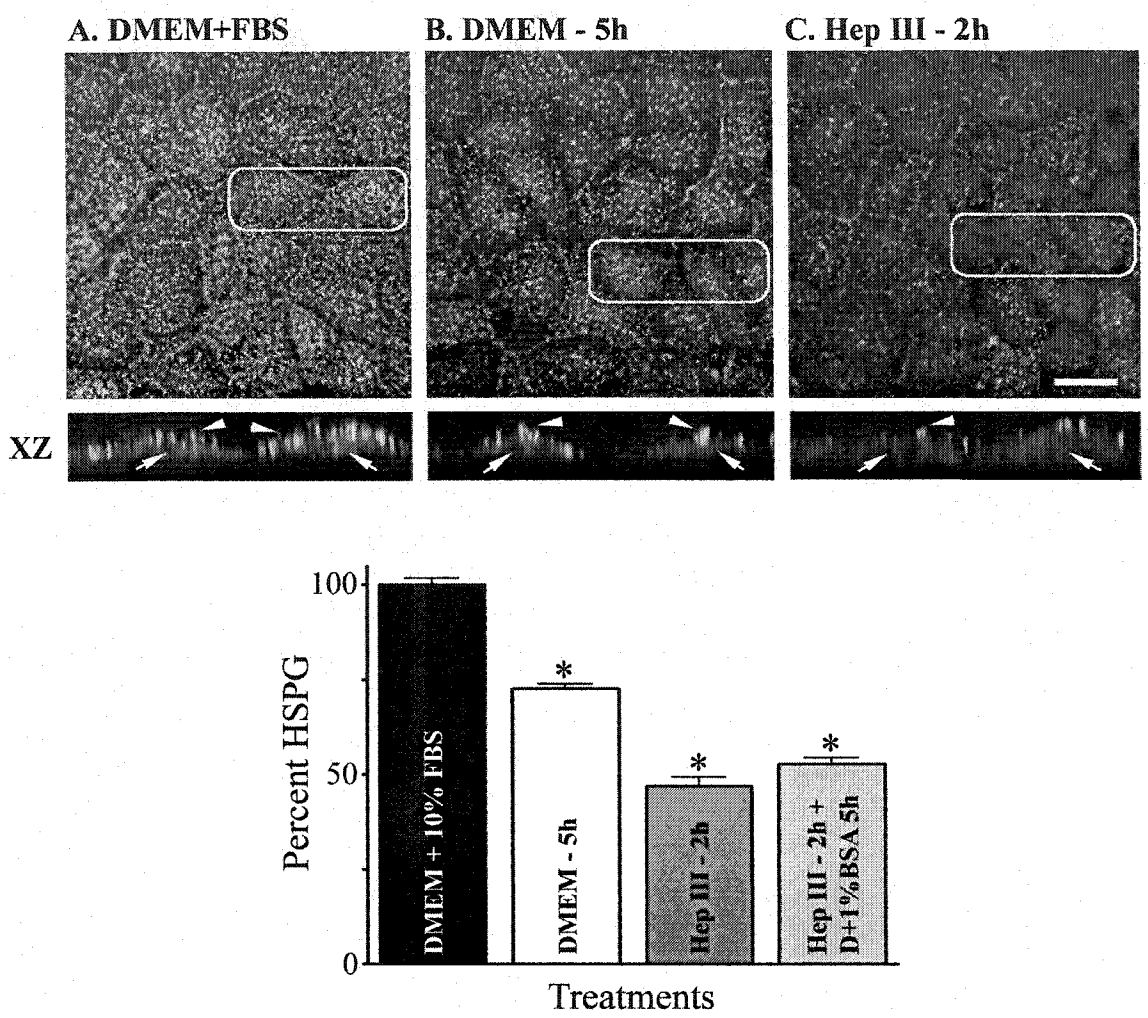

Figure 3.1. Confocal analysis of cell surface HSPG in EG layer. Cells were cultured in DMEM with (A) and without (B) 10% FBS for 5 h, with 15mU/ml of heparinase III (C) for 2 h and post cultured in DMEM + 1% BSA for 5 h (graph). To visualize cell surface HSPG, cell were stained with HSPG antibody (arrowheads) and with CellTracker orange dye (arrows). XZ views from the highlighted boxes of various control conditions show different degrees of cell surface HSPG distributions. Expression of HSPG was quantified and plotted using Scion Image. Eight images per experiment, total of 4 experiments, were taken for each treatment condition. All data are presented as mean ± SEM, n = 32 (*, $p < 0.05$). Scale bar: 20 μm.

F-actin (Fig. 3.2, arrowheads), as noted in previous studies (Girard and Nerem, 1995; Galbraith et al., 1998). As shown in Fig. 3.2, graph insert, this behavior was augmented when ECs were exposed to HSSG. Kurtosis analyses suggested that there was increased SF formation near cell borders and throughout the cell (Fig. 3.2).

Focal Adhesions (FAs). To investigate effects of USS and HSSG in the presence of the EG on focal adhesion remodeling, we studied changes of vinculin and paxillin localization in ECs. In no flow controls vinculin distribution was mostly random with some localization around cell borders and mainly situated near the basal membrane (Fig. 3.3). Exposure to fluid shear stress with DMEM perfusion medium led to no apparent changes in vinculin localization (Fig. 3.3, graph). As for Hep III treated samples there was a slight increase in localization of vinculin at cell-cell borders (Fig. 3.3, graph). With either 1% BSA or 10% FBS in the perfusion media, vinculin became notably redistributed towards appositional membranes (Fig. 3.3, arrowheads). Paxillin was distributed randomly throughout control ECs, with slightly more near appositional membranes (data not shown). Unlike vinculin, presence of the EG did not affect paxillin distribution.

Junctional Complexes. To examine the role of EG in tight and gap junction distribution, we analyzed the TJ associated protein ZO-1 and the gap junction protein Cx43. In controls, ZO-1 expression was mostly continuous and occasionally brush-stroke like at TJ, and Cx43 was abundantly punctate with linear appositional staining at cell borders. Immunoreactivity of Cx43 in perinuclear regions was also observed (Figs. 3.4 and 3.5

thin arrows). Greater disruption of ZO-1 and Cx43 at cell borders was observed in HSSG region when the glycocalyx was present (Figs. 3.4 and 3.5, arrowheads).

Discussion

Previous studies have reported that fluid shear stress disrupts DPABs (Dewey, Jr. et al., 1981; Girard and Nerem, 1995; Galbraith et al., 1998) and leads to formation of basal SFs and focal adhesions (Davies et al., 1994; Girard and Nerem, 1995), presumably due to activation of signaling pathways (Kuchan and Frangos, 1994) and autacoid release (Pohl et al., 1991; Hecker et al., 1993). The possibility that the EG might serve as a mechanotransducer for fluid shear stress was raised by the findings that the presence of cell surface proteoglycans is intimately linked to the ability of cultured ECs to release NO in response to shear (Florian et al., 2003).

In the present study we have manipulated the EG through the presence or absence of BSA and FBS in perfusion solution and digestion of glycocalyx proteins with heparinase, which was reported to completely abolish NO release (Florian et al., 2003) and to attenuate agonist-mediated reorganization of actin (Dull et al., 2003). The efficacy of heparinase is presumably due to the high ratio of heparan to chondroitin sulfate (~ 4:1) at the apical EC membrane (Mulivor and Lipowsky, 2004).

Under conditions manipulating the EG, we have determined the relationship of the ACW to the two other actin filament structures in the EC, the DPAB and the α-actinin bundled SFs, and their associated binding partners, vinculin, paxillin, ZO-1, and

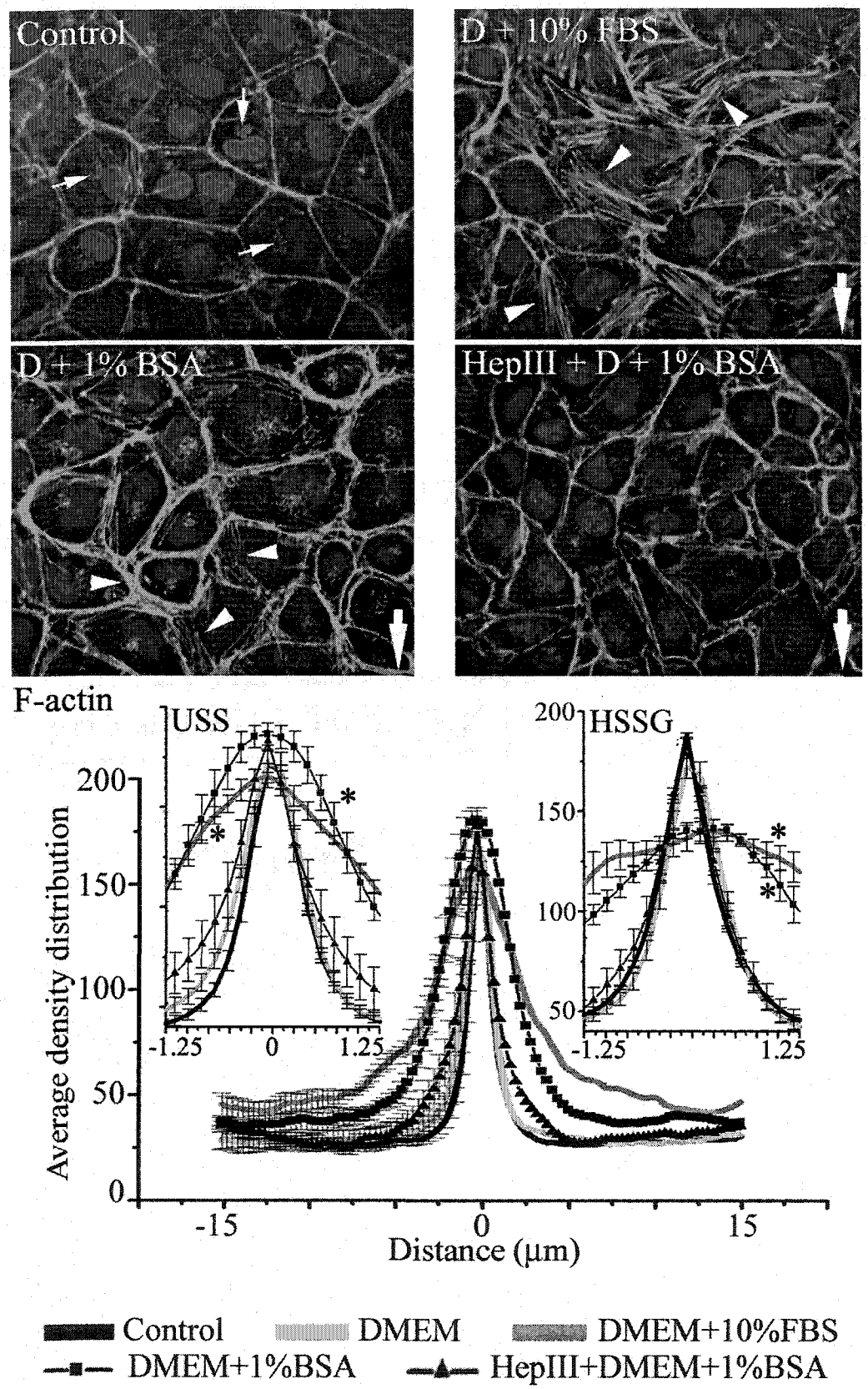

Figure 3.2. Reorganization of EC cytoskeleton in response to fluid shear stress with various flow media. Cells were exposed to USS of 10.5 dyn/cm^2 and HSSG of 0 ~ 2500 dyn/cm^2/cm for 5 h. Effects of USS and HSSG on distribution of F-actin was analyzed using confocal microscopy. Overall average protein density profiles from stacked images of different treatments were plotted using Scion Image. Changes in the distributions of F-actin were detected using kurtosis analysis. Four images per experiment, total of 4 experiments, were taken from USS and HSSG regions. All data are presented as mean ± SEM, n = 160 (*, $p < 0.05$). Flow direction: arrows; transverse SFs: thin arrows; redistribution of F-actin: arrowheads; scale bar: 20 μm.

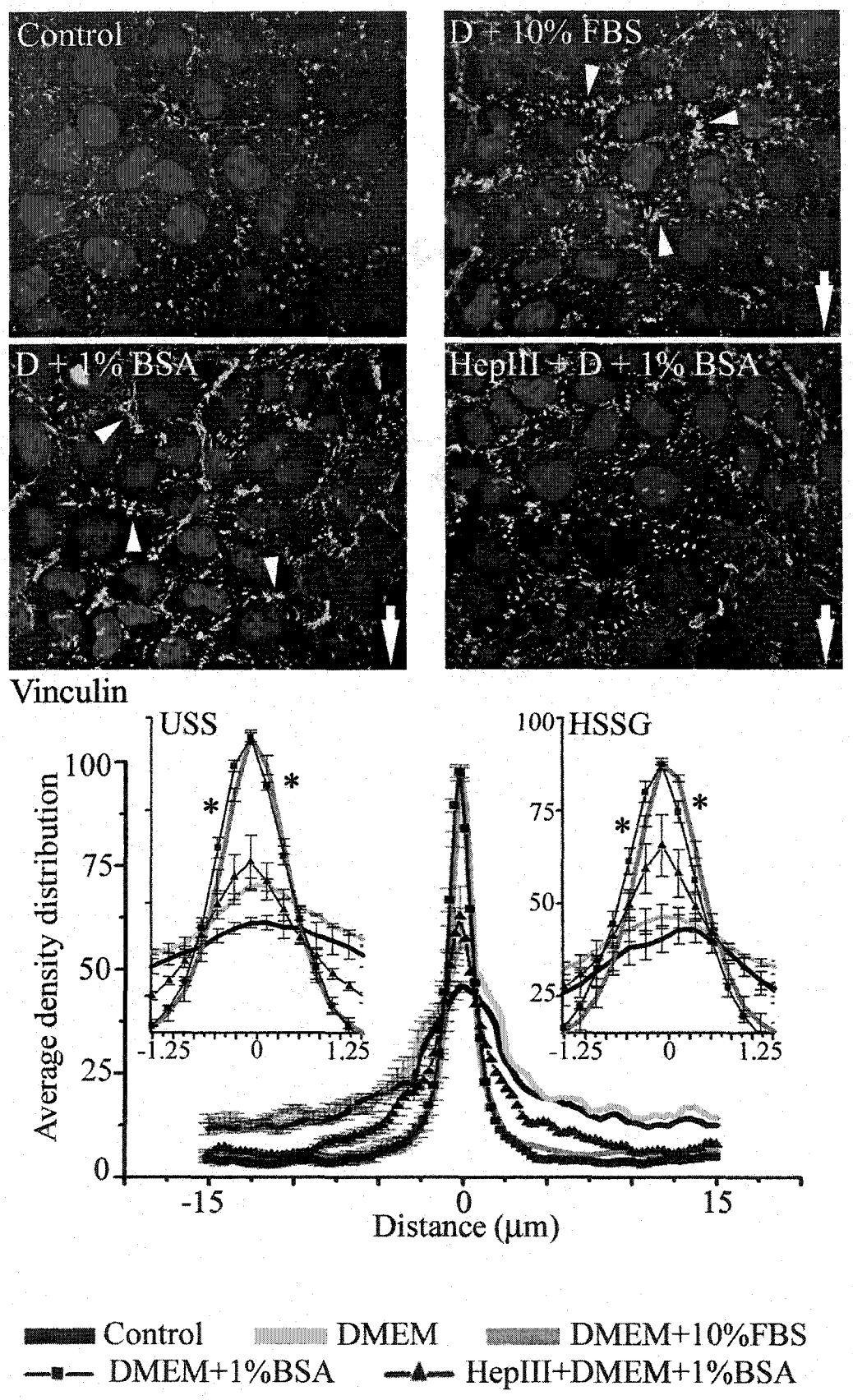

Figure 3.3. Reorganization of EC focal adhesions in response to fluid shear stress with various flow media. Cells were exposed to USS of 10.5 dyn/cm^2 and HSSG of 0 ~ 2500 dyn/cm^2/cm for 5 h. Effects of USS and HSSG on distribution of vinculin were analyzed using confocal microscopy. Overall average protein density profiles from stacked images of different treatments were plotted using Scion Image. Changes in the distributions of vinculin were detected using kurtosis analysis. Four images per experiment, total of 4 experiments, were taken from USS and HSSG regions. All data are presented as mean ± SEM, n = 160 (*, $p < 0.05$). Flow direction: arrows; redistribution of vinculin: arrowheads; scale bar: 20 μm.

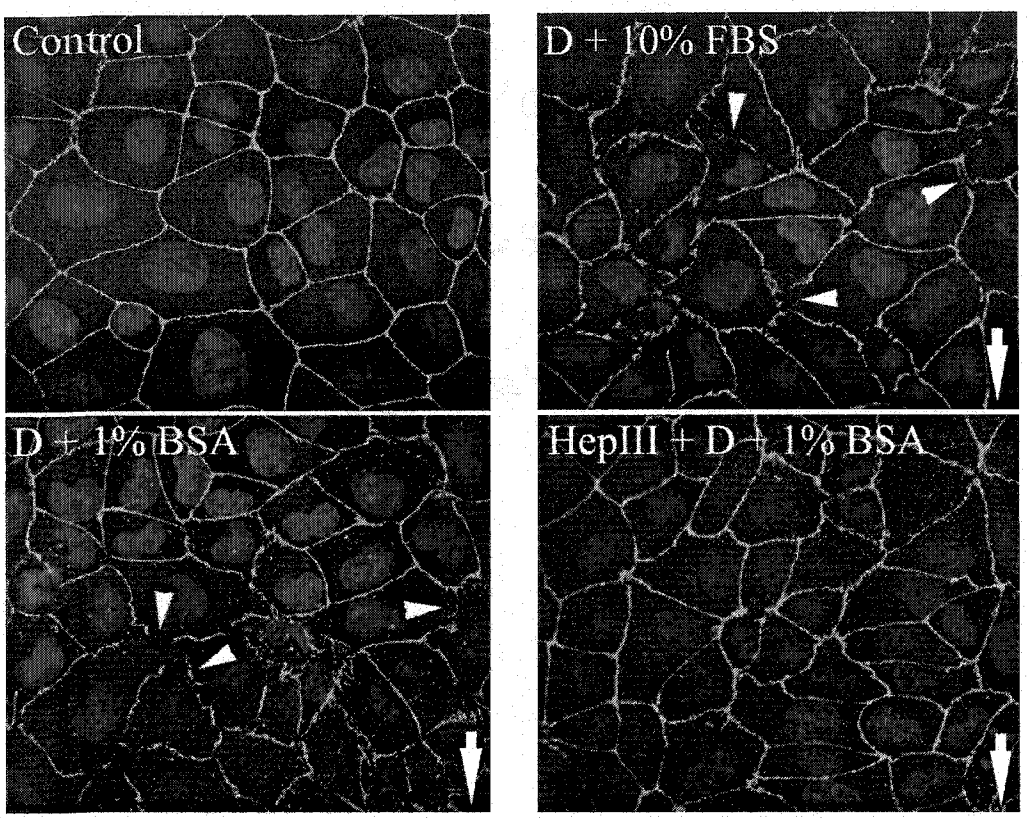

ZO-1

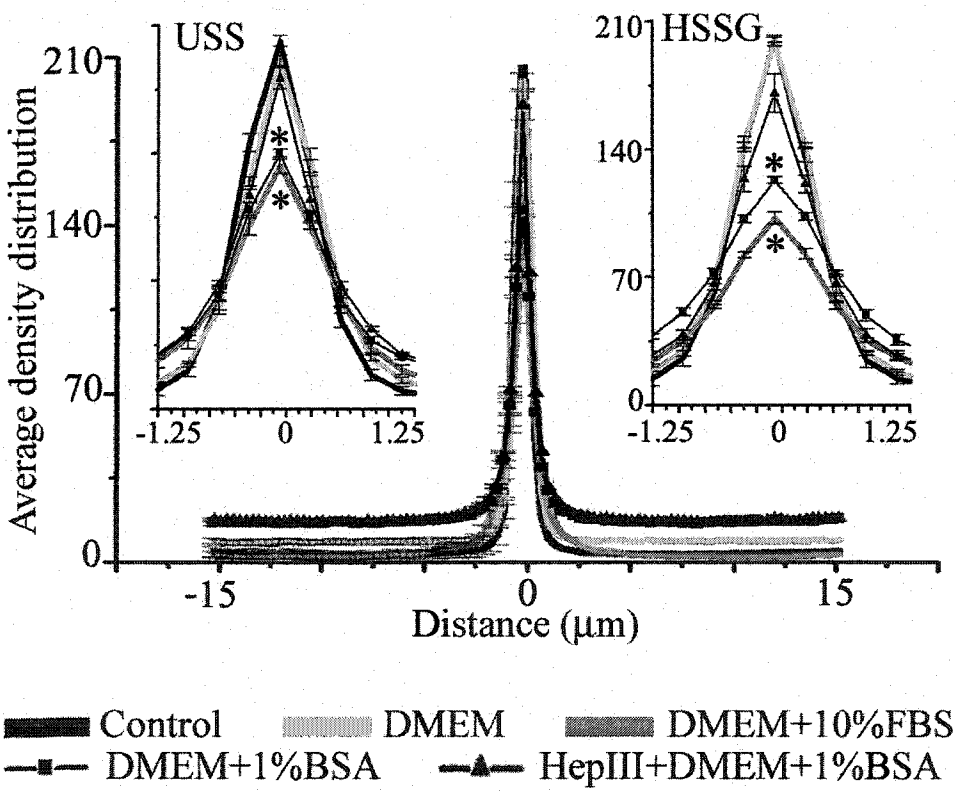

Figure 3.4. Junctional adaptation of EC in response to fluid shear stress with various flow media. Cells were exposed to USS of 10.5 dyn/cm^2 and HSSG of 0 ~ 2500 dyn/cm^2/cm for 5 h. Effects of USS and HSSG on the distribution of ZO-1 was analyzed using confocal microscopy. Overall average protein density profiles from stacked images of different treatments were plotted using Scion Image. Disruption of ZO-1 was detected using kurtosis analysis. Four images per experiment, total of 4 experiments, were taken from USS and HSSG regions. All data are presented as mean ± SEM, n = 160 (*, $p < 0.05$). Flow direction: arrow; disruption of ZO-1 at cell-cell borders: arrowheads; scale bar: 20 μm.

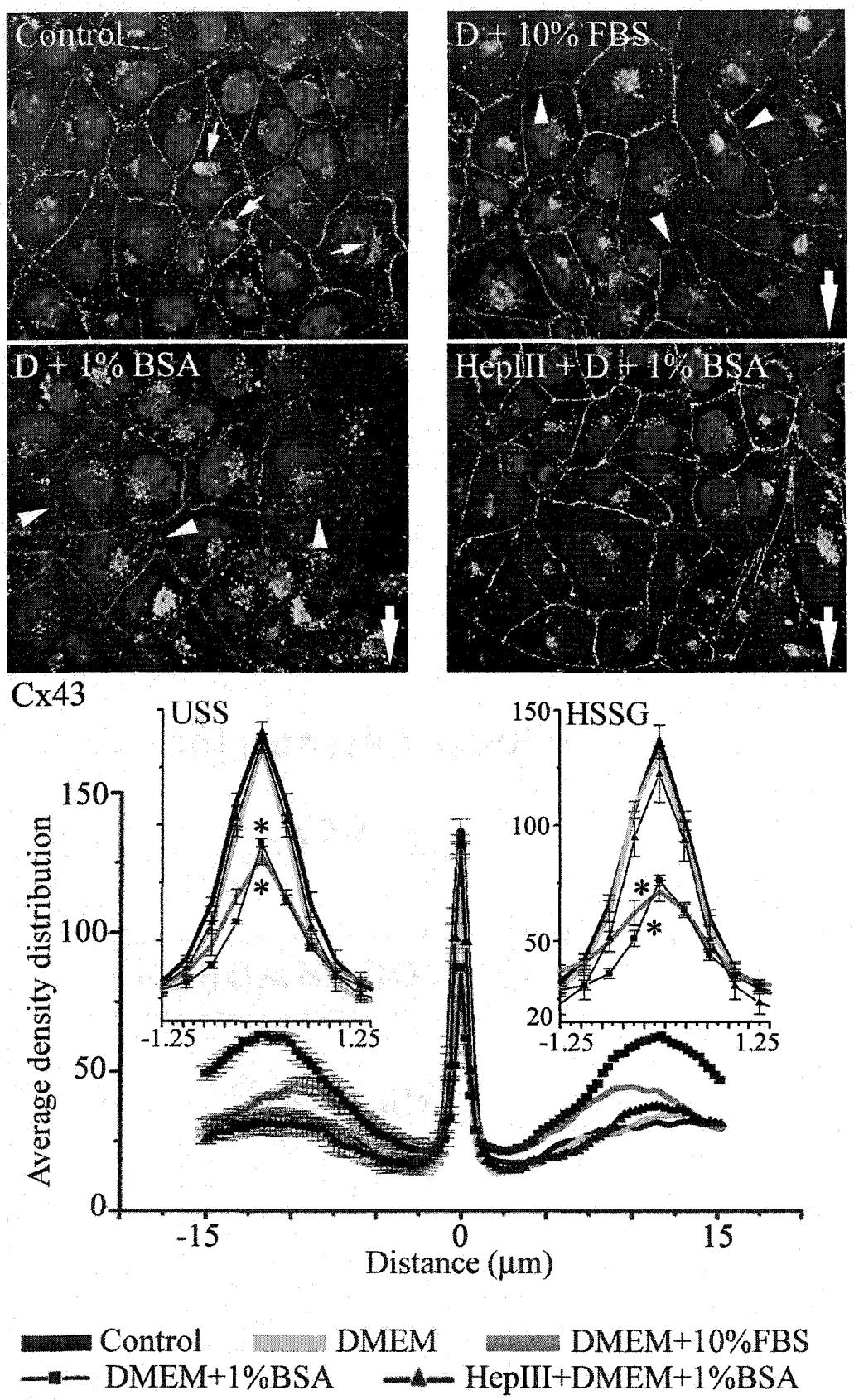

Figure 3.5. Junctional adaptation of EC in response to fluid shear stress with various flow media. Cells were exposed to USS of 10.5 dyn/cm^2 and HSSG of 0 ~ 2500 dyn/cm^2/cm for 5 h. Effects of USS and HSSG on the distribution of Cx43 were analyzed using confocal microscopy. Overall average protein density profiles from stacked images of different treatments were plotted using Scion Image. Disruption and distribution of Cx43 were detected using kurtosis analysis. Four images per experiment, total of 4 experiments, were taken from USS and HSSG regions. All data are presented as mean ± SEM, n = 160 (*, $p < 0.05$). Flow direction: arrow; perinuclear Cx43: thin arrows; disruption of Cx43 at cell-cell borders: arrowheads; scale bar: 20 μm.

Cx43. Our observation that there is virtually no actin cytoskeletal reorganization or vinculin redistribution in DMEM and that the redistribution in serum or BSA can be largely arrested by heparinase treatment strikingly demonstrates that the transmission of fluid shear stress to the actin filament system of the EC is very different when the shear stress is applied at the level of the apical plasmalemma, when the EG is collapsed, or at the edge of the EG. A key insight into the mechanism that might allow for such behavior is predicted in Weinbaum et al. (2003) where it is shown that the core proteins of the EG proteoglycans behave much like stiff fibers that are exquisitely designed to function as mechanotransducers at physiological flow rates. Syndecan I is the logical candidate for this mechanosensor since it has an extracellular domain of variable length and a cytoplasmic tail that links to F-actin (Bass and Humphries, 2002). In contrast, the plasmalemma is a viscous bilayer that can easily flow around membrane proteins (Sako and Kusumi, 1995). The principal restriction to this diffusion is the TJ where serial section electron microscopy has revealed one or more nearly continuous junction strands with occasional breaks (Adamson and Michel, 1993). Therefore, the plasmalemma might ripple under flow but should be incapable of transmitting fluid shear stress to the ACW beneath it since it has little structural rigidity. Although Weinbaum et al. (2003) predict a fundamentally different transmission of the fluid shear stress at the apical surface with and without the EG, the traction force on the focal adhesions at the basal surface will be the same for a given shear stress since the total reaction force at the base of the EC is identical.

Our hypothesis for the organization and function of the three basic actin structures (ACW, DPAB and SFs) and their coordinated response to fluid shear stress with and

without an EG are illustrated in Fig 3.6. The hypothesized essential features of the DPAB (Fig. 3.6A) are: (1) It is a nearly free floating rim that is flexibly attached by SFs to focal adhesions at the basal surface and ACW. It functions much like a rubber fender on a 'bumper car' that is constantly undergoing small collisions with its neighbors; (2) Under equilibrium or low shear flow conditions the DPAB is kept in lateral register with the DPAB in neighboring cells by the weak VE-cadherin linkages in the adherens junction (Ogunrinade et al., 2002). These linkages suffice for small flow disturbances where the DPAB bumper prevents collisions between neighboring cells in unprotected regions above and below the DPAB; (3) The DPAB and the ACW function as a single unit that can either move laterally or undergo small rotations about axes parallel to the cell surface, similar to what one would observe if one jumped on the bumper of a car. The SFs that tether the DPAB to the basal adhesions are weak compression elements that support tension; (4) When forces and torques exceed the weak bonds of the VE-cadherins these bonds rupture and the DPAB gradually breaks up into fragments that are recruited for the formation of new SFs in the rest of the cell. These changes are needed to stabilize the cell during a transient state in which the shape of the cell is changing dramatically.

The mechanism that causes fragmentation of the DPAB when the ECs are subject to fluid shear stresses above a critical magnitude and the EG is intact is illustrated in Fig. 3.6B. Drag on the tips of the core proteins at the edge of the EG causes a torque on the ACW that produces a clockwise rotation as shown in Fig. 3.6B. The bending moment on each core protein is small but the collective behavior of all the core proteins acts to produce a clockwise rotation of the DPAB. This creates a disjoining torque that is resisted by the VE-cadherins in the adherens junction. The quantitative feasibility of this

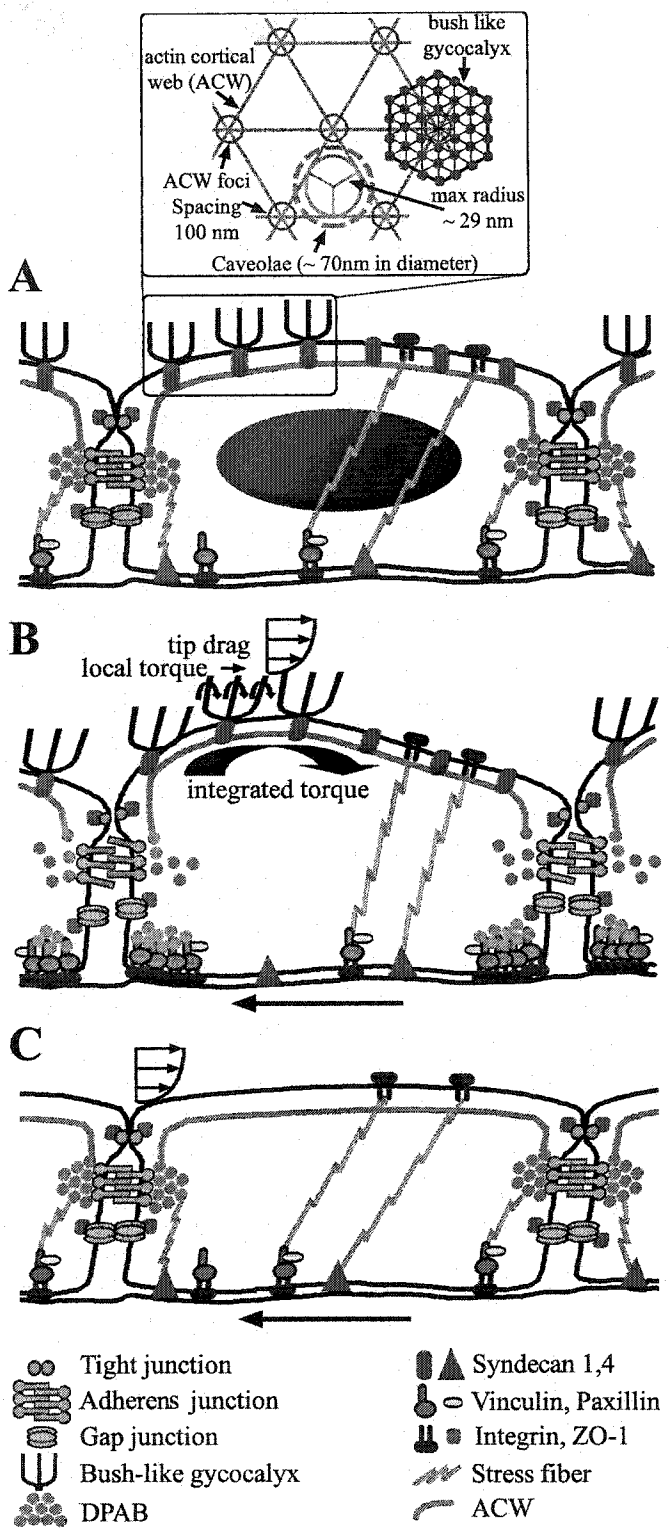

Figure 3.6. A conceptual 'bumper car' model for the structural organization of the EC in response to fluid shear stress. In its confluent control state (A) ECs displays an intact

DPAB that is localized to the adherens junction where it serves as the base for the ACW that we hypothesize is the underlying cortical scaffold for the entire apical surface. The ACW is invisible in immunofluorescence studies since it is comprised of a geodesic-like network of individual actin filaments in contrast to SFs and the DPAB, which are bundles of hundreds of α-actinin cross-linked anti-parallel microfilaments. The polygonal nature of the ACW was first reported in optical tweezer experiments (Sako and Kusumi, 1995). Recent freeze fracture EMs by Squire et al. (2001) in regions close to the plasmalemma have revealed a highly ordered hexagonal lattice with a characteristic spacing of 100 nm between junctional nodes (inset). Schematic diagrams showing adaptation steps for confluent ECs predicted by the bumper car model for intact (B) and compromised (C) EG in response to fluid shear stress. See text for detailed discussion.

hypothesis is demonstrated in *Appendix C*, where a simple model for the disjoining torque on the VE-cadherins predicts a disjoining force (~ 70 pN) that closely agrees with the 35-120 pN unbinding force estimated in Baumgartner et al. (Baumgartner et al., 2000).

We hypothesize that when this torque exceeds a threshold the adherens junction ruptures and the DPAB starts to fragment as seen in Fig. 3.2. The EC is now in an unstable configuration at its lateral margins and for the ECs to remain confluent, new focal adhesions and SFs need to be formed in the junctional region at the basal margins of the ECs. This requires the migration of vinculin to the EC borders seen in Fig. 3.3 to form new basal peripheral adhesions. This is a transient reorganization that, given sufficient

time, will approach a new stable configuration provided the cells are in a region of USS. In this scenario new DPABs form and the vinculin at the cell borders is dispersed once the basal SFs in the junctional region are no longer needed.

The sequence of events just described never occurs if the EG is compromised, as shown in Fig. 3.6C. The fluid shear stress now acts directly on the apical plasmalemma and the transmission of fluid shear stress is largely from the apical membrane of one EC to the next via the TJ complex, since the plasma membrane cannot flow through these nearly continuous junction strands. This type of shear stress transmission is described in (Fung and Liu, 1993). The important observation is that when the EG is collapsed the fluid shear stress is never transmitted to the ACW and, hence, no disjoining torque acts on the DPAB. The adherens junction is stable and the DPAB remains intact consistent with Fig. 3.2.

The question as to whether there is a torque threshold and whether the torque acts locally on individual core protein clusters or globally over the entire geodesic canopy in stimulating mechanical signaling is subtle. Weinbaum et al. (2003) predict that the torque on each core protein cluster can produce forces on the microfilaments in the ACW of the order of 0.1 pN. Forces of this magnitude have been shown to produce significant deformations in the microfilaments comprising the ACW (Sako and Kusumi, 1995). While this highly localized mechano-signaling is possible, it is not consistent with the observations in Florian et al. (2003). These investigators noticed that the release of NO was completely inhibited after a heparinase treatment that removed only 45% of HSPG. Our data also suggested that 30% reduction of HSPG (collapsed EG) was sufficient to inhibit cytoskeletal reorganization. Such behavior suggests a threshold response that

could be mediated by a minimum rotation and torque on the DPAB in our 'bumper car' model. This threshold would be difficult to explain if transmission occurred through each core protein cluster.

There are numerous signaling cascades that are activated by focal adhesions on the basal surface, leading to protein kinase C activation, tyrosine phosphorylation and the phosphorylation of focal adhesion kinase (FAK) (Burridge et al., 1992; Hu and Chien, 1997; Li et al., 1997). Paxillin is a marker for FAK in the Src kinase pathway (Turner, 2000). Thus, it is striking that the present results indicate virtually no change in the distribution of paxillin whether the EG is present or not. This strongly suggests a weak coupling between SFs at the basal membrane and the ACW associated with the DPAB. The key to this behavior would seem to be the fact that the total traction force at the basal surface does not depend on the existence of the EG. As pointed out previously, the total reaction force that is carried by the focal adhesions at the basal surface is equal and opposite to total fluid shear force acting at the apical plasmalemma whether the EG is removed or intact. These forces are transmitted to basal focal adhesions via SFs that attach at apical plaques (Kano et al., 2000) and via tensile forces that are transmitted to the basal membrane through the TJ complexes.

In the second part of this study we examined the effect of HSSGs on actin filament organization, vinculin distribution, and junction complex formation. For F-actin, regions of HSSG exhibited behavior similar to USS regions except that the fragmentation of the DPAB was more accentuated and there was a wider dispersion of the actin filaments. There was no distinguishable difference in vinculin distribution between HSSG and USS regions whether EG was present or not. These results suggest that

HSSGs play only a secondary role in the reorganization of actin filaments and their associated linker protein vinculin. Previous studies (Depaola et al., 1999; Thi et al., 2003) have shown that ZO-1 and Cx43 expression are sensitive to fluid shear stress in USS and HSSG regions since stable junctions are not able to form. Recent studies suggest that in addition to organizing TJ proteins, such as occludin and ZO-2 and enabling Cx43 to dock at the cell surface, ZO-1 serves as a linker between tight junction proteins and F-actin (Giepmans and Moolenaar, 1998; Fanning et al., 1998). Thus, we further speculate that it might also serve as a tertiary mechanotransducer at cell-cell junctions. In general, ECs in the HSSG region experience more significant junctional disruption than those in the USS region. Therefore, we conclude that apparent differences in distributions of F-actin and vinculin, as well as severe ZO-1 and Cx43 disruption commonly associated with ECs in the HSSG region, demonstrate cell-cell inability to stabilize and establish steady state adhesion and hence, permanent contact-inhibition. Although our studies were performed in a 5 h period, we predict that changes corresponding to USS regions are only transient until the cells are fully adapted to the flow, whereas changes corresponding to HSSG regions are permanent as shown by others with 24-30 h studies (Davies et al., 1986; Girard and Nerem, 1995; Depaola et al., 1999).

In summary, the model in Fig. 3.6 suggests a dichotomy of structure and function with the DPAB and the ACW acting nearly independently of the SFs associated with the integrin complexes at the basal and apical membranes. This could account for the observation that degradation of the EG blocks NO formation (Pohl et al., 1991; Hecker et al., 1993; Florian et al., 2003), but has no influence on PGI_2 production (Hecker et al., 1993). Our 'bumper car' model predicts that signaling through basal adhesion plaques

linked to the apical plasma membrane by SFs, which can mediate prostaglandin production (Ponik and Pavalko, 2004), would be unaffected by degradation of the EG. In addition, the 'bumper car' model predicts that a partially deformed ACW, which is triggered by the disruption of the adherens junction and its associated DPAB, is needed for caveolae (~ 70 nm diameter) to invaginate in caveolin rich areas. The inset in Fig 3.4A shows that the intact ACW may be expected to inhibit caveolae formation since their diameters exceed the largest sphere (~ 60 nm diameter) that can easily fit through an ordered ACW. This may explain why shear stress increases caveolae density at the luminal surface of endothelial cells, as observed between 6 h and 3 days after application of shear (Boyd et al., 2003; Rizzo et al., 2003).

Acknowledgements

We thank Drs. Andrei Iacobas, Alejandra Bosco and Karen Cusato for advice on confocal image analysis, Dr. Elliot Hertzberg (AECOM) for generous supply of Cx43 antibody, and Dr. Anthony Ashton (AECOM) for providing the RFPEC cell line. Supported by PO1 (DK06037), NS41282 and HL 35549.

Appendix A

Derivation of an infinite series solution of the two-dimensional steady Navier-Stokes equation.

Governing Equations

Fluid flow in a conventional flow chamber has usually been modeled as fully developed laminar flow between infinite parallel plates. In our study, we have modified the gasket of the conventional parallel plate flow chamber to obtain a very narrow flow space (4×60 mm) which has enabled us to analyze the effects of uniform shear stress (USS) as well as spatial high shear stress gradients (HSSGs) in the same flow cross-section. Our model below describes steady unidirectional flow through a rectangular conduit.

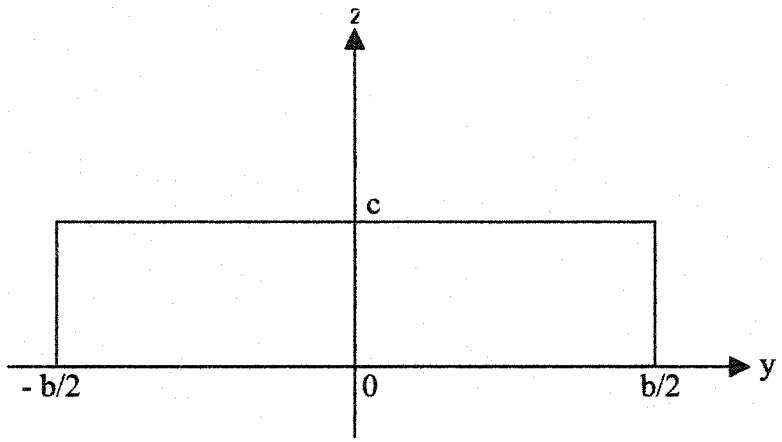

Fig. A1. Cross-sectional geometry of rectangular conduit; flow is symmetric with respect to z axis. b: channel width; c: channel height.

As shown in Fig.A1, flow is assumed to be in the x direction. The reduced

governing equation derived from the full Navier-Stokes equation is

$$\mu\left(\frac{\partial^2}{\partial y^2}+\frac{\partial^2}{\partial z^2}\right)u=-K, \qquad \textbf{[A1]}$$

where the constant $K = -\partial p/\partial x$, μ is the viscosity and u is the velocity.

Boundary conditions which satisfy Eq. **A1** are:

$u = 0$ at $z = 0, c$ and $y = \pm b/2$, where b is the channel width and c is the channel height. From symmetry $\partial u/\partial y = 0$ at $y = 0$.

The infinite series solution to Eq. **A1**, which satisfies these conditions is,

$$u=\frac{-K}{\mu}\left[\frac{z^2}{2}-\frac{cz}{2}-\sum_{n=1}^{\infty}\frac{2c^2(\cos(n\pi)-1)}{(n\pi)^3\cosh\left(\frac{n\pi b}{2c}\right)}\cosh\left(\frac{n\pi}{c}y\right)\sin\left(\frac{n\pi}{c}z\right)\right]. \qquad \textbf{[A2]}$$

Using Eq. **A2,** one can calculate the volumetric flow rate, Q, as follows:

$$Q=\int_0^c\int_{-\frac{b}{2}}^{\frac{b}{2}}u\,dy\,dz=\frac{-K}{\mu}\left[-\frac{bc^3}{12}+4c^4\sum_{n=1}^{\infty}\frac{(\cos(n\pi)-1)}{(n\pi)^5}\tanh\left(\frac{n\pi b}{2c}\right)(\cos(n\pi)-1)\right]. \qquad \textbf{[A3]}$$

The expression for the shear stress distribution along the bottom wall of the flow channel is given by

$$\tau\big|_{z=0}=\mu\frac{\partial u}{\partial z}=-K\left[-\frac{c}{2}-\sum_{n=1}^{\infty}\frac{2c\,(\cos(n\pi)-1)}{(n\pi)^2\cosh\left(\frac{n\pi b}{2c}\right)}\cosh\left(\frac{n\pi}{c}y\right)\right]. \qquad \textbf{[A4]}$$

From Eq. **A4**, shear stress gradients can be obtained by differentiating the shear stress distribution,

$$\left.\frac{d\tau}{dy}\right|_{z=0} = -K\left[-\sum_{n=1}^{\infty}\frac{2\,(\cos(n\pi)-1)}{n\pi\cosh\left(\frac{n\pi b}{2c}\right)}\sinh\left(\frac{n\pi}{2c}y\right)\right]. \qquad \textbf{[A5]}$$

The distributions of the shear stress and its gradients are plotted in Fig. A2.

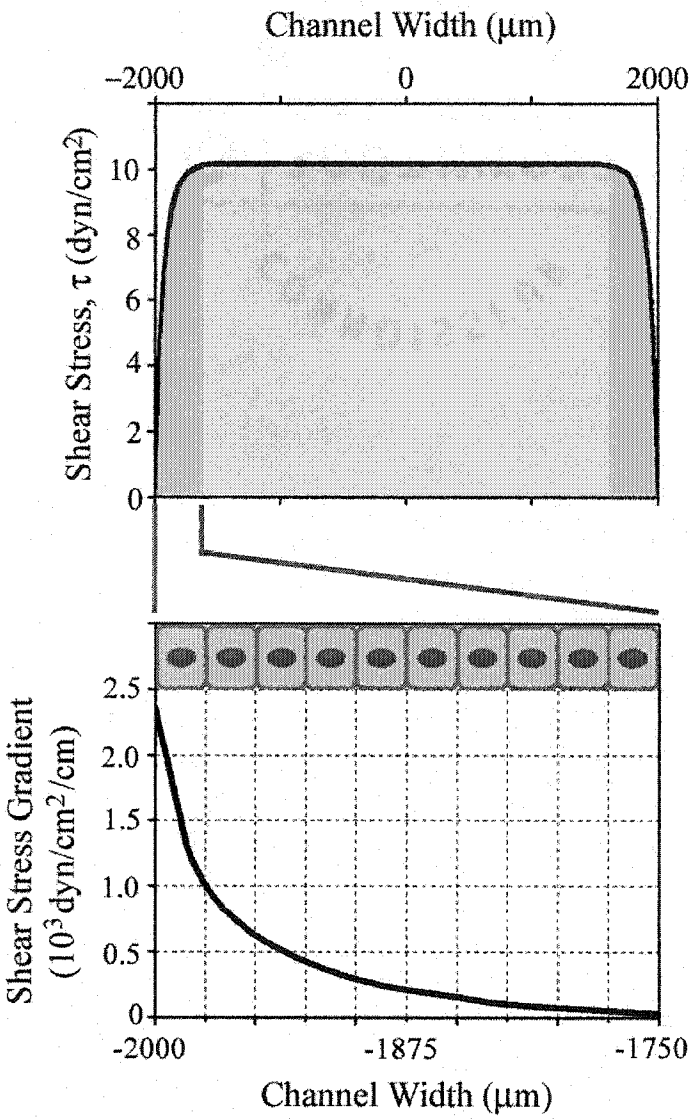

Fig. A2. Shear stress and spatial shear gradient distributions in narrow rectangular conduit. (A) Shear stress is uniform in the central region and tapered off to zero in the corner region. (B) Cells in the corner region, about 250μm (10-cell length scale) from the edge of the chamber, experienced spatial high shear stress gradients. Results shown for a flow chamber with 4×60 mm cross-section whose wall shear stress in the central region is 10.5 dyn/cm^2.

Appendix B

Detailed Methods

Immunofluorescence and Confocal Microscopy

Both controls and shear stress exposed cells were fixed with 2% formaldehyde, permeabilized with 0.4% Triton-X100 (Sigma) and blocked with 10% goat serum (GibcoBRL) in 1X PBS as described in (Thi et al., 2003). Cells were incubated with primary antibodies overnight at 4°C and secondary antibodies for 1 hour at room temperature with intervening washes. Antibodies used were polyclonal antibodies Cx43 (courtesy of Dr. E. Hertzberg, AECOM), 1:1000; and ZO-1 (Zymed), 1:250; and monoclonal antibodies Vinculin (Chemicon), 1:200; and Paxillin (Chemicon), 1:200. Secondary antibodies (Molecular Probes) conjugated to Alexa 488 or 594 were used at 1:1000. For filamentous actin (F-actin) staining, cells were incubated with rhodamine-labeled phalloidin (Sigma), 1:200, for 30 minutes at room temperature immediately after fixation. Coverslips were mounted with medium containing the nucleophilic dye Dapi (Vector) on slides.

Heparinase III (Sigma) was used at 15 mU/ml to selectively digest heparan sulfate within the glycocalyx as described in (Florian et al., 2003). Detection of cell surface heparan sulfate was performed on live cells as follows: prior to the HSPG labeling, cells were incubated with CellTracker Orange CMTMR (Molecular Probes), 5 μM, for 45 minutes at 37°C to identify the cell body. Cells were chilled briefly on ice and rinsed three times with ice cold 1X PBS. Cell were then incubated on ice with primary heparan

sulfate antibody (US Biological), 1:200, for 1 hour, followed by ice cold 1X PBS rinses and fixation with intervening washes. Secondary antibody Alexa 488 (Molecular Probes) was used at 1:200. Coverslips were mounted as described above.

All the control, HSSG and USS regions were examined on an Olympus FluoView FV500 Laser Scanning Confocal Microscope (Olympus). Images were taken serially from top to bottom of each cell field using a 'z' plane motorized sub-stage. The upper and lower z-axis positions were carefully selected so that the entire sample was imaged to generate the same number of images in each series. Image stacks (typically 13-23 optical sections per stack relative to different protein stainings) of cells in HSSG and USS regions were collected at 0.31-0.41 μm *z*-axis steps. Four images from both the corner and the mid regions were taken for each set of experiments. For HSPG, eight images per experiment were taken for each set of experiments.

Protein Distribution

Overall average protein density profiles of 10 cell pairs from each stacked image, where each cell pair was randomly selected as long as the nuclei were within the fixed range of 30μm with the apposition membrane approximately in the middle, were plotted using Scion Image (NIH). Changes in protein distribution and reorganization among the cell pairs were detected using kurtosis analysis (peakness or flatness vs. normal distribution). Similarly, to quantify HSPG removal or reduction, the average protein density profile for the whole image field was plotted and measured using Scion Image. Multi-plane view analyses were performed using Imaris (Bitplane AG).

Appendix C

Estimation of the disjoining torque on the actin cortical web (ACW) and the resulting disjoining force acting on the adherens junction.

The theoretical model developed in Weinbaum et al. (2003) shows that the fluid shear stress acting at the edge of the endothelial glycocalyx (EG) is converted to a drag that acts on the tips of the core proteins within <20 nm of the EG edge. This creates a torque on the core proteins of the EG that bypasses the membrane and acts directly on the actin cortical web (ACW) where it is transmitted to the plane of the adherens junction and the dense peripheral actin band (DPAB) at the base of ACW. There are three components to the total lever arm as sketched in Fig. C1, the thickness of the EG, L_G, the average height of the nuclear bulge above the apical membrane, $L_N/2$, and the distance from the plane of the DPAB to the apical surface at the edge of the cell, L_B. The total lever arm is the sum of these three components.

Each of these three components can be estimated as follows. The measured thickness L_G of the EG layer varies from, $150 < L_G < 400$ nm. We need next to locate the plane of the adherens junctions and the DPAB. We shall assume that this plane lies midway between the tight junction (TJ) complex, which has been measured in Adamson et al. (2004) to be ~ 60 nm below the entrance to the endothelial cell (EC) cleft at the apical surface, and the location of the gap junctions. Our multi-plane view analyses of stacked confocal images indicate that the average maximum height of the EC in the

nuclear region is approximately 4.2 μm and the average height of the tight junction above the focal adhesions at the base of the cell, as indicated by ZO-1 fluorescence, is ~ 1.75 μm. The height of the gap junctions above this base as indicated by Cx43 labeling, is ~ 0.54 μm. Since we assume the adherens junction lies midway between these two junctions it is ~ 0.6 μm below the tight junction. This would place the DPAB at a distance L_B ~ 660 nm below the apical surface of the EC at its edge and the latter 1.8 μm above the focal adhesions at its base. Thus, the maximum height of the nuclear region of the EC is L_N = 2.4 μm higher on average than this edge region. If we assume the average height of the nuclear bulge at the apical surface is ~ $L_N/2$, then the average elevation of the apical surface above its height at the EC edge is 1.2 μm. Thus, as shown in Fig. C1 the total lever arm is $L_G + L_B + L_N/2$. If A_c is the en face of the EC and τ is the fluid shear stress at the EC edge, then the torque, $\mathbf{T} = T\mathbf{i}$, imposed by the EG on the DPAB is

$$\mathbf{T} = \tau A_c(L_G + L_B + L_N/2)\mathbf{i}, \qquad \textbf{[C1].}$$

For an elliptical cell 30μm in length and 20 μm in width, $A_c = \pi \times 15 \times 10\ \mu m^2 \approx 500\ \mu m^2$. For $\tau = 10$ dyn/cm^2 and $L_G + L_B + L_N/2 \approx 200 + 660 + (2400/2) \approx 2060$ nm then $\mathbf{T} = 103 \times 10^{-3}$ pN.cm. A more sophisticated model needs to be developed for the restraining force exerted on the VE-cadherins but if **T** were restrained by a counterclockwise moment due to a concentrated force acting on the edge of a cell with an effective diameter of 30 μm (15 μm lever arm) the disjoining force, **F**, on the adherens junction can be calculated by requiring that $\mathbf{T} = \mathbf{F} \times \mathbf{R}$, where **R** is the effective radius. Thus, the disjoining force on the adherens junction would be ≈ 70 pN. This exceeds the disjoining force measured for single VE-cadherin interaction that lies between 35-55 pN and falls in the range of higher order disjoining forces for multiple interactions that lies

between 70-120 pN (Baumgartner et al. 2000). This larger force would be required to unzipper the adherens junction.

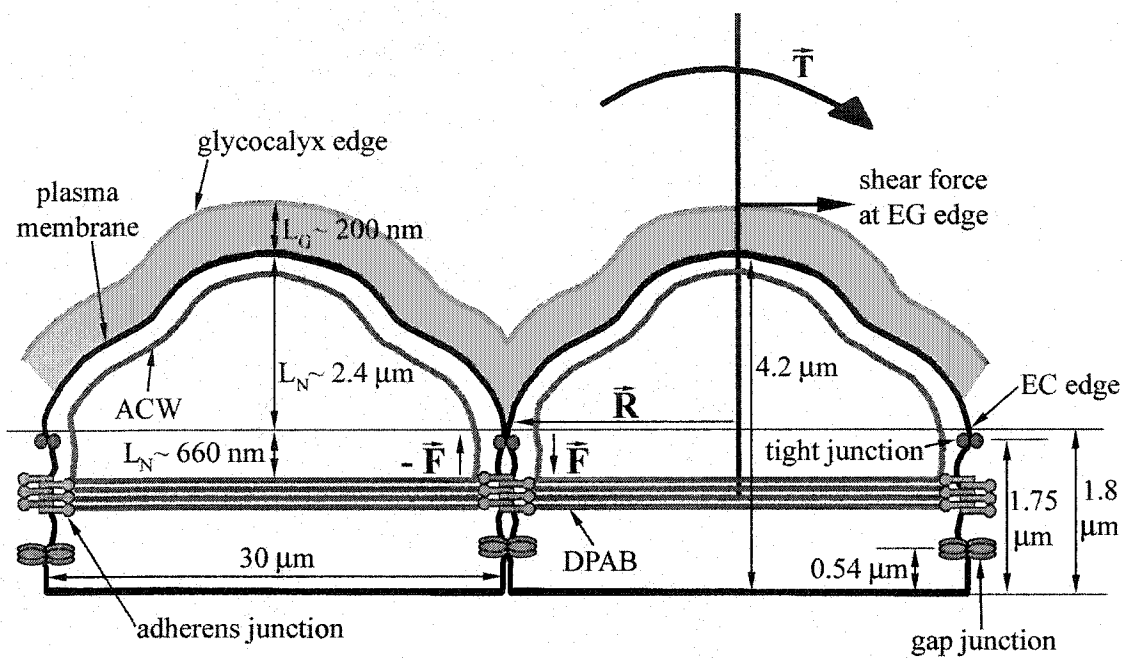

Fig. C1. Sketch of disjoining torque (**T**) acting directly on the actin cortical web (ACW) and the resulting disjoining force (**F**) on the adherens junction and the dense peripheral band (DPAB) showing the three components of the total lever arm from the adherens junction or DPAB (not drawn to scale). **R**: the effective EC radius; L_G: the thickness of the glycocalyx; L_N: the height of the nuclear bulge above the apical membrane; L_B: the distance from the plane of the DPAB to the apical surface at the edge of EC.

Chapter 4

Summary and Discussion

Summary

In this chapter, we summarize our studies with regard to past and present key insights on cell-cell mechanotransduction and propose future directions for this research. It is widely recognized that mechanotransduction plays an important role in homeostasis of various fluid filled organs such as bone and vessel wall endothelium and their cellular functions. It has been well accepted that possible mechanosensors are located either on the apical or basal surface of the cell (transmembrane proteins on the cell surface, stress activated channels, mechanosensitive ion channels, integrins and focal adhesions) and the signal transmission is carried out via the cell cytoskeleton. Over the past several decades many researchers who were attempting to better understand the mechanisms involved in shear induced signal transduction pathways generally focused their attentions on cytoskeletal rearrangement either via focal adhesions or junctional pathways, and on mechanochemical signaling pathways such as Ca^{++}, NO, PGE_2, PGI_2, and protein kinase pathways. Regardless of the cell types, either bone or endothelial cells, the adaptation processes and signaling pathways in response to various flow dynamics are very similar.

Although past flow studies have made the cellular mechanotransduction mechanisms more comprehensible with regard to activation of many of the specific signaling pathways, they have been unable to identify likely mechanosensor(s) for those pathways. This is partly due to lack of knowledge on the detailed architecture of the cytoskeleton and surface glycocalyx of various cell types. The detailed structure of the glycocalyx in both bone and endothelial cells has been largely unknown until very recently. Therefore the majority of *in vitro* experiments in the past were unaware of the

existence of the glycocalyx on cultured cells, and consequently its role as a possible mechanosensor has often been ignored. The knowledge prior to the discovery of the glycocalyx as a mechanosensor is recapitulated below.

The cell cytoskeleton possesses a structure that may very well be capable of serving as a signal transmission structure. Therefore, the influence of shear stress on the cytoskeleton has been widely studied for the both bone cell network and endothelial cells. It is commonly observed that bone and endothelial cells initially respond to fluid shear stress by increased formation of stress fibers to enhance the focal and lateral attachments, followed by the disruption of dense peripheral actin band to facilitate the cellular realignment during longer exposure times (~ 6h), and eventually realigning in the direction of the flow with far more stress fibers and complex actin network structures during a 24 h flow period (Ookawa et al., 1992; Girard and Nerem, 1995; Satcher et al., 1997; Galbraith et al., 1998; Schnittler et al., 2001). Initial bursts of intracellular Ca^{++} (via IP_3), upregulation of integrins, c-fos and cyclooxygenase-2 (COX-2) have been shown to play some important roles in shear induced SF formations. Depolymerizing actin (cytochalasin B and D) or chelating intracellular Ca^{++} or blocking α-actinin mediated pathways failed to realign cells, produce c-fos and COX-2 expression and prostaglandin (PGI_2 and PGE_2) release, or form SFs (Ajubi et al., 1996; Pavalko et al., 1998; Chen et al., 2000). Rapid activation of FAK and Src are also shown to associated with fluid-induced shear stress (Li et al., 1997; Takahashi et al., 1997). The vital role of focal adhesions in shear stress induction of COX-2 and PGE_2 release in osteoblast cells was demonstrated by specifically blocking integrin-fibronectin binding with Arg-GLy-Asp-Ser (RGDS) peptides (Ponik and Pavalko, 2004). These data suggest that focal

adhesions and SF polymerization play a close knit role in response to fluid shear stress.

While Cx43 knockout (KO) mice exhibit delayed ossification and dysfunctioning of bone cells (Lecanda et al., 2000) and vascular endothelial cell-specific KO mice express hypertension and bradycardia (Liao et al., 2001), little attention has been paid to shear modulation of the gap junctional complex compared to widely studied changes in cytoskeleton and other signaling pathways. Striking effects of shear stress on expression of gap junction proteins have been observed in multiple cell types (osteoblasts, osteocytes, and endothelial cells). We and others observed marked disruption of membrane bound connexins and regulation of connexin gene expressions in a shear dependent manner on bone and endothelial cells (Depaola et al., 1999; Thi et al., 2003). In addition, gap junctions are believed to regulate steady or oscillating fluid shear stress induced PGE_2 release (Saunders et al., 2001; Cheng et al., 2001a; Saunders et al., 2003). Little is known about shear stress regulation of tight junctions although their physiological control is critically important in permeability of endothelial cells. Similar to changes in connexins, the tight junction associated proteins occludin and ZO-1 have been shown to be severely downregulated at the appositional membrane during 1-3 h of laminar flow exposure (DeMaio et al., 2001; Thi et al., 2003). Moreover, shear stress regulation of adherens junctions has been routinely studied especially in endothelial cells. During the initial adaptation phase (~8h) stabilized VE-cadherins, α-, β-catenins in the junctions become disarrayed and during the recovery phase (24-48 h) these junctions become colocalized with the ends of SFs along the lateral side of the cells (Schnittler et al., 1997; Noria et al., 1999). In addition, findings by Noria et al. (1999) show that plakoglobin gradually disappears from the junctions during 24 h of shear stress exposure

and reappears at 48 h. Studies by Schnittler et al. (1997) indicate that these junction integrities are highly dependent on extracellular Ca^{++} and plakoglobin; depleting plakoglobin from the cells by microinjection with antisense oligonucleotides results in junctional disruption in response to 1 h of fluid shear stress. These data suggest that under shear stress or low extracellular Ca^{++}, loss of plakoglobin may cause cadherins to disconnect either from the cytoskeleton or the neighboring cadherins and thus affect the state of junctional assembly.

A more thoroughly explored area in mechanotransduction of bone and endothelial cells is flow mediated release of numerous factors such as NO, PGI_2, and PGE_2. Both cell types display the same pattern of NO release (biphasic) in response to fluid flow; a rapid and transient production phase (2-5 min) and a sustained production phase (Pohl et al., 1991; Hecker et al., 1993; Kuchan et al., 1994; Kuchan and Frangos, 1994; Klein-Nulend et al., 1996; Smalt et al., 1997; Klein-Nulend et al., 1998). Studies by Kuchan and coworkers (Kuchan et al., 1994; Kuchan and Frangos, 1994) suggest that the transient phase of NO production depends on Ca^{++}-Calmodulin and G-protein pathways whereas the sustained phase depends on shear stress. Similarly PGI_2 release mediated by fluid shear stress also displays an initial burst and steady state production in endothelial cells (Frangos et al., 1985; Hecker et al., 1993). On the other hand, shear stress regulation on bone cells exhibits slow PGE_2 (after 10 min) and even slower PGI_2 release (Reich and Frangos, 1993; Klein-Nulend et al., 1995b; Ajubi et al., 1996; Klein-Nulend et al., 1997; Reich et al., 1997; Smalt et al., 1997; Cheng et al., 2001a; Saunders et al., 2003; Norvell et al., 2004; Ponik and Pavalko, 2004). The studies above suggested that PGI_2 and PGE_2 release is regulated by focal adhesions, G-proteins, and gap junction mediated

intercellular diffusion of Ca^{++} and IP_3. Recently, caveolae have emerged as another candidate for mechanosensors. Caveolae were first identified in endothelial cells but appear on the surfaces of most cells (Anderson, 1993). They are 50-90 nm in diameter and are located on or within 100 nm below the plasma membrane. They are the sites of Ca^{++} entry, enriched with caveolin-1, calmodulin, nitric oxide synthase (eNOS), prostacyclin synthase (PGIS), and COX-2 (Isshiki and Anderson, 2003; Spisni et al., 2003). Recent evidence indicates the localization of several actin binding proteins in caveolae, which in turn suggests the possible linkage between caveolae and the actin cytoskeleton (Anderson, 1993; Isshiki and Anderson, 2003). Gap junction protein Cx43 has also been shown to interact with caveolae associated protein caveolin-1(Schubert et al., 2002). In addition enhanced NO production resulting from eNOS regulation appears to be associated with caveolin-1 KO mice (Isshiki and Anderson, 2003). Studies have demonstrated that fluid shear stress upregulates membrane bound caveolin-1, eNOS and caveolae (Boyd et al., 2003; Rizzo et al., 2003; Sun et al., 2003). The elevated caveolae expression is observed between 6 h to 3 days after the flow exposure.

Discussion

Very little attention has been paid to the importance of the glycocalyx in the bone cell network and the endothelium, in part due to the wide disparity in the function of the cells and the organs in which they reside. While these cells may have different functional responses to maintain their organs' homeostasis, they appear to have two common links:

1) a thin surface layer called the glycocalyx which is highly likely to serve as a sensor for the mechanical shearing forces in their fluid filled environments, and 2) the actin cytoskeleton that connects apical, basal, and lateral parts of the cells.

While numerous theoretical models for the bone cell network have considered the presence of a pericellular matrix and predicted the potential structure in the fluid annulus surrounding the bone cells (Weinbaum et al., 1994; Cowin et al., 1995; Weinbaum et al., 2001; You et al., 2001) (Harrigan and Hamilton, 1993) have been very few experimental studies to verify its existence (Sauren et al., 1992). Although we were aware of the existence of a pericellular matrix *in vivo*, like many investigators we overlooked the possible existence of this layer in *in vitro* cell culture studies and failed to recognize it as a possible mechanosensor. In addition there are some limitations to the studies we performed in Chapter 2. Even though the shear forces that we applied to the bone cells are in the physiological range, the flow pattern was not. Current experimental studies on bone cells use either oscillatory or pulsatile flow profiles. At present, we realized from model predictions as well as the morphological evidence of You and coworkers (You et al., 2001; You et al., 2004) that the transverse elements of the pericellular matrix form a bridge between the cell membrane and mineralized canalicular wall and have the capability of amplifying the fluid drag force to produce cell cytoskeletal strains 20-100 fold larger than bone tissue strain. This behavior can not be mimicked in flow chamber studies since the cell monolayer or cell processes are not tethered by the transverse elements to a supporting structure and, therefore, hampering the means for further experimental investigation. Recent *in vitro* experiments demonstrated that cultured bone cells possess a hyaluronic acid rich layer (Reilly et al., 2003) and further suggested that

the signaling pathway for PGE_2 is glycocalyx dependent whereas the pathway for Ca^{++} is not. Apparently more studies need to be done to clarify the role of bone pericellular matrix as well as its specific protein components.

On the other hand many investigators are aware of the presence of the endothelial glycocalyx, mostly as a molecular sieve or barrier between blood cells and endothelial cells. A recent breakthrough model by Squire et al. (Squire et al., 2001) identified the detailed structure of the glycocalyx for the first time. Based on the suggested structure, a new theoretical model has predicted a primary mechanotransduction pathway through the glycocalyx to the underlying actin cytoskeleton (Weinbaum et al., 2003). This prediction was confirmed by Florian et al. (Florian et al., 2003) who for the first time verified the presence of a heparan sulfate rich glycocalyx in cultured endothelial cells. We further explored the role of the glycocalyx under various conditions (presence, absence, or collapse) with respect to cell cytoskeleton, junctional complexes, and focal adhesions and came across the two possible signaling pathways for NO and PGI_2 release that are overlooked in many previous studies.

In the past decade several investigators studying the shear induced NO and PGI_2 release in the small arteries observed that when sialic acids or heparan sulfate proteoglycans were removed from the endothelial glycocalyx by neuraminidase or heparinase the shear induced NO was abolished whereas PGI_2 was not (Pohl et al., 1991; Hecker et al., 1993; Florian et al., 2003). In addition, our studies from the Chapter 3 showed no reorganization of the actin cytoskeleton, junctional complexes and focal adhesions when the glycocalyx was compromised. These striking results suggest that the surface layer glycocalyx is the primary mechanosensor of the fluid shearing forces that

directly regulates the underlying actin cytoskeleton.

There is increasing evidence that PGI_2 and PGE_2 production relies on focal adhesions and the cytoskeleton and it has become apparent that cells with either disrupted actin cytoskeleton or compromised focal contacts fail to release shear induced PGI_2 and PGE_2 (Ajubi et al., 1996; Sawyer et al., 2001; Ponik and Pavalko, 2004). These observations have led us to believe that there must be two distinct pathways for NO and PGI_2 or PGE_2 production. Since the cell cytoskeleton is linked to every aspect of the cell, we have proposed in Chapter 3 that there must be several cytoskeletal structures regulating various pathways; one possible structure, the actin cortical web and dense peripheral actin band, regulates the apical portion of the cell and the other structure, transverse stress fibers bridging apical and basal surfaces of the cell, regulates basal attachements. Collectively piecing together these key insights we propose a conceptual 'bumper car' model for the cytoskeleton of the endothelial cells with a major dichotomy in structure and function at the basal and apical aspects of the cells: one signaling cascade probably originating from the actin cortical web and dense peripheral band at the apical surface of the cell involving the release of NO via caveolae, and the other from focal adhesions and stress fibers at the basal aspect of the cell involving the release of PGI_2 and PGE_2. In our model caveolae formation depends on the integrity of actin cortical web. Based on numerous studies on cytoskeletal adaptation many of us have assumed that the actin cytoskeleton reaches its steady state once the cell is fully aligned in the direction of the flow (> 24 h flow exposure). That is to assume that the actin cortical web and the dense peripheral band have reformed to its control state. Studies on shear induced caveolae, on the other hand, show that caveolae density is increased up to 3 days after

application of shear (Boyd et al., 2003). Taking these factors and our proposed actin cortical web model into account, we intuitively concluded that the actual time needed for the actin cortical web to reach its steady state might be longer than 3 days.

There are various conflicting data on the role of the cytoskeleton and the shear induced NO and PGI_2 or PGE_2 releases. Knudsen and Frangos (Knudsen and Frangos, 1997) reported that shear induced NO production is independent of the actin and microtubule cytoskeletons. This finding is in contrast to similar studies in which the production of shear induced NO or dilation is attenuated by treating the isolated rabbit arteries with either cytochalasin B or colchicine (Hutcheson and Griffith, 1996; Sun et al., 2001). Likewise, it has been shown that the production of PGI_2 and PGE_2 in response to shear stress does not require intact actin or microtubules in cultured osteoblasts (Norvell et al., 2004). This observation contradicted the finding that disrupting the cytoskeleton using cytochalasin B completely abolished the shear induced PGI_2 and PGE_2 release in cultured osteocytes (Ajubi et al., 1996). These contradictory results are based on the findings of different cell or tissue experiments with various flow conditions using a variety of flow media. Therefore, it is very difficult to interpret these results. Evidently, more experiments are needed to verify these pathways.

Now that the significance of the glycocalyx is apparent, the specific roles of proteoglycans that reside on the surfaces of bone and endothelial cells need to be identified. There are many on going studies on the functions of endothelial cell surface proteoglycans, heparan and chondroitin sulfate proteoglycans. The same needs to be done for the bone cells, since recent in vitro studies in bone cells have failed to detect the presence of sulfated proteoglycans. In addition, more studies are required to study the

interaction between the cytoskeleton and these proteoglycans. Studies using cDNA microarrys to analyze the many genes that are up- or down-regulated by fluid shearing forces would give us a broader scope of shear force affects. In addition, investigating knockout animal models such as animals lacking actin, vimentin, actin binding proteins, heparan sulfate (Syndecan I), eNOS, or COX-2 would allow us to elucidate some unsolved cellular mechanisms that are associated with mechanotransduction.

The current state of the knowledge of the mechanical properties of the key structures of the cells is in its infancy. Most cells possess an ACW that can resist forces in the vicinity of 0.1 pN with the elastic constant of 700-900 dyn/cm^2. Focal adhesive contacts can withstand forces up to 0.9-1.45 nN, and the adherens junctions that can bear forces in the range of 35-120 pN. Some crucial measurements with regard to resistance forces of the DPAB, or tight and gap junction binding forces need to be measured for future theoretical models.

Our efforts in elucidating various mechanisms associated with cell-cell mechanotransduction have brought us to a new level of understanding. Predictions from our 'bumper car' model have opened new avenues to explore and may very well lead us to explain long standing fundamental questions regarding cellular mechanotransduction.

Bibiliography

Adamson,R.H. 1990. Permeability of frog mesenteric capillaries after partial pronase digestion of the endothelial glycocalyx. *J. Physiol* 428:1-13.:1-13.

Adamson,R.H. and G.Clough. 1992. Plasma proteins modify the endothelial cell glycocalyx of frog mesenteric microvessels. *J. Physiol* 445:473-86.:473-486.

Adamson,R.H., J.F.Lenz, X.Zhang, G.N.Adamson, S.Weinbaum, and F.E.Curry. 2004. Oncotic pressures opposing filtration across non-fenestrated rat microvessels. *J. Physiol* 557:889-907.

Adamson,R.H. and C.C.Michel. 1993. Pathways through the intercellular clefts of frog mesenteric capillaries. *J. Physiol* 466:303-27.:303-327.

Ai,Z., A.Fischer, D.C.Spray, A.M.Brown, and G.I.Fishman. 2000. Wnt-1 regulation of connexin43 in cardiac myocytes. *J. Clin. Invest* 105:161-171.

Ajubi,N.E., J.Klein-Nulend, P.J.Nijweide, T.Vrijheid-Lammers, M.J.Alblas, and E.H.Burger. 1996. Pulsating fluid flow increases prostaglandin production by cultured chicken osteocytes--a cytoskeleton-dependent process. *Biochem. Biophys. Res. Commun.* 225:62-68.

Alford,A.I., C.R.Jacobs, and H.J.Donahue. 2003. Oscillating fluid flow regulates gap junction communication in osteocytic MLO-Y4 cells by an ERK1/2 MAP kinase-dependent mechanism small star, filled. *Bone* 33:64-70.

Anderson,R.G. 1993. Caveolae: where incoming and outgoing messengers meet. *Proc. Natl. Acad. Sci. U. S. A* 90:10909-10913.

Angst,B.D., C.Marcozzi, and A.I.Magee. 2001. The cadherin superfamily: diversity in form and function. *J. Cell Sci.* 114:629-641.

Arana-Chavez,V.E., A.M.Soares, and E.Katchburian. 1995. Junctions between early developing osteoblasts of rat calvaria as revealed by freeze-fracture and ultrathin section electron microscopy. *Arch. Histol. Cytol.* 58:285-292.

Bailly,M. 2003. Connecting cell adhesion to the actin polymerization machinery: vinculin as the missing link? *Trends Cell Biol.* 13:163-165.

Bao,X., C.B.Clark, and J.A.Frangos. 2000. Temporal gradient in shear-induced signaling pathway: involvement of MAP kinase, c-fos, and connexin43. *Am. J. Physiol Heart Circ. Physiol* 278:H1598-H1605.

Barakat,A.I. and P.F.Davies. 1998. Mechanisms of shear stress transmission and transduction in endothelial cells. *Chest* 114:58S-63S.

Bass,M.D. and M.J.Humphries. 2002. Cytoplasmic interactions of syndecan-4 orchestrate adhesion receptor and growth factor receptor signalling. *Biochem. J.* 368:1-15.

Baumgartner,W., P.Hinterdorfer, W.Ness, A.Raab, D.Vestweber, H.Schindler, and D.Drenckhahn. 2000. Cadherin interaction probed by atomic force microscopy. *Proc. Natl. Acad. Sci. U. S. A* 97:4005-4010.

Berk,B.C., M.A.Corson, T.E.Peterson, and H.Tseng. 1995. Protein kinases as mediators of fluid shear stress stimulated signal transduction in endothelial cells: a hypothesis for calcium-dependent and calcium-independent events activated by flow. *J. Biomech.* 28:1439-1450.

Beyer,E.C. 1990. Molecular cloning and developmental expression of two chick embryo gap junction proteins. *J. Biol. Chem.* 265:14439-14443.

Boo,Y.C. and H.Jo. 2003. Flow-dependent regulation of endothelial nitric oxide synthase: role of protein kinases. *Am. J. Physiol Cell Physiol* 285:C499-C508.

Boyd,N.L., H.Park, H.Yi, Y.C.Boo, G.P.Sorescu, M.Sykes, and H.Jo. 2003. Chronic shear induces caveolae formation and alters ERK and Akt responses in endothelial cells. *Am. J. Physiol Heart Circ. Physiol* 285:H1113-H1122.

Bruzzone,R., J.A.Haefliger, R.L.Gimlich, and D.L.Paul. 1993. Connexin40, a component of gap junctions in vascular endothelium, is restricted in its ability to interact with other connexins. *Mol. Biol. Cell* 4:7-20.

Burger,E.H. and J.Klein-Nulend. 1999. Mechanotransduction in bone--role of the lacuno-canalicular network. *FASEB J.* 13 Suppl:S101-12.:S101-S112.

Burger,E.H., J.Klein-Nulend, P.A.van der, and P.J.Nijweide. 1995. Function of osteocytes in bone--their role in mechanotransduction. *J. Nutr.* 125:2020S-2023S.

Burr,D.B. and R.B.Martin. 1993. Calculating the probability that microcracks initiate resorption spaces. *J. Biomech.* 26:613-616.

Burr,D.B., C.Milgrom, D.Fyhrie, M.Forwood, M.Nyska, A.Finestone, S.Hoshaw, E.Saiag, and A.Simkin. 1996. In vivo measurement of human tibial strains during vigorous activity. *Bone* 18:405-410.

Burr,D.B., A.G.Robling, and C.H.Turner. 2002. Effects of biomechanical stress on bones in animals. *Bone* 30:781-786.

Burridge,K., K.Fath, T.Kelly, G.Nuckolls, and C.Turner. 1988. Focal adhesions: transmembrane junctions between the extracellular matrix and the cytoskeleton. *Annu. Rev. Cell Biol.* 4:487-525.:487-525.

Burridge,K., C.E.Turner, and L.H.Romer. 1992. Tyrosine phosphorylation of paxillin and pp125FAK accompanies cell adhesion to extracellular matrix: a role in cytoskeletal assembly. *J. Cell Biol.* 119:893-903.

Burstone,M.S. 1961. Histochemical demonstration of phosphatases in frozen sections with naphthol AS-phosphates. *J. Histochem. Cytochem.* 9:146-153.

Carter,D.R. and W.C.Hayes. 1977. Compact bone fatigue damage: a microscopic examination. *Clin. Orthop.*265-274.

Chen,N.X., K.D.Ryder, F.M.Pavalko, C.H.Turner, D.B.Burr, J.Qiu, and R.L.Duncan. 2000. Ca(2+) regulates fluid shear-induced cytoskeletal reorganization and gene expression in osteoblasts. *Am. J. Physiol Cell Physiol* 278:C989-C997.

Cheng,B., Y.Kato, S.Zhao, J.Luo, E.Sprague, L.F.Bonewald, and J.X.Jiang. 2001a. PGE(2) is essential for gap junction-mediated intercellular communication between osteocyte-like MLO-Y4 cells in response to mechanical strain. *Endocrinology* 142:3464-3473.

Cheng,B., S.Zhao, J.Luo, E.Sprague, L.F.Bonewald, and J.X.Jiang. 2001b. Expression of functional gap junctions and regulation by fluid flow in osteocyte-like MLO-Y4 cells. *J. Bone Miner. Res.* 16:249-259.

Civitelli,R., E.C.Beyer, P.M.Warlow, A.J.Robertson, S.T.Geist, and T.H.Steinberg. 1993. Connexin43 mediates direct intercellular communication in human osteoblastic cell networks. *J. Clin. Invest* 91:1888-1896.

Cowan,D.B., S.J.Lye, and B.L.Langille. 1998. Regulation of vascular connexin43 gene expression by mechanical loads. *Circ. Res.* %20;82:786-793.

Cowin,S.C. and S.Weinbaum. 1998. Strain amplification in the bone mechanosensory system. *Am. J. Med. Sci.* 316:184-188.

Cowin,S.C., S.Weinbaum, and Y.Zeng. 1995. A case for bone canaliculi as the anatomical site of strain generated potentials. *J. Biomech.* 28:1281-1297.

Critchley,D.R. 2000. Focal adhesions - the cytoskeletal connection. *Curr. Opin. Cell Biol.* 12:133-139.

Damiano,E.R. and T.M.Stace. 2002. A mechano-electrochemical model of radial deformation of the capillary glycocalyx. *Biophys. J.* 82:1153-1175.

Darrow,B.J., V.G.Fast, A.G.Kleber, E.C.Beyer, and J.E.Saffitz. 1996. Functional and structural assessment of intercellular communication. Increased conduction velocity and enhanced connexin expression in dibutyryl cAMP-treated cultured cardiac myocytes. *Circ. Res.* 79:174-183.

Darrow,B.J., J.G.Laing, P.D.Lampe, J.E.Saffitz, and E.C.Beyer. 1995. Expression of multiple connexins in cultured neonatal rat ventricular myocytes. *Circ. Res.* 76:381-387.

Davies,P.F. 1995. Flow-mediated endothelial mechanotransduction. *Physiol Rev.* 75:519-560.

Davies,P.F. 1997. Overview: temporal and spatial relationships in shear stress-mediated endothelial signalling. *J. Vasc. Res.* 34:208-211.

Davies,P.F., K.A.Barbee, M.V.Volin, A.Robotewskyj, J.Chen, L.Joseph, M.L.Griem, M.N.Wernick, E.Jacobs, D.C.Polacek, N.Depaola, and A.I.Barakat. 1997. Spatial relationships in early signaling events of flow-mediated endothelial mechanotransduction. *Annu. Rev. Physiol* 59:527-49.:527-549.

Davies,P.F., A.Remuzzi, E.J.Gordon, C.F.Dewey, Jr., and M.A.Gimbrone, Jr. 1986. Turbulent fluid shear stress induces vascular endothelial cell turnover in vitro. *Proc. Natl. Acad. Sci. U. S. A* 83:2114-2117.

Davies,P.F., A.Robotewskyj, and M.L.Griem. 1994. Quantitative studies of endothelial cell adhesion. Directional remodeling of focal adhesion sites in response to flow forces. *J. Clin. Invest* 93:2031-2038.

DeMaio,L., Y.S.Chang, T.W.Gardner, J.M.Tarbell, and D.A.Antonetti. 2001. Shear stress regulates occludin content and phosphorylation. *Am. J. Physiol Heart Circ. Physiol* 281:H105-H113.

Depaola,N., P.F.Davies, W.F.Pritchard, Jr., L.Florez, N.Harbeck, and D.C.Polacek. 1999. Spatial and temporal regulation of gap junction connexin43 in vascular endothelial cells exposed to controlled disturbed flows in vitro. *Proc. Natl. Acad. Sci. U. S. A* 96:3154-3159.

Dermietzel,R., Y.Gao, E.Scemes, D.Vieira, M.Urban, M.Kremer, M.V.Bennett, and D.C.Spray. 2000. Connexin43 null mice reveal that astrocytes express multiple connexins. *Brain Res. Brain Res. Rev.* 32:45-56.

Desjardins,C. and B.R.Duling. 1990. Heparinase treatment suggests a role for the endothelial cell glycocalyx in regulation of capillary hematocrit. *Am. J. Physiol* 258:H647-H654.

Dewey,C.F., Jr., S.R.Bussolari, M.A.Gimbrone, Jr., and P.F.Davies. 1981. The dynamic response of vascular endothelial cells to fluid shear stress. *J. Biomech. Eng* 103:177-185.

Donahue,H.J. 2000. Gap junctions and biophysical regulation of bone cell differentiation. *Bone* 26:417-422.

Donahue,H.J., Z.Li, Z.Zhou, and C.E.Yellowley. 2000. Differentiation of human fetal osteoblastic cells and gap junctional intercellular communication. *Am. J. Physiol Cell Physiol* 278:C315-C322.

Donahue,H.J., K.J.McLeod, C.T.Rubin, J.Andersen, E.A.Grine, E.L.Hertzberg, and P.R.Brink. 1995. Cell-to-cell communication in osteoblastic networks: cell line-dependent hormonal regulation of gap junction function. *J. Bone Miner. Res.* 10:881-889.

Donahue,T.L., T.R.Haut, C.E.Yellowley, H.J.Donahue, and C.R.Jacobs. 2003. Mechanosensitivity of bone cells to oscillating fluid flow induced shear stress may be modulated by chemotransport. *J. Biomech.* 36:1363-1371.

Doty,S.B. 1981. Morphological evidence of gap junctions between bone cells. *Calcif. Tissue Int.* 33:509-512.

Drenckhahn,D. and W.Ness. 1997. The endothelial contractile cytoskeleton. *Vascular Endothelium: Physiology, Pathology, and Therapeutic Opportunities* 3:1-25.

Drenckhahn,D. and J.Wagner. 1986. Stress fibers in the splenic sinus endothelium in situ: molecular structure, relationship to the extracellular matrix, and contractility. *J. Cell Biol.* 102:1738-1747.

Duffy,H.S., M.Delmar, and D.C.Spray. 2002. Formation of the gap junction nexus: binding partners for connexins. *J. Physiol Paris* 96:243-249.

Dull,R.O., R.Dinavahi, L.Schwartz, D.E.Humphries, D.Berry, R.Sasisekharan, and J.G.Garcia. 2003. Lung endothelial heparan sulfates mediate cationic peptide-induced barrier dysfunction: a new role for the glycocalyx. *Am. J. Physiol Lung Cell Mol. Physiol* 285:L986-L995.

Duncan,R.L. and C.H.Turner. 1995. Mechanotransduction and the functional response of bone to mechanical strain. *Calcif. Tissue Int.* 57:344-358.

Fanning,A.S., B.J.Jameson, L.A.Jesaitis, and J.M.Anderson. 1998. The tight junction protein ZO-1 establishes a link between the transmembrane protein occludin and the actin cytoskeleton. *J. Biol. Chem.* 273:29745-29753.

Fleming,I., J.Bauersachs, B.Fisslthaler, and R.Busse. 1998. Ca2+-independent activation of the endothelial nitric oxide synthase in response to tyrosine phosphatase inhibitors and fluid shear stress. *Circ. Res.* 82:686-695.

Florian,J.A., J.R.Kosky, K.Ainslie, Z.Pang, R.O.Dull, and J.M.Tarbell. 2003. Heparan sulfate proteoglycan is a mechanosensor on endothelial cells. *Circ. Res.* 93:e136-e142.

Frangos,J.A., S.G.Eskin, L.V.McIntire, and C.L.Ives. 1985. Flow effects on prostacyclin production by cultured human endothelial cells. *Science* 227:1477-1479.

Frangos,J.A., T.Y.Huang, and C.B.Clark. 1996. Steady shear and step changes in shear stimulate endothelium via independent mechanisms--superposition of transient and sustained nitric oxide production. *Biochem. Biophys. Res. Commun.* 224:660-665.

Fritton,S.P., K.J.McLeod, and C.T.Rubin. 2000. Quantifying the strain history of bone: spatial uniformity and self-similarity of low-magnitude strains. *J. Biomech.* 33:317-325.

Fung,Y.C. and S.Q.Liu. 1993. Elementary mechanics of the endothelium of blood vessels. *J. Biomech. Eng* 115:1-12.

Furuse,M., M.Itoh, T.Hirase, A.Nagafuchi, S.Yonemura, S.Tsukita, and S.Tsukita. 1994. Direct association of occludin with ZO-1 and its possible involvement in the localization of occludin at tight junctions. *J. Cell Biol.* 127:1617-1626.

Galbraith,C.G., R.Skalak, and S.Chien. 1998. Shear stress induces spatial reorganization of the endothelial cell cytoskeleton. *Cell Motil. Cytoskeleton* 40:317-330.

Giepmans,B.N. 2004. Gap junctions and connexin-interacting proteins. *Cardiovasc. Res.* 62:233-245.

Giepmans,B.N. and W.H.Moolenaar. 1998. The gap junction protein connexin43 interacts with the second PDZ domain of the zona occludens-1 protein. *Curr. Biol.* 8:931-934.

Girard,P.R. and R.M.Nerem. 1995. Shear stress modulates endothelial cell morphology and F-actin organization through the regulation of focal adhesion-associated proteins. *J. Cell Physiol* 163:179-193.

Guan,X., S.Wilson, K.K.Schlender, and R.J.Ruch. 1996. Gap-junction disassembly and connexin 43 dephosphorylation induced by 18 beta-glycyrrhetinic acid. *Mol. Carcinog.* 16:157-164.

Harrigan,T.P. and J.J.Hamilton. 1993. Bone strain sensation via transmembrane potential changes in surface osteoblasts: Loading rate and microstructural implications. *J. Biomech.* 26:183-200.

Hecker,M., A.Mulsch, E.Bassenge, and R.Busse. 1993. Vasoconstriction and increased flow: two principal mechanisms of shear stress-dependent endothelial autacoid release. *Am. J. Physiol* 265:H828-H833.

Helmke,B.P., R.D.Goldman, and P.F.Davies. 2000. Rapid displacement of vimentin intermediate filaments in living endothelial cells exposed to flow. *Circ. Res.* 86:745-752.

Henry,C.B. and B.R.Duling. 1999. Permeation of the luminal capillary glycocalyx is determined by hyaluronan. *Am. J. Physiol* 277:H508-H514.

Hillsley,M.V. and J.A.Frangos. 1994. Bone tissue engineering: the role of interstitial fluid flow. *Biotechnol. Bioeng.* 43:573-581.

Hillsley,M.V. and J.A.Frangos. 1997. Alkaline phosphatase in osteoblasts is down-regulated by pulsatile fluid flow. *Calcif. Tissue Int.* 60:48-53.

Hirokawa,N. and J.E.Heuser. 1981. Quick-freeze, deep-etch visualization of the cytoskeleton beneath surface differentiations of intestinal epithelial cells. *J. Cell Biol.* 91:399-409.

Howarth,A.G., M.R.Hughes, and B.R.Stevenson. 1992. Detection of the tight junction-associated protein ZO-1 in astrocytes and other nonepithelial cell types. *Am. J. Physiol* 262:C461-C469.

Hu,X. and S.Weinbaum. 1999. A new view of Starling's hypothesis at the microstructural level. *Microvasc. Res.* 58:281-304.

Hu,Y.L. and S.Chien. 1997. Effects of shear stress on protein kinase C distribution in endothelial cells. *J. Histochem. Cytochem.* 45:237-249.

Hung,C.T., F.D.Allen, S.R.Pollack, and C.T.Brighton. 1996. Intracellular Ca2+ stores and extracellular Ca2+ are required in the real-time Ca2+ response of bone cells experiencing fluid flow. *J. Biomech.* 29:1411-1417.

Hung,C.T., S.R.Pollack, T.M.Reilly, and C.T.Brighton. 1995. Real-time calcium response of cultured bone cells to fluid flow. *Clin. Orthop.*256-269.

Hutcheson,I.R. and T.M.Griffith. 1996. Mechanotransduction through the endothelial cytoskeleton: mediation of flow- but not agonist-induced EDRF release. *Br. J. Pharmacol.* 118:720-726.

Huxley,V.H. and D.A.Williams. 2000. Role of a glycocalyx on coronary arteriole permeability to proteins: evidence from enzyme treatments. *Am. J. Physiol Heart Circ. Physiol* 278:H1177-H1185.

Ihrcke,N.S., L.E.Wrenshall, B.J.Lindman, and J.L.Platt. 1993. Role of heparan sulfate in immune system-blood vessel interactions. *Immunol. Today* 14:500-505.

Isshiki,M. and R.G.Anderson. 2003. Function of caveolae in Ca2+ entry and Ca2+-dependent signal transduction. *Traffic.* 4:717-723.

Itoh,M., A.Nagafuchi, S.Moroi, and S.Tsukita. 1997. Involvement of ZO-1 in cadherin-based cell adhesion through its direct binding to alpha catenin and actin filaments. *J. Cell Biol.* 138:181-192.

Itoh,M., A.Nagafuchi, S.Yonemura, T.Kitani-Yasuda, S.Tsukita, and S.Tsukita. 1993. The 220-kD protein colocalizing with cadherins in non-epithelial cells is identical to ZO-1, a tight junction-associated protein in epithelial cells: cDNA cloning and immunoelectron microscopy. *J. Cell Biol.* 121:491-502.

Jeansonne,B.G., F.F.Feagin, R.W.McMinn, R.L.Shoemaker, and W.S.Rehm. 1979. Cell-to-cell communication of osteoblasts. *J. Dent. Res.* 58:1415-1423.

Johnson,D.L., T.N.McAllister, and J.A.Frangos. 1996. Fluid flow stimulates rapid and continuous release of nitric oxide in osteoblasts. *Am. J. Physiol* 271:E205-E208.

Kano,Y., K.Katoh, and K.Fujiwara. 2000. Lateral zone of cell-cell adhesion as the major fluid shear stress-related signal transduction site. *Circ. Res.* 86:425-433.

Kato,Y., J.J.Windle, B.A.Koop, G.R.Mundy, and L.F.Bonewald. 1997. Establishment of an osteocyte-like cell line, MLO-Y4. *J. Bone Miner. Res.* 12:2014-2023.

King,G.J. and M.E.Holtrop. 1975. Actin-like filaments in bone cells of cultured mouse calvaria as demonstrated by binding to heavy meromyosin. *J. Cell Biol.* 66:445-451.

Klein-Nulend,J., E.H.Burger, C.M.Semeins, L.G.Raisz, and C.C.Pilbeam. 1997. Pulsating fluid flow stimulates prostaglandin release and inducible prostaglandin G/H synthase mRNA expression in primary mouse bone cells. *J. Bone Miner. Res.* 12:45-51.

Klein-Nulend,J., M.H.Helfrich, J.G.Sterck, H.MacPherson, M.Joldersma, S.H.Ralston, C.M.Semeins, and E.H.Burger. 1998. Nitric oxide response to shear stress by human bone cell cultures is endothelial nitric oxide synthase dependent. *Biochem. Biophys. Res. Commun.* 250:108-114.

Klein-Nulend,J., C.M.Semeins, N.E.Ajubi, P.J.Nijweide, and E.H.Burger. 1995b. Pulsating fluid flow increases nitric oxide (NO) synthesis by osteocytes but not periosteal fibroblasts--correlation with prostaglandin upregulation. *Biochem. Biophys. Res. Commun.* 217:640-648.

Klein-Nulend,J., C.M.Semeins, and E.H.Burger. 1996. Prostaglandin mediated modulation of transforming growth factor-beta metabolism in primary mouse osteoblastic cells in vitro. *J. Cell Physiol* 168:1-7.

Klein-Nulend,J., P.A.van der, C.M.Semeins, N.E.Ajubi, J.A.Frangos, P.J.Nijweide, and E.H.Burger. 1995a. Sensitivity of osteocytes to biomechanical stress in vitro. *FASEB J.* 9:441-445.

Knudsen,H.L. and J.A.Frangos. 1997. Role of cytoskeleton in shear stress-induced endothelial nitric oxide production. *Am. J. Physiol* 273:H347-H355.

Kojima,T., N.Sawada, H.Chiba, Y.Kokai, M.Yamamoto, M.Urban, G.H.Lee, E.L.Hertzberg, Y.Mochizuki, and D.C.Spray. 1999. Induction of tight junctions in

human connexin 32 (hCx32)-transfected mouse hepatocytes: connexin 32 interacts with occludin. *Biochem. Biophys. Res. Commun.* 266:222-229.

Krutovskikh,V.A., M.Mesnil, G.Mazzoleni, and H.Yamasaki. 1995. Inhibition of rat liver gap junction intercellular communication by tumor-promoting agents in vivo. Association with aberrant localization of connexin proteins. *Lab Invest* 72:571-577.

Ku,D.N., D.P.Giddens, C.K.Zarins, and S.Glagov. 1985. Pulsatile flow and atherosclerosis in the human carotid bifurcation. Positive correlation between plaque location and low oscillating shear stress. *Arteriosclerosis* 5:293-302.

Kuchan,M.J. and J.A.Frangos. 1994. Role of calcium and calmodulin in flow-induced nitric oxide production in endothelial cells. *Am. J. Physiol* 266:C628-C636.

Kuchan,M.J., H.Jo, and J.A.Frangos. 1994. Role of G proteins in shear stress-mediated nitric oxide production by endothelial cells. *Am. J. Physiol* 267:C753-C758.

Kusumi,A. and Y.Sako. 1996. Cell surface organization by the membrane skeleton. *Curr. Opin. Cell Biol.* 8:566-574.

Kwak,B.R., F.Mulhaupt, N.Veillard, D.B.Gros, and F.Mach. 2002. Altered pattern of vascular connexin expression in atherosclerotic plaques. *Arterioscler. Thromb. Vasc. Biol.* 22:225-230.

Laing,J.G., R.N.Manley-Markowski, M.Koval, R.Civitelli, and T.H.Steinberg. 2001. Connexin45 interacts with zonula occludens-1 and connexin43 in osteoblastic cells. *J. Biol. Chem.* 276:23051-23055.

Lanyon,L.E. 1984. Functional strain as a determinant for bone remodeling. *Calcif. Tissue Int.* 36 Suppl 1:S56-61.:S56-S61.

Lecanda,F., D.A.Towler, K.Ziambaras, S.L.Cheng, M.Koval, T.H.Steinberg, and R.Civitelli. 1998. Gap junctional communication modulates gene expression in osteoblastic cells. *Mol. Biol. Cell* 9:2249-2258.

Lecanda,F., P.M.Warlow, S.Sheikh, F.Furlan, T.H.Steinberg, and R.Civitelli. 2000. Connexin43 deficiency causes delayed ossification, craniofacial abnormalities, and osteoblast dysfunction. *J. Cell Biol.* 151:931-944.

Li,S., M.Kim, Y.L.Hu, S.Jalali, D.D.Schlaepfer, T.Hunter, S.Chien, and J.Y.Shyy. 1997. Fluid shear stress activation of focal adhesion kinase. Linking to mitogen-activated protein kinases. *J. Biol. Chem.* 272:30455-30462.

Li,Z., Z.Zhou, C.E.Yellowley, and H.J.Donahue. 1999. Inhibiting gap junctional intercellular communication alters expression of differentiation markers in osteoblastic cells. *Bone* 25:661-666.

Liao,Y., K.H.Day, D.N.Damon, and B.R.Duling. 2001. Endothelial cell-specific knockout of connexin 43 causes hypotension and bradycardia in mice. *Proc. Natl. Acad. Sci. U. S. A* 98:9989-9994.

Liu,S.M., K.E.Magnusson, and T.Sundqvist. 1993. Microtubules are involved in transport of macromolecules by vesicles in cultured bovine aortic endothelial cells. *J. Cell Physiol* 156:311-316.

Luegmayr,E., H.Glantschnig, F.Varga, and K.Klaushofer. 2000. The organization of adherens junctions in mouse osteoblast-like cells (MC3T3-E1) and their modulation by triiodothyronine and 1,25-dihydroxyvitamin D3. *Histochem. Cell Biol.* 113:467-478.

Luft,J.H. 1966. Fine structures of capillary and endocapillary layer as revealed by ruthenium red. *Fed. Proc.* 25:1773-1783.

Mack,P.J., M.R.Kaazempur-Mofrad, H.Karcher, R.T.Lee, and R.D.Kamm. 2004. Force-induced focal adhesion translocation: Effects of force amplitude and frequency. *Am. J. Physiol Cell Physiol* ..

Marzioni,D., M.Banita, A.Felici, F.J.Paradinas, E.Newlands, M.De Nictolis, J.Muhlhauser, and M.Castellucci. 2001. Expression of ZO-1 and occludin in normal human placenta and in hydatidiform moles. *Mol. Hum. Reprod.* 7:279-285.

Matthews,B.D., D.R.Overby, F.J.Alenghat, J.Karavitis, Y.Numaguchi, P.G.Allen, and D.E.Ingber. 2004. Mechanical properties of individual focal adhesions probed with a magnetic microneedle. *Biochem. Biophys. Res. Commun.* 313:758-764.

Michel,C.C. 1997. Starling: the formulation of his hypothesis of microvascular fluid exchange and its significance after 100 years. *Exp. Physiol* 82:1-30.

Minkoff,R., E.S.Bales, C.A.Kerr, and W.E.Struss. 1999. Antisense oligonucleotide blockade of connexin expression during embryonic bone formation: evidence of functional compensation within a multigene family. *Dev. Genet.* 24:43-56.

Minkoff,R., V.R.Rundus, S.B.Parker, E.L.Hertzberg, J.G.Laing, and E.C.Beyer. 1994. Gap junction proteins exhibit early and specific expression during intramembranous bone formation in the developing chick mandible. *Anat. Embryol. (Berl)* 190:231-241.

Mitic,L.L. and J.M.Anderson. 1998. Molecular architecture of tight junctions. *Annu. Rev. Physiol* 60:121-42.:121-142.

Mulivor,A.W. and H.H.Lipowsky. 2002. Role of glycocalyx in leukocyte-endothelial cell adhesion. *Am. J. Physiol Heart Circ. Physiol* 283:H1282-H1291.

Mulivor,A.W. and H.H.Lipowsky. 2004. Inflammation- and ischemia-induced shedding of venular glycocalyx. *Am. J. Physiol Heart Circ. Physiol* 286:H1672-H1680.

Musil,L.S., B.A.Cunningham, G.M.Edelman, and D.A.Goodenough. 1990. Differential phosphorylation of the gap junction protein connexin43 in junctional communication-competent and -deficient cell lines. *J. Cell Biol.* 111:2077-2088.

Musil,L.S. and D.A.Goodenough. 1991. Biochemical analysis of connexin43 intracellular transport, phosphorylation, and assembly into gap junctional plaques. *J. Cell Biol.* 115:1357-1374.

Noria,S., D.B.Cowan, A.I.Gotlieb, and B.L.Langille. 1999. Transient and steady-state effects of shear stress on endothelial cell adherens junctions. *Circ. Res.* 85:504-514.

Norvell,S.M., S.M.Ponik, D.K.Bowen, R.Gerard, and F.M.Pavalko. 2004. Fluid shear stress induction of COX-2 protein and prostaglandin release in cultured MC3T3-E1 osteoblasts does not require intact microfilaments or microtubules. *J. Appl. Physiol* 96:957-966.

Nusrat,A., J.A.Chen, C.S.Foley, T.W.Liang, J.Tom, M.Cromwell, C.Quan, and R.J.Mrsny. 2000. The coiled-coil domain of occludin can act to organize structural and functional elements of the epithelial tight junction. *J. Biol. Chem.* 275:29816-29822.

Nusrat,A., M.Giry, J.R.Turner, S.P.Colgan, C.A.Parkos, D.Carnes, E.Lemichez, P.Boquet, and J.L.Madara. 1995. Rho protein regulates tight junctions and

perijunctional actin organization in polarized epithelia. *Proc. Natl. Acad. Sci. U. S. A* 92:10629-10633.

Ogunrinade,O., G.T.Kameya, and G.A.Truskey. 2002. Effect of fluid shear stress on the permeability of the arterial endothelium. *Ann. Biomed. Eng* 30:430-446.

Ookawa,K., M.Sato, and N.Ohshima. 1992. Changes in the microstructure of cultured porcine aortic endothelial cells in the early stage after applying a fluid-imposed shear stress. *J. Biomech.* 25:1321-1328.

Ookawa,K., M.Sato, and N.Ohshima. 1993. Morphological changes of endothelial cells after exposure to fluid-imposed shear stress: differential responses induced by extracellular matrices. *Biorheology* 30:131-140.

Owan,I., D.B.Burr, C.H.Turner, J.Qiu, Y.Tu, J.E.Onyia, and R.L.Duncan. 1997. Mechanotransduction in bone: osteoblasts are more responsive to fluid forces than mechanical strain. *Am. J. Physiol* 273:C810-C815.

Park,H., Y.M.Go, R.Darji, J.W.Choi, M.P.Lisanti, M.C.Maland, and H.Jo. 2000. Caveolin-1 regulates shear stress-dependent activation of extracellular signal-regulated kinase. *Am. J. Physiol Heart Circ. Physiol* 278:H1285-H1293.

Pavalko,F.M., N.X.Chen, C.H.Turner, D.B.Burr, S.Atkinson, Y.F.Hsieh, J.Qiu, and R.L.Duncan. 1998. Fluid shear-induced mechanical signaling in MC3T3-E1

osteoblasts requires cytoskeleton-integrin interactions. *Am. J. Physiol* 275:C1591-C1601.

Pavalko,F.M. and C.A.Otey. 1994. Role of adhesion molecule cytoplasmic domains in mediating interactions with the cytoskeleton. *Proc. Soc. Exp. Biol. Med.* 205:282-293.

Pina-Benabou,M.H., M.Srinivas, D.C.Spray, and E.Scemes. 2001. Calmodulin kinase pathway mediates the K+-induced increase in Gap junctional communication between mouse spinal cord astrocytes. *J. Neurosci.* 21:6635-6643.

Pohl,U., K.Herlan, A.Huang, and E.Bassenge. 1991. EDRF-mediated shear-induced dilation opposes myogenic vasoconstriction in small rabbit arteries. *Am. J. Physiol* 261:H2016-H2023.

Polacek,D., F.Bech, J.F.McKinsey, and P.F.Davies. 1997. Connexin43 gene expression in the rabbit arterial wall: effects of hypercholesterolemia, balloon injury and their combination. *J. Vasc. Res.* 34:19-30.

Polacek,D., R.Lal, M.V.Volin, and P.F.Davies. 1993. Gap junctional communication between vascular cells. Induction of connexin43 messenger RNA in macrophage foam cells of atherosclerotic lesions. *Am. J. Pathol.* 142:593-606.

Ponik,S.M. and F.M.Pavalko. 2004. Formation of Focal Adhesions on Fibronectin Promotes Fluid Shear Stress Induction of COX-2 and PGE2 Release in MC3T3-E1 Osteoblasts. *J. Appl. Physiol* 97:135-142.

Reed,K.E., E.M.Westphale, D.M.Larson, H.Z.Wang, R.D.Veenstra, and E.C.Beyer. 1993. Molecular cloning and functional expression of human connexin37, an endothelial cell gap junction protein. *J. Clin. Invest* 91:997-1004.

Reich,K.M. and J.A.Frangos. 1991. Effect of flow on prostaglandin E2 and inositol trisphosphate levels in osteoblasts. *Am. J. Physiol* 261:C428-C432.

Reich,K.M. and J.A.Frangos. 1993. Protein kinase C mediates flow-induced prostaglandin E2 production in osteoblasts. *Calcif. Tissue Int.* 52:62-66.

Reich,K.M., C.V.Gay, and J.A.Frangos. 1990. Fluid shear stress as a mediator of osteoblast cyclic adenosine monophosphate production. *J. Cell Physiol* 143:100-104.

Reich,K.M., T.N.McAllister, S.Gudi, and J.A.Frangos. 1997. Activation of G proteins mediates flow-induced prostaglandin E2 production in osteoblasts. *Endocrinology* 138:1014-1018.

Reilly,G.C., T.R.Haut, C.E.Yellowley, H.J.Donahue, and C.R.Jacobs. 2003. Fluid flow induced PGE2 release by bone cells is reduced by glycocalyx degradation whereas calcium signals are not. *Biorheology* 40:591-603.

Rizzo,V., C.Morton, N.Depaola, J.E.Schnitzer, and P.F.Davies. 2003. Recruitment of endothelial caveolae into mechanotransduction pathways by flow conditioning in vitro. *Am. J. Physiol Heart Circ. Physiol* 285:H1720-H1729.

Romanello,M., L.Moro, D.Pirulli, S.Crovella, and P.D'Andrea. 2001. Effects of cAMP on intercellular coupling and osteoblast differentiation. *Biochem. Biophys. Res. Commun.* %20;282:1138-1144.

Rubin,C.T. and L.E.Lanyon. 1984. Regulation of bone formation by applied dynamic loads. *J. Bone Joint Surg. Am.* 66:397-402.

Rubin,C.T. and L.E.Lanyon. 1985. Regulation of bone mass by mechanical strain magnitude. *Calcif. Tissue Int.* 37:411-417.

Ryeom,S.W., D.Paul, and D.A.Goodenough. 2000. Truncation mutants of the tight junction protein ZO-1 disrupt corneal epithelial cell morphology. *Mol. Biol. Cell* 11:1687-1696.

Sako,Y. and A.Kusumi. 1995. Barriers for lateral diffusion of transferrin receptor in the plasma membrane as characterized by receptor dragging by laser tweezers: fence versus tether. *J. Cell Biol.* 129:1559-1574.

Satcher,R., C.F.Dewey, Jr., and J.H.Hartwig. 1997. Mechanical remodeling of the endothelial surface and actin cytoskeleton induced by fluid flow. *Microcirculation.* 4:439-453.

Sato,M., D.P.Theret, L.T.Wheeler, N.Ohshima, and R.M.Nerem. 1990. Application of the micropipette technique to the measurement of cultured porcine aortic endothelial cell viscoelastic properties. *J. Biomech. Eng* 112:263-268.

Saunders,M.M., J.You, J.E.Trosko, H.Yamasaki, Z.Li, H.J.Donahue, and C.R.Jacobs. 2001. Gap junctions and fluid flow response in MC3T3-E1 cells. *Am. J. Physiol Cell Physiol* 281:C1917-C1925.

Saunders,M.M., J.You, Z.Zhou, Z.Li, C.E.Yellowley, E.L.Kunze, C.R.Jacobs, and H.J.Donahue. 2003. Fluid flow-induced prostaglandin E2 response of osteoblastic ROS 17/2.8 cells is gap junction-mediated and independent of cytosolic calcium. *Bone* 32:350-356.

Saunders,S., M.Jalkanen, S.O'Farrell, and M.Bernfield. 1989. Molecular cloning of syndecan, an integral membrane proteoglycan. *J. Cell Biol.* 108:1547-1556.

Sauren,Y.M., R.H.Mieremet, C.G.Groot, and J.P.Scherft. 1992. An electron microscopic study on the presence of proteoglycans in the mineralized matrix of rat and human compact lamellar bone. *Anat. Rec.* 232:36-44.

Sawyer,S.J., S.M.Norvell, S.M.Ponik, and F.M.Pavalko. 2001. Regulation of PGE(2) and PGI(2) release from human umbilical vein endothelial cells by actin cytoskeleton. *Am. J. Physiol Cell Physiol* 281:C1038-C1045.

Schiller,P.C., B.A.Roos, and G.A.Howard. 1997. Parathyroid hormone up-regulation of connexin 43 gene expression in osteoblasts depends on cell phenotype. *J. Bone Miner. Res.* 12:2005-2013.

Schnittler,H.J. 1998. Structural and functional aspects of intercellular junctions in vascular endothelium. *Basic Res. Cardiol.* 93 Suppl 3:30-9.:30-39.

Schnittler,H.J., B.Puschel, and D.Drenckhahn. 1997. Role of cadherins and plakoglobin in interendothelial adhesion under resting conditions and shear stress. *Am. J. Physiol* 273:H2396-H2405.

Schnittler,H.J., S.W.Schneider, H.Raifer, F.Luo, P.Dieterich, I.Just, and K.Aktories. 2001. Role of actin filaments in endothelial cell-cell adhesion and membrane stability under fluid shear stress. *Pflugers Arch.* 442:675-687.

Schubert,A.L., W.Schubert, D.C.Spray, and M.P.Lisanti. 2002. Connexin family members target to lipid raft domains and interact with caveolin-1. *Biochemistry* 41:5754-5764.

Secomb,T.W., R.Hsu, and A.R.Pries. 2001. Effect of the endothelial surface layer on transmission of fluid shear stress to endothelial cells. *Biorheology* 38:143-150.

Seebach,J., P.Dieterich, F.Luo, H.Schillers, D.Vestweber, H.Oberleithner, H.J.Galla, and H.J.Schnittler. 2000. Endothelial barrier function under laminar fluid shear stress. *Lab Invest* 80:1819-1831.

Shaklai,M., D.Loskutoff, and M.Tavassoli. 1978. Membrane characteristics of cultured endothelial cells: identification of gap junction. *Isr. J. Med. Sci.* 14:306-313.

Smalt,R., F.T.Mitchell, R.L.Howard, and T.J.Chambers. 1997. Induction of NO and prostaglandin E2 in osteoblasts by wall-shear stress but not mechanical strain. *Am. J. Physiol* 273:E751-E758.

Spisni,E., M.C.Bianco, C.Griffoni, M.Toni, R.D'Angelo, S.Santi, M.Riccio, and V.Tomasi. 2003. Mechanosensing role of caveolae and caveolar constituents in human endothelial cells. *J. Cell Physiol* 197:198-204.

Spray,D.C. 1996. Molecular physiology of gap junction channels. *Clin. Exp. Pharmacol. Physiol* 23:1038-1040.

Spray,D.C. 1998. Gap junction proteins: where they live and how they die. *Circ. Res.* 83:679-681.

Spray,D.C., H.S.Duffy, and E.Scemes. 1999. Gap junctions in glia. Types, roles, and plasticity. *Adv. Exp. Med. Biol.* 468:339-59.:339-359.

Squire,J.M., M.Chew, G.Nneji, C.Neal, J.Barry, and C.Michel. 2001. Quasi-periodic substructure in the microvessel endothelial glycocalyx: a possible explanation for molecular filtering? *J. Struct. Biol.* 136:239-255.

Steinberg,T.H., R.Civitelli, S.T.Geist, A.J.Robertson, E.Hick, R.D.Veenstra, H.Z.Wang, P.M.Warlow, E.M.Westphale, J.G.Laing, and . 1994. Connexin43 and connexin45 form gap junctions with different molecular permeabilities in osteoblastic cells. *EMBO J.* 13:744-750.

Sun,D., A.Huang, S.Sharma, A.Koller, and G.Kaley. 2001. Endothelial microtubule disruption blocks flow-dependent dilation of arterioles. *Am. J. Physiol Heart Circ. Physiol* 280:H2087-H2093.

Sun,R.J., S.Muller, F.Y.Zhuang, J.F.Stoltz, and X.Wang. 2003. Caveolin-1 redistribution in human endothelial cells induced by laminar flow and cytokine. *Biorheology* 40:31-39.

Takahashi,M., T.Ishida, O.Traub, M.A.Corson, and B.C.Berk. 1997. Mechanotransduction in endothelial cells: temporal signaling events in response to shear stress. *J. Vasc. Res.* 34:212-219.

Tanaka-Kamioka,K., H.Kamioka, H.Ris, and S.S.Lim. 1998. Osteocyte shape is dependent on actin filaments and osteocyte processes are unique actin-rich projections. *J. Bone Miner. Res.* 13:1555-1568.

Tarbell,J.M. 2003. Mass transport in arteries and the localization of atherosclerosis. *Annu. Rev. Biomed. Eng* 5:79-118.

Tepass,U. 2002. Adherens junctions: new insight into assembly, modulation and function. *Bioessays* 24:690-695.

Thi,M.M., T.Kojima, S.C.Cowin, S.Weinbaum, and D.C.Spray. 2003. Fluid shear stress remodels expression and function of junctional proteins in cultured bone cells. *Am. J. Physiol Cell Physiol* 284:C389-C403.

Toyofuku,T., Y.Akamatsu, H.Zhang, T.Kuzuya, M.Tada, and M.Hori. 2001. c-Src regulates the interaction between connexin-43 and ZO-1 in cardiac myocytes. *J. Biol. Chem.* 19;276:1780-1788.

Toyofuku,T., M.Yabuki, K.Otsu, T.Kuzuya, M.Hori, and M.Tada. 1998. Direct association of the gap junction protein connexin-43 with ZO-1 in cardiac myocytes. *J. Biol. Chem.* 273:12725-12731.

Tsukita,S. and M.Furuse. 2002. Claudin-based barrier in simple and stratified cellular sheets. *Curr. Opin. Cell Biol.* 14:531-536.

Tsukita,S., K.Oishi, N.Sato, J.Sagara, A.Kawai, and S.Tsukita. 1994. ERM family members as molecular linkers between the cell surface glycoprotein CD44 and actin-based cytoskeletons. *J. Cell Biol.* 126:391-401.

Turner,C.E. 2000. Paxillin and focal adhesion signalling. *Nat. Cell Biol.* 2:E231-E236.

Turner,C.H., M.R.Forwood, and M.W.Otter. 1994. Mechanotransduction in bone: do bone cells act as sensors of fluid flow? *FASEB J.* 8:875-878.

Turner,C.H. and F.M.Pavalko. 1998. Mechanotransduction and functional response of the skeleton to physical stress: the mechanisms and mechanics of bone adaptation. *J. Orthop. Sci.* 3:346-355.

Urban,M., R.Rozental, and D.C.Spray. 1999. A simple RT-PCR-based strategy for screening connexin identity. *Braz. J. Med. Biol. Res.* 32:1029-1037.

Vander Molen,M.A., C.T.Rubin, K.J.McLeod, L.K.McCauley, and H.J.Donahue. 1996. Gap junctional intercellular communication contributes to hormonal responsiveness in osteoblastic networks. *J. Biol. Chem.* 271:12165-12171.

Vink,H. and B.R.Duling. 1996. Identification of distinct luminal domains for macromolecules, erythrocytes, and leukocytes within mammalian capillaries. *Circ. Res.* 79:581-589.

Vink,H. and B.R.Duling. 2000. Capillary endothelial surface layer selectively reduces plasma solute distribution volume. *Am. J. Physiol Heart Circ. Physiol* 278:H285-H289.

Wang,L., S.C.Cowin, S.Weinbaum, and S.P.Fritton. 2000. Modeling tracer transport in an osteon under cyclic loading. *Ann. Biomed. Eng* 28:1200-1209.

Warner,A. 1992. Gap junctions in development--a perspective. *Semin. Cell Biol.* 3:81-91.

Wassermann,F. and J.A.Yaeger. 1965. Fine structure of the osteocyte capsule and of the wall of lacunae in bone. *Zeitschrift fur Zellforschung.* 67:636-652.

Weinbaum,S. 1998. 1997 Whitaker Distinguished Lecture: Models to solve mysteries in biomechanics at the cellular level; a new view of fiber matrix layers. *Ann. Biomed. Eng* 26:627-643.

Weinbaum,S., S.C.Cowin, and Y.Zeng. 1994. A model for the excitation of osteocytes by mechanical loading-induced bone fluid shear stresses. *J. Biomech.* 27:339-360.

Weinbaum,S., P.Guo, and L.You. 2001. A new view of mechanotransduction and strain amplification in cells with microvilli and cell processes. *Biorheology* 38:119-142.

Weinbaum,S., X.Zhang, Y.Han, H.Vink, and S.C.Cowin. 2003. Mechanotransduction and flow across the endothelial glycocalyx. *Proc. Natl. Acad. Sci. U. S. A* 100:7988-7995.

White,C.R., M.Haidekker, X.Bao, and J.A.Frangos. 2001. Temporal gradients in shear, but not spatial gradients, stimulate endothelial cell proliferation. *Circulation* 103:2508-2513.

Willecke,K., J.Eiberger, J.Degen, D.Eckardt, A.Romualdi, M.Guldenage, U.Deutsch, and G.Sohl. 2002. Structural and Functional Diversity of Connexin genes in the Mouse and Human Genome. *Biol. Chem.* 383:725-737.

Yamaguchi,D.T., D.Ma, A.Lee, J.Huang, and H.E.Gruber. 1994. Isolation and characterization of gap junctions in the osteoblastic MC3T3-E1 cell line. *J. Bone Miner. Res.* 9:791-803.

Yellowley,C.E., Z.Li, Z.Zhou, C.R.Jacobs, and H.J.Donahue. 2000. Functional gap junctions between osteocytic and osteoblastic cells. *J. Bone Miner. Res.* 15:209-217.

You,J., C.E.Yellowley, H.J.Donahue, Y.Zhang, Q.Chen, and C.R.Jacobs. 2000. Substrate deformation levels associated with routine physical activity are less stimulatory to bone cells relative to loading-induced oscillatory fluid flow. *J. Biomech. Eng* 122:387-393.

You,L., S.C.Cowin, M.B.Schaffler, and S.Weinbaum. 2001. A model for strain amplification in the actin cytoskeleton of osteocytes due to fluid drag on pericellular matrix. *J. Biomech.* 34:1375-1386.

You,L.D., S.Weinbaum, S.C.Cowin, and M.B.Schaffler. 2004. Ultrastructure of the osteocyte process and its pericellular matrix. *Anat. Rec.* 278A:505-513.

Zeng,Y., S.C.Cowin, and S.Weinbaum. 1994. A fiber matrix model for fluid flow and streaming potentials in the canaliculi of an osteon. *Ann. Biomed. Eng* 22:280-292.

Zhang,D., S.C.Cowin, and S.Weinbaum. 1997. Electrical signal transmission and gap junction regulation in a bone cell network: a cable model for an osteon. *Ann. Biomed. Eng* 25:357-374.

Zhang,D., S.Weinbaum, and S.C.Cowin. 1998. Electrical signal transmission in a bone cell network: the influence of a discrete gap junction. *Ann. Biomed. Eng* 26:644-659.

Ziambaras,K., F.Lecanda, T.H.Steinberg, and R.Civitelli. 1998. Cyclic stretch enhances gap junctional communication between osteoblastic cells. *J. Bone Miner. Res.* 13:218-228.